Functional Modification of Textile Fabrics Using New Technologies

Functional Modification of Textile Fabrics using New Technologies
（各種技術を用いる織物の高機能加工）

平成24年3月　鄭光洪

福　井　大　学
学　位　論　文［博士（工学）］

Functional Modification of Textile Fabrics Using New Technologies

（各種技術を用いる織物の高機能加工）

平成 24 年 3 月

氏名：　鄭光洪

UNIVERSITY OF FUKUI
GRADUATE SCHOOL OF ENGINEERING
FIBER AMENITY ENGINEERING

Functional Modification of Textile Fabrics Using New Technologies

By
Zheng Guanghong

A thesis submitted in partial fulfillment of the
requirements for the degree of
Doctor of Philosophy

NOVEMBER 2011

ABSTRACT

With the increasing awareness of environmental pollution and the extensive consideration of mankind health, there has been an increased demand for natural fibers in textile materials recently. As a typical natural fiber, ramie is an increasingly popular because of its excellent properties including a high tensile strength, excellent thermal conductivity, coolness, ventilation function, moisture absorption, and antibacterial function. However, ramie fiber and ramie fabric have some disadvantages such as poor elasticity, low wrinkle recovery, low resilience, itchiness, harsh handle, which decreases the competitiveness of ramie fabric in the high-grade garment-fabric market. It is necessary to use the advanced technologies in the dyeing and finishing for enhancing the competitiveness of ramie fabric. This study is aimed to study the natural dyeing and functional finishing of ramie fabric.

At present, ramie fabrics are mostly dyed with synthetic colorants which can give rise to serious environmental pollution and potential harm to mankind health. Thus the natural and healthy features of ramie fabric are greatly weakened. In this study, ramie fabrics were dyed with the several natural extracts. But heavy metal ions, which lead to environmental pollution, are usually used as mordant in natural dyeing. In this study, the eco-friendly rare earth was used as mordant in natural dyeing of ramie fabrics. The influences of dyeing conditions were studied. The ramie fabrics dyed using rare earth as mordant exhibited higher color shade stability against pH variation. Using rare earth as mordant in natural dyeing apparently enhanced the color fastness to washing, rubbing and light of the ramie fabrics. As compared with Fe^{2+} and Cr^{6+}, rare earth was more efficient, resulting in decrease of mordant concentration in natural dyeing. Thus rare earth was effective mordant in the natural dyeing of ramie fabrics.

One of the shortcomings of ramie fabric is its lower wrinkle recovery. The typical wrinkle resistant finishing via cross-linking usually decreases strength of cellulose fabrics. In this study, ramie fabrics were pretreated with liquid ammonia (NH_3) prior to wrinkle resistant finishing. Meanwhile, a kind of thermally reactive polyurethane (PU) emulsion was used as strength protector. The liquid NH_3 pretreatment was proved to

decrease crystallinity of ramie fiber and bring about apparent swelling effect. As a result, the accessibility of the ramie fabrics treated by liquid NH_3 was elevated. The liquid NH_3 pretreatment prior to resin finishing gave rise to better wrinkle resistant effect and less strength loss. The thermally reactive PU emulsion was proved to decrease strength loss of ramie fabric without influencing wrinkle resistant effect. Using liquid NH_3 pretreatment and employing reactive PU as protector in the wrinkle resistant finishing of ramie fabric can raise strength retention up to 80%. After 10 laundry cycles, the flat appearance and the crease retention of these ramie fabrics were over grade 3.0.

Developing electromagnetic shielding textiles has drawn increasing attention recently since electromagnetic pollution is harmful to mankind health. In this study, super critical carbon dioxide ($scCO_2$) fluid technology was used to develop electromagnetic shielding ramie fabric. The $scCO_2$ treatment could remove the impurities of the ramie fibers prominently. The $scCO_2$ fluid could result in the swelling of ramie fiber and thus increase the absorbency of ramie fiber to additives. Using $scCO_2$ fluid, the Palladium (II)-hexafluoroacetylacetonate could be impregnated into the ramie fiber under appropriate conditions. After thermal decomposition at high temperature, the Palladium film formed on ramie fibers. The ramie fabrics bearing Palladium catalyst were plated with a cooper film via electroless cooper plating. The cooper coated ramie fabrics exhibited good shielding effect. This study presented a new way for developing electromagnetic shielding fabric.

Nanoparticles have been extensively used for the functional finishing of textiles. But the nano finishing of ramie fabrics has less been studied. In this study, the multifunctional ramie fabrics coated by TiO_2 nanoparticle were developed. The optimal dispersion conditions of TiO_2 nanoparticles in aqueous suspension were studied in details. A kind of hydrophilic silica aerogel product was proved to be suitable for serving as dispersant for dispersion of TiO_2. Using the TiO_2 suspension prepared in optimal conditions, ramie fabrics were coated with TiO_2 via a dip-pad-dry process. In order to enhance the finishing durability the ramie fabric were pretreated by citric acid prior to nano finishing. The ramie fabric finished with working bath containing 0.8g/L TiO_2 was proved exhibited excellent UV protection and antibacterial property, and high

capability for decomposing formaldehyde. Treating fabric with citric acid before coating could improve the washing durability of the resultant TiO_2 loaded ramie fabrics.

This study explored several ways for developing healthy and highly functional ramie fabrics with high added value. The resultant ramie fabrics exhibited high quality. The newly developed dyeing and finishing processes are supposed to be helpful for raising the competitiveness of ramie and expanding its application.

TABLE OF CONTENT

CHAPTER 1
INTRODUCTION

1.1 Research background

As a classic fiber, ramie has been used in many countries since time immemorial. Ramie has been grown in the Far East for centuries and its fiber was used for textiles and cloth even before the introduction of cotton. Nowadays, ramie is mainly grown in China, Brazil, South Korea, the Philippines, Taiwan, Thailand, India and a few other countries. Ramie fibers are stripped from stem bast of a hardy perennial herbaceous plant of the Urticaceae family which is also called China grass. The ramie fabrics are used in the textile industry for manufacturing various types of high quality clothing materials. Ramie is used frequently in blends with other textile fibers such as cotton, viscose, polyester, wool, hemp, jute, etc. A great variety of textile products such as canvas, towels, twines, sewing threads, knitted cloths and garments can be produced from ramie fibers. Recent fashion trends have an increased demand for ramie fibers because of its outstanding performance and aesthetic properties.

Ramie has excellent properties such as high tensile strength when they are used as textile materials. It is reported that ramie has a tensile strength eight times that of cotton and seven times greater than silk. It possesses excellent thermal conductivity, coolness, ventilation function, moisture absorption function and therefore is comfortable to wear, especially during warm weather. Ramie also shows prominent resistance to bacteria, mildew, alkalis, light and insect attack. Ramie fabric has natural stain resisting ability with ease of stain removal and is better than cotton fabric thereby. It also gives a high luster.

However, ramie fibers are suffered from low elasticity, poor wrinkle recovery, low abrasion resistance, harsh handle and itching when worn next to the skin. The dyeing

property of ramie is not as good as that of cotton. Because of its high molecular crystallinity, ramie lacks resiliency and is low in elongation potential. Spinning the ramie fibers is difficult by their brittle quality and low elasticity; and weaving is complicated by the hairy surface of the yarn, resulting from lack of cohesion between the fibers. Ramie fabrics tend to show wrinkle appearance easily because of the higher stiffness of ramie fiber. In addition, ramie fiber is high cost which reduces its competitiveness against other textile fibers. The shortcomings decrease the competitiveness of ramie fabric in the high-grade garment-fabric market. Natural dyeing and functional finishing bring about high added value to ramie fabric and thus can enhance its competiveness against other textile materials.

At present, ramie fabrics are mostly dyed with synthetic colorants which can give rise to serious environmental pollution and potential harm to mankind health. Thus the natural and healthy features of ramie fabric are greatly weakened. Replacing the synthetic dyes with natural extract colorants in the dyeing of ramie fabric can not only reduce environmental pollution but also retain the natural and healthy features of ramie fabric and thus is favorable for increasing its competitiveness. However, heavy metal ions are usually used as mordant in the natural dyeing of cellulose fabrics, resulting in environmental pollution and potential harm to human being. Rare earth elements can be used as mordant in natural dyeing due to their higher capability for forming complexion. Using rare earth as mordant in the natural dyeing of ramie fabric is supposed to develop high-quality healthy textile material, which has never been reported.

Poor wrinkle recovery is a major disadvantage of ramie fabric. Carrying out wrinkle resistant finishing on ramie fabric is significant for upgrading the performance of ramie. It is well documented, the typical wrinkle resistant finishing of cellulose fabrics using the cross-linking agents such as dimethyloldihydroxyethyleneurea (DMDHEU) and 1,2,3,4-butanetetracarboxylic acid (BTCA) can result in significant strength loss. Liquid NH_3 treatment prior to resin finishing has been proved to reduce strength loss for cotton fabrics. The application of the combination of liquid NH_3 pretreatment and resin finishing for ramie fabrics has not been studied systematically.

With the development of science and technology, electromagnetic (EM) pollution increases as well, resulting in the rising attention to electromagnetic shielding (EMS) fabrics. Most of investigations on the EMS fabrics are based on synthetic fibers. Fewer attempts have been made on the development of EMS fabrics with natural fibers. Developing EMS fabrics with ramie fabric is essential for expanding the application of ramie fabric. Electroless copper (Cu) plating is a simple and effective method for developing EMS fabrics. But ramie fabric has to be pretreated prior to Cu plating for increasing the absorbency of ramie fibers to Palladium catalyst. As an environmentally benign process, $scCO_2$ fluid technique has been proved to result in the swelling of cellulose fibers and thus raise their accessibility. Using $scCO_2$ fluid technique for the impregnation of Palladium catalyst in the development of EMS fabrics has never been studied.

With the advent of nanoscience and technology, a new area has developed in the area of textile finishing called "Nano finishing". Growing awareness of health and hygiene has increased the demand for bioactive or antimicrobial and UV-protecting textiles. Coating the surface of textiles and clothing with nanoparticles can produce high functional textiles having UV protective, antibacterial, water repellant and self-cleaning characteristics which greatly enhance added values and competiveness of fabrics. However, most of the nano finishing investigations were conducted on cotton or polyester fabric. As compared with case of cotton and polyester, few attempts have been made on the nano finishing of ramie fabric.

1.2 Objectives of the study

This study is mainly concerning with the application of new techniques for the dyeing and finishing of ramie fabrics in order to overcome some major difficult problems in the processing of ramie fabrics and develop high-value-added ramie textile materials. The primary objectives of this thesis are summarized as follows:

(1) To study the natural dyeing of ramie fabrics using rare earth as mordant.

(2) To study the wrinkle resistant finishing of ramie fabric using liquid ammonia technology

(3) To investigate the application of super critical carbon dioxide technique for the electromagnetic shielding finishing of ramie fabric.

(4) To develop multifunctional ramie fabrics through finishing with TiO_2 nanoparticles.

1.3 Methodology

In order to achieve the above objectives, the following methods were adopted in this study.

(1) A literature review was conducted in order to get the background knowledge, especially the comprehensive understanding of the unique structure of ramie fibers so that the appropriate investigating routes can be adopted.

(2) According to the structural feature, i.e. high crystallinity, and the dyeing and finishing properties of ramie fibers, the new technologies including liquid ammonia (NH_3) and super critical carbon dioxide ($scCO_2$) processes were employed to treat ramie fabric prior to wrinkle resistant finishing and electromagnetic shielding treatment. On one hand the two kinds of technologies can greatly reduce crystallinity and result in swelling of ramie fiber. On the other hand, the two kinds of technologies are eco-friendly. The eco-friendly pretreatments can avoid or reduce chemical residual and match the natural feature of ramie fabric.

(3) Owing to its natural feature, this study conducted the study on the natural dyeing of ramie fabric. Moreover, the eco-friendly light rare earth chlorides were used to replace heavy metal as mordant, which is aimed to further reduce harmful chemical residual of ramie fabric and decrease environmental pollution in dyeing.

(4) The poor wrinkle resistance is a major shortcoming of ramie fabric. This study used the combination of liquid NH_3 and chemical cross-linking to perform the wrinkle resistant finishing. In order to reduce the strength damage, a thermally reactive polyurethane emulsion was utilized as protector.

(5) The combination of pretreatment by $scCO_2$ and precursor impregnation by $scCO_2$ was used for electroless cooper plating. This can promote the swelling of ramie fiber and reduce pollution.

(6) In the study of nano finishing of ramie fabric, the hydrophilic silica aerogel was used as dispersant of TiO_2 nanoparticles. The chemical cross-linking pretreatment on ramie fabric was used to improve the finishing durability. In addition, the influencing factors on dispersion of TiO_2 were studied, which favors the production of stable TiO_2 suspension.

(7) The techniques including scanning electron microscopy (SEM), X ray diffraction (XRD), thermogravimetric analysis (TGA), X-ray photoelectron spectroscopy (XPS) were used to study structural change. In addition, the CIELAB colorimetric values of dyed fabric were measured by Datacolor SF600 Computer Color Matching System. The UV protection of fabric specimens was measured using UV-visible spectrophotometer.

1.4 Outline of the thesis

(1) Chapter 1 introduces the research background and proposes the study contents and objectives. In addition, the main study methods employed in the study were explained. At last, the outline of the thesis was given.

(2) Chapter 2 presents a short overview on the documents of the relevant investigations. In particular, the structural characteristics of ramie fibers were stressed. Because the structural characteristics of ramie fiber was the basis of its dyeing and finishing. The new developments of finishing were also simply introduced.

(3) Chapter 3 shows the study results of natural dyeing of ramie fabric. The mordant function of rare earth in natural dyeing was verified. The advantage of rare earth over heavy metals for serving as mordant was manifested.

(4) Chapter 4 presents the findings in the wrinkle resistant finishing of ramie fabric using liquid NH_3 pretreatment. It was found that the liquid NH_3 pretreatment could improve wrinkle resistant effect and reduce strength damage. Using thermally reactive PU emulsion as protector could further decrease strength damage with

influencing wrinkle resistant effect.

(5) Chapter 5 reports the experimental results achieved from the study of electromagnetic shielding finishing using $scCO_2$ technique. It can be drawn from this part that the $scCO_2$ could result in the swelling of ramie fiber which is favorable for the impregnation of Palladium catalyst. The electroless plated ramie fabrics were proved to show good electromagnetic shielding effect.

(6) Chapter 6 introduces the achievements attained from the study on the multifunctional finishing of ramie fabric using titanium dioxide (TiO_2) nanoparticles. It was found that TiO_2 coated ramie fabrics exhibited excellent UV protection and antibacterial property, and high capability of decomposing formaldehyde. In addition, the pretreatment of ramie fabric with citric acid could greatly enhance the finishing durability in multiple launderings.

(7) Chapter 7 summarizes the conclusions obtained in all the investigations of my PhD study.

CHAPTER 2
LITERATURE REVIEW

2.1 Ramie fiber

Ramie is one of the oldest vegetable fibers and has been used for thousands of years. It was used for Chinese burial shrouds over 2,000 years ago, long before cotton was introduced in the Far East [1-3]. Ramie is classified chemically as a cellulosic fiber, just like cotton, linen and rayon. Leading producers of ramie are China, Taiwan, Korea, Philippines and Brazil. However, the research studies conducted on ramie fiber began much later than on cotton. The comfort quality of ramie involves its cool nature and ability to absorb perspiration, both are related to the structure of the fiber bundle. Since it is a good conductor of heat, thus ramie goods are especially suitable for North American and European countries where quick weather changes, i.e. cool in the morning but mild or hot in the afternoon. The high perspiration absorption rate of ramie coupled with improved dyeing techniques enables it to be used for making basic garments with a classic look. Ramie fabrics are easily laundered without suffering any strength loss, and are therefore ideal for making bed sheets, tablecloths and towels [4]. Ramie has also been used to produce seat covers due to its excellent thermal conductivity, and reinforced composites due to its high tenacity [5].

2.1.1 Fiber pretreatment

Decortication

The ramie fibers are removed from the stalks by the process of decortication. This is always carried out by hand; the process consists of peeling or beating the bark and bast material from the stalk soon after harvesting. The fibers are freed by soaking the bark in water and scraping with knives made from shells, bamboo, bronze or iron. The long strands of ramie fiber are then dried and bleached in the sun.

The decortication process varies in detail in different regions [1]. Sometimes the stalks are beaten against rocks before being peeled; the bark is battered with wooden mallets to free the fiber from adhering woody matter. In Indonesia the stalks are scraped in such a way as to leave the bast fibers clinging to the woody cores. These are then washed and the fibers are peeled away in the form of long ribbon-like strands. During the 1930s, great interest was aroused in the large-scaled commercial possibilities of ramie as a textile fiber. However, development of ramie production was held up by the primitive methods used in decortication, and attempts were made to devise machinery that could strip the fibers from the stalk. Several machines are now in commercial use, and decortication has been mechanised.

Degumming

In their natural state, ramie fibers are present in the plants' stems in the form of fiber bundles, consisting of individual ultimate fibers that are cemented to each other by waxes and pectins. As these bundles are too thick and too long to be used for textile purposes the fibers within the bundles need to be separated by removing the waxes and pectins. This process is called degumming and produces 'technical' fibers which can be spun into yarns [1-3, 6-9]. Usually, degumming is done in spinning mills prior to spinning. The process involves soaking in alkali baths for the prescribed periods of time at prescribed temperatures. The most common chemical used is caustic soda; others which can be used alone or in combination with caustic soda are sodium tripolyphosphate, sodium sulphate, sodium carbonate, sodium pyrophosphate, sodium silicate and sodium citrate. However, such a process requires high energy input and produces hazardous waste.

Degumming of bast fibers has also been carried out with the help of microorganisms. Pectinolytic enzymes produced by microorganisms, which are generally part of the micro-flora residing on the stalk, have gained most attention [1-3, 6, 8, 9]. These enzymes degrade the pectin of the middle lamella and primary cell wall, leading to separation of the cellulosic fibers. Combined chemical-biochemical processes have been proposed for degumming ramie bast fibers, but no reports are available on the successful introduction of a bio-technical degumming process at industrial scale.

However, the search for new microorganisms and enzymes for such an application is still a challenging task.

Bleaching

Bleaching of ramie fiber is strongly affected by the high percentage of their non-cellulosic components [1, 4]. The hemicelluloses, which are the main constituent of the middle lamella, are of a low degree of polymerisation and are highly soluble in alkali. The loss in weight of up to 25% may be obtained in alkaline bleaching treatment. The major objective of bleaching bast fibers is to remove the lignin with which most of the colouring matters are associated. The removal of woody matter remaining in the fibers after the mechanical processing stages, if any, is also essential. A two-stage combination bleaching is often applied, usually with sodium chlorite followed by hydrogen peroxide. The more severe the conditions used in bleaching, the higher the degree of whiteness obtained and the greater the loss in weight will be. The bleaching processes used for bast fibers are usually milder, with longer treatment times than those used for cotton, in order to preserve the strand structure as much as possible.

2.1.2 Fiber structure

When defining the structure of a polymeric substrate such as ramie fiber, one has to distinguish three structure levels:

(1) The molecular level, i.e., the chemical composition, steric conformation, molecular mass, molecular mass distribution, the presence of functional sites and the existence of intra-molecular interactions.
(2) The supermolecular level, i.e., the aggregation of the chain molecules to elementary crystals and fibrils, the degree of order within and around these fibrils, and the perfection of their orientation with respect to the fiber axis.
(3) The morphological level, i.e., the spatial position of the fibrillar aggregations in the "cross-morphology" of the fiber, the existence of distinct cell wall layers in native cellulosic fibers or of skin-core structures in man-made cellulosic fibers, and the presence of voids or interfibrillar interstices.

Molecular Structure

Bast fibers including ramie are natural vegetable fibers based on cellulose. They are derived from the vascular bundles of plant stems which are used for food and water conduction in the living plant. The fibers are constructed of long thick-walled cells overlapping and cementing together by non-cellulosic materials to form continuous strands that may run the entire length of plant stem. The process of retting or degumming can release the strands of bast fibers from the cellular and woody tissue of plant stem.

Table 2.1 Chemical composition of ramie fiber.

Chemical components	Content (%)
Cellulose	68.6 - 76.2
Hemi-cellulose	13.1 - 16.7
Pectin	1.9
Lignin	0.6 - 0.7
Water solubles	5.5
Wax	0.3
Moisture	8.0-10.0

The natural and chemical composition of ramie fiber may vary widely. The main factors are the generic characteristics of the plant, conditions of growth, type of soil, age, part of the plant from which the sample originates, mode of cultivation, and the atmospheric conditions to which the fibers are directly exposed. To some extent the divergence in values may also be due to different methods employed for the determination. Table 2.1 shows the chemical composition of a typical ramie fiber [1, 4, 10].

Cellulose is a linear macromolecule formed by b-d anhydroglucose units (AGU), linked together by 1,4-glucosidic bonds. Each of the AGUs possesses hydroxyl groups at C-2, C-3 and C-6 position, capable of undergoing typical reactions known for primary and secondary alcohols. The hydroxyl groups at both ends of cellulose chain show different behaviour. The C-1 end has reducing properties, while the glucose end group with a free C-4 hydroxyl group is non-reducing. The bridging and chain show different behaviour. The C-1 end has reducing properties, while the glucose end group with a free C-4 hydroxyl group is non-reducing. The bridging and the ring oxygen atom are predominately involved in intra- and inter-molecular interactions, mainly hydrogen bonds. The molecular size of cellulose can be defined by its average degree of polymerisation (*DP*). Among all the natural cellulosic fibers, ramie has the highest *DP* around 2150-3300 [4].

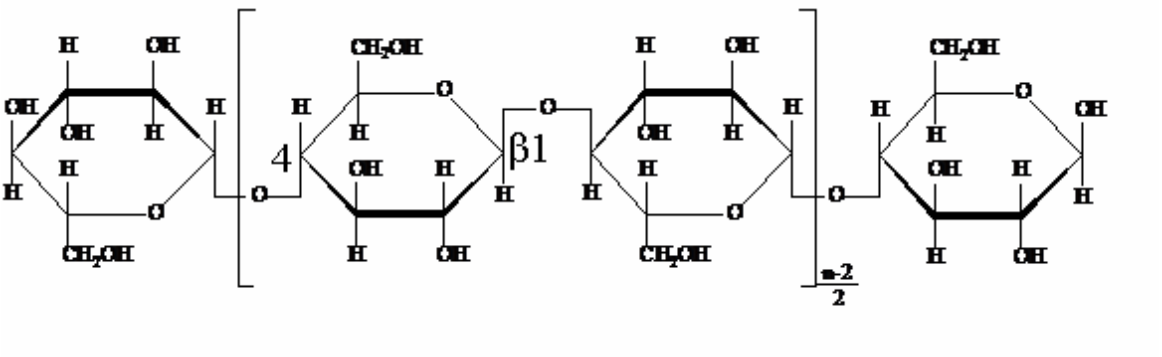

Figure 2.1 Chemical structure of cellulose

Supramolecular Structure

The order of the macromolecules in a cellulosic fiber is not uniform throughout the whole structure, and so amorphous regions as well as cyrstalline regions coexist [10, 11]. Marchessaault R. H. *et al* proposed the model of a continuous order spectrum of solid state cellulose [12]. This model, however, is abandoned today as obvious regions of medium order play a minor role only, and the experimental evidence available today is adequately interpreted by a two-phase model assuming amorphous and crystalline regions, and neglecting the rather

small amount of matter with an intermediate state of order.

In a simplified two-phase model, the supramolecular structure of a polymer is considered as a system of crystalline and amorphous phases. Based on this two-phase model, a considerable work has been done to estimate the crystallinity of cellulosic fibers including ramie using the X-ray diffraction technique over the last several decades. These methods of measuring crystallinity are based on the assumption that it is possible to separate the X-ray diffraction diagram of polymer into "sharp reflections" and "diffuse scatter" and assign these respectively to crystalline and amorphous components. Based on this two-phase method, most of the results obtained showed that the crystallinity of ramie fiber was around 80% which was higher than that of cotton (~70%). However, various results were obtained by different researchers. The divergences in data could be attributed to the differences in the morphological structures of the ramie varieties tested and the differences in testing condition.

Over the past years, considerable experimental works had shown that the two-phase model was oversimplified and some experimental phenomena of ramie fiber could not be fully explained by the traditional two-phase model. Knight, J. A., *et al* used deuterated water (D_2O) to treat ramie and cotton fiber [13]. The hydrogen (H) of the hydroxyl of the cellulose molecule in the D_2O accessible region was substituted by deuterium (D). It was found that the amount of H substituted by D in ramie was more than that in cotton. Ray P. K *et al* treated ramie fiber with 24% NaOH at both high and room temperature for 30 minutes, and then the samples were investigated by X-ray diffraction [14]. The result showed that the cellulose I of ramie fiber was transferred completely to cellulose II, while the cotton fiber only had partial transformation. In addition, some researchers studied the lowest concentration of NaOH that could cause the change of X-ray diagram of the cellulosic fibers. The concentrations used for cotton and ramie were 17% and 12% respectively. All the above results showed that the accessibility of ramie fiber to some chemicals was more than that of cotton, and the crystalline structure of ramie was easier to be destructed than cotton. Hence it

was considered that there were some defects in the crystallite of ramie fiber and the three-phase model containing crystalline, para-crystalline and amorphous regions was advanced by scientists.

A lot of work has been devoted to get a much deeper understanding of the supramolecular structure in ramie fiber. Nishimura, H. *et al* studied the mechanism of mercerization and crystallite sizes using ramie substrate [15]. They suggested that the overall morphology of ramie fiber could be divided into three regions namely the highly oriented amorphous one, another one consisting of small and distorted crystalline region, and the third one consisting of a well-ordered crystalline region. The difference between the former two regions was not distinct. Sao, K. P. *et al* measured various structure parameters of ramie such as crystallinity and disorder parameters using the Ruland and Vonk method [16]. They found that the simple two-phase model of completely ordered and disordered phases had little validity for ramie fiber. The existence of intermediate ordered regions had to be considered for a satisfactory explanation of the phenomenon of swelling. They suggested a model of ramie cellulose structure consisting of crystalline, oriented amorphous, highly distorted crystalline, and amorphous regions respectively.

Morphological Structure

Unlike cotton, ramie fiber is a multiple cellular system [4, 10]. It is found as bundles (aggregates) of multiple cells also called ultimate cells. The ultimate cells in the aggregate bundle are bound together by natural polymers, variously called resins, gums, cementing materials, encrusting materials and middle lamella. The morphological structure of the multi-cellular fibers makes them analogous to the modern-day fiber reinforced, rigid-matrix composites.

According to this picture, the middle lamella in bast fibers plays the role of the matrix. It is, however, a complex role. First, the middle lamella holds the ultimate cells together in the fiber bundle or strands. This is termed the "inner middle lamella". Owing to its close packing and possible penetration into the fiber walls, as well as the possibility of being chemically linked to the cellulose of the cell wall, it is relatively stable to

chemical and microorganism attack. A second function of the middle lamella is to glue together the fiber bundles in the bast layer and this layer to the other layers of the stem. This is termed the "outer middle lamella." It is less closely packed than is the inner middle lamella, and it is probably less chemically linked to the other layers. The possibility of selective attack on the outer middle lamella by microorganisms had been recognized by the ancients and was used in practice to this day in the retting and degumming operations.

Microscopic examination reveals that ramie fiber is a bundle of ultimate cells. The cells are rounded polygons with a thin, well-defined lumen, both are of irregular shapes. The cells also have a tendency to develop radial cracks. More recent SEM of the fiber's ultimates reveal kidney-shaped, ribbon-like and multi-lobal cross sections with or without lumens; the lumens in the ribbon-like cross sections appear like cracks oriented in the longer direction of the cross section. The longitudinal view of the ultimates shows cross-striations. Detailed examination of these striations reveals that they are not cracks or fissures; but the dislocation-folds or constructions in the straight continuity of fibrils in the secondary wall. Evidence has been presented to suggest that cross-markings on the fiber surface are developed due to the presence of contiguous cross-walls of adjacent parenchyma cells during the period when fiber is a functioning member of the plant stem. It has been suggested that such striations are indeed the location of the paths through which nutrients are supplied to the fiber by the parenchyma cells. It was further demonstrated that, through swelling treatment with the Krais- Viertel reagent and lateral compression, the cross-markings can be made to disappear. Under lateral compression, the fiber is shown to be composed of a series of well-defined, parallel bundle of fibrils, nearly parallel to the fiber axis.

It has been shown that the outside layer of ramie has Z spiral followed by an S spiral layer and a core intermediate is almost in parallel orientation. Native ramie fiber has lower cellulose but higher hemi-cellulose and lignin content than cotton.

2.2 Ramie fiber modification

The wearing properties of fabric are determined mostly by the properties of the textile fiber. As for ramie, it has much higher initial modulus than cotton. Hence, the ramie fiber is very rigid, and the breaking elongation and elastic recovery are very poor. As a result, the ramie fabric suffers from harsh handle and poor wrinkle recovery, imparting a feeling of itchiness when used in garments worn next to the skin. In the recent 30 years, a considerable work has been done to ameliorate these undesirable properties by modifying the chemical structure and surface properties of ramie. The usual modification of ramie fiber can be grouped into the following three kinds of methods: (1) alternating the structure of cellulose molecules of ramie fiber to change the degree of fiber orientation and crystallinity such as alkali modification. (2) grafting of the reactive cellulose hydroxyl group with the other functional groups such as sulphonation, acetylation and alkylation, so as to create a new modified cellulose; (3) chemical cross-linking of cellulose molecular chains which is a common method used to improve the crease-resistance of the cellulosic fabric.

2.2.1 Alakli modification

Alkali treatment is one of the most important methods used to modify the ramie fiber. The swelling of ramie cellulose in aqueous solutions of sodium hydroxide has been observed already 70 years ago and has since been the topic of a large number of experimental investigations and theoretical considerations. Several studies have focused on the effect of sodium hydroxide on the fine structure of ramie. X-ray studies have shown that mercerisation of ramie will result in a complete conversion from cellulose I to cellulose II and a decrease in the degree of crystallinity to 50%.

Sao, K. P. *et al* found that the transition of ramie cellulose from cellulose I to cellulose II lattice took place in 12-15% NaOH at room temperature through the infrared spectra studies, and X-ray diffraction patterns further confirmed the result [17]. Liu, Q. H. *et al* also studied the fine structure of ramie fiber which was treated with various concentrations of NaOH solution at 20^{o}C for 5 minutes [18]. It was found that

when the concentration of NaOH was below 12%, the crystallinity, orientation, density and absorption of the treated ramie fiber were changed unremarkably. However, when the concentration of NaOH reached 12% or higher, these parameters would decrease markedly; and all the fine structures had the maximum change at 16% NaOH.

The swelling process of ramie fiber in NaOH solution has also' been thoroughly investigated. Okano, T. *et al* studied the alkali-cellulose structures as intermediates during the conversion of cellulose I to cellulose II when ramie cellulose was mercerized [19]. Five unique alkali celluloses were identified in their research. In the later research, they studied the crystal of three of the intermediates and provided with the information on the interactions between cellulose and sodium ions, as well as the formation of these structures and the probable conversion mechanism.

It is difficult to generalize the changes in the mechanical properties of ramie induced by alkali treatment since the data in literature vary considerably. The overall results were qualitatively coincident such that the slack mercerization of ramie would bring about considerable losses in yam strength, greatly increased breaking elongation and very greatly decreased initial modulus, resulting in improved elasticity and soft handle. Tension mercerization would bring about increased strength, slight decrease in breaking elongation and increased initial modulus, resulting in a much more rigid handle [18, 20]. The reduction of the strength in slack mercerized ramie fiber has been attributed to the decrease in crystalline orientation as a function of the unrestrained lateral swelling of the fibrils. Under tension mercerization, the lateral movement of the polymer chains in ramie is limited, thus strength loss does not occur as in the slack treatment. The increase in cotton strength under both slack and tension swelling is well documented and has been attributed to the restraining primary wall and S1 layer oriented transverse to the axis.

After alkali modification, the accessibility of the ramie fiber increased which resulted in increased dye absorption. Cheek, L. gave a comparison of mercerized ramie, flax and cotton [20, 21]. It was found that the dye up-take and color yield of ramie fiber was lower than that of cotton but higher than flax before mercerization. However, dyed

ramie exhibited a higher apparent depth of shade than cotton and flax with lower dye content. Only when the difference in dye content was considerably higher did flax appear darker than ramie. Slack mercerization produced much greater gain in the rate of dye sorption, quantity of dye exhausted at the end of the dyeing cycle, and depth of shade produced than that of tension mercerization for all three fibers.

2.2.2 Chemical grafting

To improve the physical properties of ramie fiber, especially elastic recovery, many efforts besides alkali modification have also been taken since 1960s'. Sulphonation is one of the earliest methods applied to modify ramie fiber. The mechanism includes using carbon disulphide (CS_2) to react with the hydroxyl group of cellulose under alkali condition. The process is very complicated and has tremendous pollution to the environment. The modified fiber has a serious strength loss while its rigidity is much less than the untreated one. Alkylating is another method applied to ramie fiber. The mechanism includes using alkylate agent such as alcohol and halo-hydrocarbon to react with the ramie cellulose under the swelling and catalysation of alkali. The process causes little pollution and many properties including handle, elastic recovery and dyeability have been improved after modification. Acylation is also an important modifying method for ramie; the process is similar to that of alkylation.

In recent years, apart from the above grafting methods, some other functional groups or monomers were also studied. Zhao, W. B. used acrylonitrile to graft ramie fiber and produced cyanoethylated ramie [22]. The supramolecular structures of the modified ramie such as crystallinity, fiber orientation and crystallite dimension were decreased. This resulted in an improvement of both physical and chemical properties such as increased elasticity and breaking energy, decreased initial modulus, improved loop strength, dyeability and rot resistance. Another grafting method involves using vinyl and related monomers for graft copolymerization of ramie and other bast fibers such as jute, flax and hemp. The modified ramie fiber has an improved elasticity but at the expense of much strength loss. Using cationic grafting to improve the dyeability has also been investigated for a long time. The results showed that the modified ramie fiber had

higher dye absorption and deeper shade. The modified ramie fiber could even be dyed by acid dyestuff with a very high colour fastness.

2.2.3 Liquid NH_3 treatment

Several workers have shown that intra-crystalline swelling takes place when native cellulosic fibers are immersed in liquid NH_3 [23-38]. Liquid NH_3 interacts with cellulose to form a hydrogen-bonded complex. The nitrogen atom in the NH_3 molecule, with its unshared pair of electrons, replaces OH—O hydrogen bonds by OH－N bonds to form a swelling complex. This complex is unstable and decomposes when the liquid NH_3 is either evaporated or washed out with water. Depending on the experimental conditions, destruction of the ammonia-cellulose complex can be accompanied by a partial or full lattice transformation from the cellulose I to III form. The use of liquid NH_3 in the cotton textile finishing industry has increased over the past several years. It has been used as a treatment for sheeting, work-wear, denim and bottom-weight fabrics. It is also applied prior to cross-linking treatments in 100% cotton shirting fabrics.

The swelling behavior of ramie fiber in liquid NH_3 has some difference with that of cotton due to its special morphology and fine structure. It was found that liquid NH_3 treatment could improve the wearing properties of ramie fabric such as shrink-proof, fabric handle and especially abrasion resistance property. More interesting is that liquid NH_3 treatment can improve the wrinkle recovery angle of ramie fabric even without cross-linking treatment. It is possible to cut down the use of cross-linking agent to obtain similar or better end-use and easy-care property.

Although a number of investigation have been made on the liquid NH_3 treatment of cotton and polyester fabrics, the researches of liquid NH_3 treatment of ramie fabric were less reported yet [26, 27].

2.2.4 Cellulase treatment

Using cellulase treatment to improve the fabric handle and surface properties of cotton-based fabric has been investigated for many years [1]. The mechanism of enzymatic hydrolysis of cellulosic materials is complicated and not yet fully understood.

Ramie fabric suffers from a harsh handle and itchiness when used in garments worn next to the skin due to its high crystallinity and high lignin content. Hence, it is much more interesting to use cellulase to treat the ramie fabric so as to improve the wearability of the ramie goods. It has higher crystallinity and the pitch of the spiral structure is less than that in cotton. Significant differences in their pore structure and crystallite sizes have also been found. There are some differences when they are subjected to the same cellulase hydrolysis. Buschle-Diller, G, *et al.* studied the enzymatic hydrolysis of cotton, linen, ramie and viscose rayon fabrics [39]. It was found that enzymatic hydrolysis employed to decrease stiffness, ease stretch-ability, and generally loosen the structure of fabrics was applicable to all cellulosic fabrics. Since the crystallinity of samples does not change after the enzymatic hydrolysis, nor does accessibility to moisture, this suggests that the ratio of crystalline to less ordered regions does not change upon enzymatic degradation.

Ishikawa, A. reported that the tensile strength of ramie fiber decreased drastically by a cellulase treatment causing a small weight loss of the fiber [40]. Scanning electron microscopic observations showed no significant morphological changes. However, confocal laser scanning microscopy of the enzyme-treated samples stained with cellobiose dehydrogenase showed the formation of characteristic node-like structures at every 30-50 μ m along the fiber axis. Fracture planes of the enzyme treated ramie fiber tended to run vertical to the fiber axis, whereas that of the untreated fiber tended to be more irregular and oblique. Prolonged enzyme treatment would bring about spontaneous disintegration of the fiber into short fragments with vertically cut ends. These observations suggested that enzymatic attacks on ramie fiber would result in the formation of node-like defects with a periodicity of 30-50 μ m along the fiber, which in

turn caused significant deterioration in tensile strength.

2.3 Natural dyeing

With the appearance of synthetic dyes the use of natural dyes for textile dyeing almost disappeared. The wide range of colors available with good fastness properties at moderate costs was the main reason for the replacement of natural dyes by their synthetic counterparts. Nowadays, the application of natural dyes in textile dyeing is increasing required because of the increasing attention on environmental protection and consideration on mankind health [41-43]. Besides ecofriendliness, natural dyes have many more technical advantages, including their uncommon and soothing shades. A good number of investigations have been carried out to elucidate the fundamental aspects of natural dyes as well as to enhance their fastness properties, especially washing and light fastness, and so on [41-64]. However, little attention has been given to the environmental pollution cause by mordants used in natural dyeing. Dyeing fabrics with natural dyes often leads to problems such as lower color fastness to washing or light of the dyed textiles [44, 55, 58]. Most attempts for overcoming these problems involved the use of metallic salts (e.g., aluminum potassium sulfate, potassium dichromate, stannous chloride, ferrous sulfate and copper sulfate) as mordants [42, 49, 51, 56, 57, 64, 65]. The metal ions can act as electron donor to form coordination bonds with the dye molecules. The wastewater containing heavy metal ions from these mordants have significant impact on the environment and public health [66]. The content of heavy-metal ions in textile is limited. Therefore, nowadays selecting new mordant to replace traditional heavy metal ions has been an important part in the development of natural dyeing of textiles.

2.4 Wrinkle-resistance treatment of cellulose fabric

Cellulosic fabrics such as cotton, rayon, flax and ramie have a tendency to wrinkle badly and have poor smooth drying properties after home laundering. Under distortion and moist conditions, the hydrogen bonds that hold the cellulose

chains together are ruptured, and then the chains slide to minimise the stress within the fibers. This phenomenon causes the hydrogen bonds to reform in a new position after the removal of the distorting force. The rupture and reformation of hydrogen bonds cause wrinkle problems on cellulosic fabrics [67-69]. To improve the performance properties, cotton or cotton-blend fabrics are often given a chemical treatment called wrinkle- resistant finishing [67-70]. This treatment involves the use of cross-linking agents which can covalently cross-link with the adjacent cellulose chains within cotton fibers. This treatment involves the use of cross-linking agents which can covalently cross-link with the adjacent cellulose chains within cotton fibbers. The new cross-linking bonds formed in the wrinkle-resistant finishing process are stronger than the former hydrogen bonds. The new cross-links pull the cellulose chains back into position after the removal of a distorting force when the fabric is under distortion and moist conditions, so that the fabric can resist wrinkling. On the other hand, if one of the long-chain molecules is pulled to one side by creasing forces prior to the condensation of small molecules and displaced, these same spring-like forces will tend to return the cellulose molecule to its displaced position. In other words, the fabric has been given a permanent crease.

Cross-linking agents in common use are generally water soluble, di- or multi-functional agents capable of reaction with cellulose under relatively mild, acidic conditions. The cross-linking agents adopted by textile industries recently are mainly made of formaldehyde adducts of ureas, melamine or carbamates, in which 1,3-dimethylol-4,5-dihydroxyethelyeneurea (DMDHEU) and modified DMDHEU with lower formaldehyde levels are the dominant Cross-linking agents. The cross-linking reaction of DMDHEU with cellulose molecules is shown in Scheme 2.1.

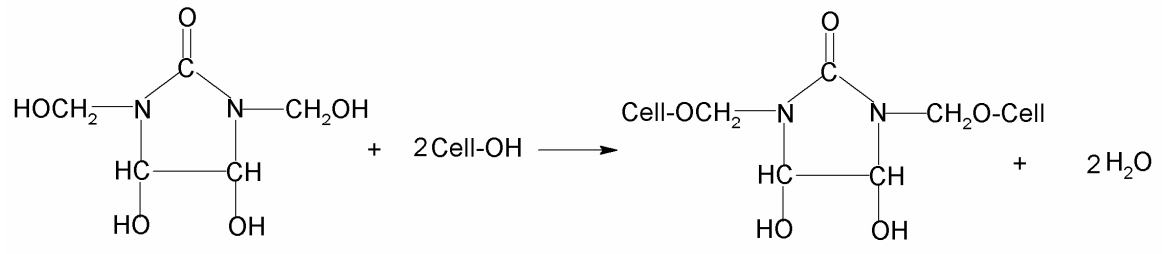

Scheme 2.1 Cross-linking reaction between DMDHEU and cellulose.

The formaldehyde reactants are the most commonly used cross-linking agents for wrinkle resistance due to their efficient and inexpensive features. But they have two serious disadvantages [67-76]. Firstly, they release formaldehyde vapors during finishing process, storage and consumer use. Secondly, formaldehyde treated fabrics suffer a major loss of such mechanical properties as tensile strength, tearing strength and abrasion resistance due to two key contributing factors. One factor is the fiber degradation caused by the acid catalysts at elevated temperatures. The other is the restriction of stress distribution within the fibers due to the cross-linked sites.

Largely due to the concern of formaldehyde hazards to workers in the textile industry and also to consumers, formaldehyde-free cross-linking agents for producing wrinkle-resistant properties are of interest to replace DMDHEU, the conventional finishing agent for wrinkle-resistant finishes. The low cost, ready availability, high functionality and high solubility in water of glyoxal make it of considerable interest as a formaldehyde-free cellulose cross-linking agent. When glyoxal is heated with cotton in the presence of an acid catalyst such as boric acid or ammonium chloride, the resultant product contains monoacetals and diacetals of glyoxal with cellulose. The reaction of glyoxal with cellulose is presented in Scheme 2.2.

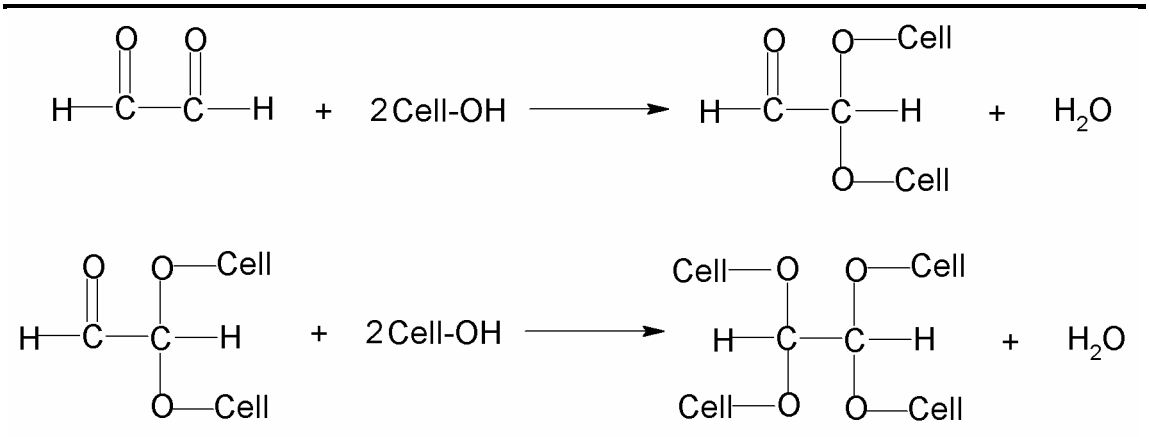

Scheme 2.2 Cross-linking reaction between glyoxal and cellulose.

Polycarboxylic acids (PCA), which are non-formaldehyde reactants, are the possible replacements for the conventional finishing reactant. The main advantages of PCA are that they are formaldehyde-free, do not have a bad odor, and produce a very soft fabric handle. Scheme 2.3 illustrates, a polycarboxylic acid esterifies cellulose through the formation of a five-membered cyclic anhydride intermediate by the dehydration of two carboxyl groups. Fabric treatment with a solution containing 1,2,3,4-butanetetracarboxylic acid (BTCA) and sodium hypophosphite has shown good results in wrinkle recovery angle and DP rate. However, the tensile strength and tearing strength of the finished fabrics are almost 50 percentages lower than those of the untreated fabrics.

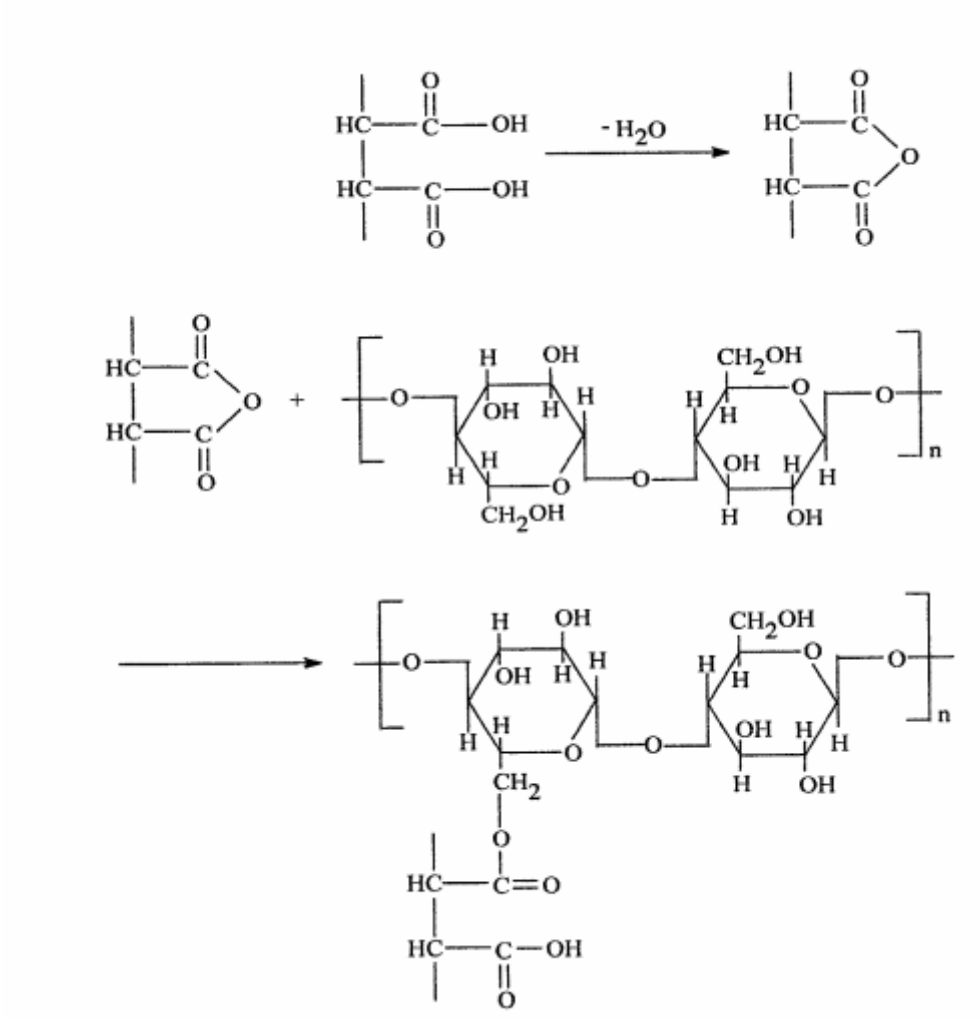

Scheme 2.3 Cross-linking reaction between glyoxal and cellulose.

Using cross-linking treatment to improve the wrinkle resistance of the ramie fabric has been researched for several years. The cross-linking agents used are nearly all the conventional wrinkle-resistant agents usually applied in cotton industry such as DMDHEU and modified DMDHEU. The results showed that the wrinkle recovery angle had been improved to a satisfactory degree, while the tensile and tearing strengths of the treated fabric were much reduced. Another problem is caused by the high degree of crystalline orientation of the ramie fiber, which prevented the cross-linking agents from evenly and deeply diffusing into the fiber, leading to localisation of cross-linking. To diminish the mechanical strength loss of the cross-linked fabrics and to get an optimum balance between the wrinkle recovery and mechanical properties, the most important task is to seek an optimum finishing condition such as recipe formulation,

curing temperature and curing time. Some additives are also recommended and there is a large quantity of works in this field. More recently, the liquid NH_3 treatment before cross-lining was successfully used in the wrinkle resistant finishing of cotton [24, 29, 30, 34, 36, 37]. But few investigations on ramie fabric have been reported [26].

2.5 Application of $scCO_2$ in textile

Gases and liquids could become supercritical fluids (SCFs) when they are compressed and heated above their critical pressure and temperature. In this state it can show properties intermediate between those of typical gas and liquid [77-81]. The phase diagram of carbon dioxide is shown in Figure 2.1 in which the critical point is indicated. The temperature and pressure corresponding to the critical point refer to the critical temperature (T_c) and the critical pressure (P_c), respectively, above which the substance will behave as a SCF. The critical point for carbon dioxide occurs at a pressure of 73.8 bar and a temperature of 31.1^oC. Although a number of substances can be used as SCFs, carbon dioxide has been studied widely. Carbon dioxide is appealing for use as a SCF because it is inexpensive, non-toxic, non-flammable, environmentally friendly, recoverable and chemically inert under many conditions [77-82] .

SCFs exhibit gas-like viscosities and diffusivities and liquid like densities. Compared with liquids, density and viscosity of SCFs are less and diffusion is greater. Hence supercritical fluids are widely used in chemical extraction, polymerization of polymers, chromatography and impregnation of desired additives into the matrices [83-85]. The technology is now employed in many fields of chemical processing (pharmaceuticals, chemicals, foodstuffs, plastics, coatings, papermaking, rubber, cosmetics, paint and pigments) [82]. Since the mid-1980s, applications of supercritical fluids have received significant attention in polymer processing and polymer synthesis. Supercritical fluid polymer impregnation is one of the prospective applications of polymer processing. As an application of polymer impregnation in supercritical fluids, supercritical fluid dyeing has been investigated since the early 1990s.

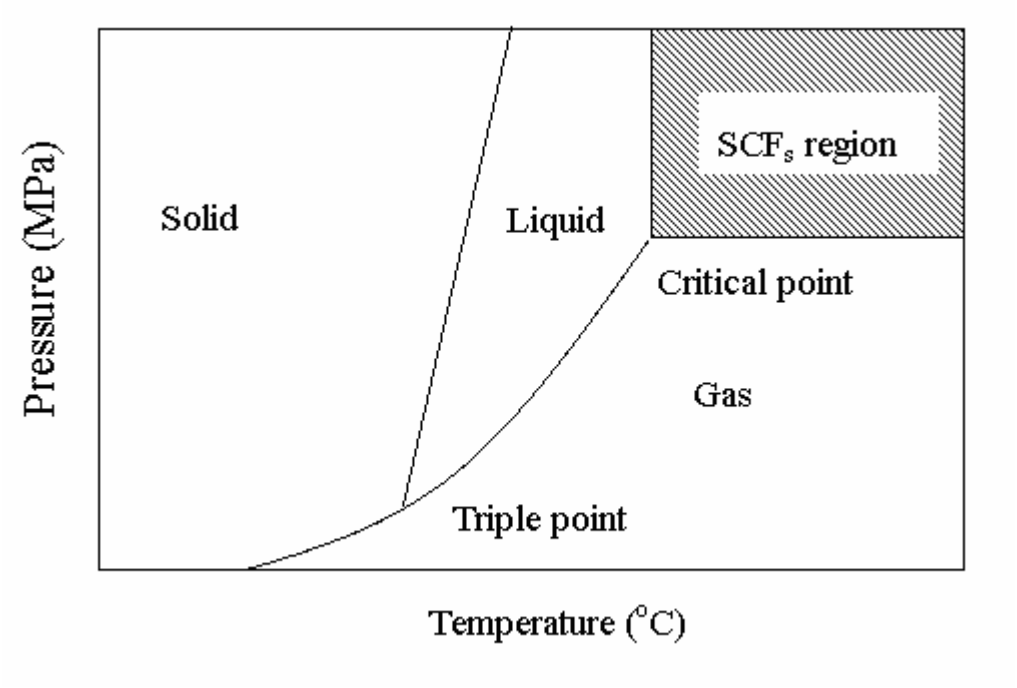

Figure 2.1 Phase diagram of carbon dioxide

The use of SCFs as solvents in the dyeing process has attracted considerable attention in recent years [77-81, 83-102]. In current industrial textile dyeing processes, large amounts of wastewater are produced. This is an environmental burden and, due to the ever more stringent regulations on water pollution, also an economical problem. The use of $scCO_2$ as dyeing medium solves this problem: the CO_2 and the residual dye remaining in the dye bath after the process can easily be separated so both can be recycled. Additional advantages are the high diffusivity and low viscosity of $scCO_2$, which make the dyeing process faster than in water. The low surface tension allows the $scCO_2$ to penetrate small pores easier than water. Furthermore, SFDs process is also energy efficient since it does not involve the washing/drying steps that are normally required in conventional dyeing.

The use of $scCO_2$ as a solvent is an attractive alternative to traditional extraction techniques, offering the potential to avoid or minimize the use of organic solvents. Supercritical CO_2 fluids have been applied in the extraction of wool wax and grease [103, 104]. Studies have focused on the extraction of wool wax from raw wool with

$scCO_2$.

Supercritical technology has also been adopted in the research of surface plating, and several studies have been conducted in this field. Zhao et al employing scCO2 to conduct electroless copper plated on aramid fibers [105]. Gittard et al developed silver deposited cotton fabrics via scCO2 process [106]. Employing the high diffusion of $scCO_2$, Ma et al impregnated nonwoven fibrous polyethylene material with a nonionic surfactant [107].

Although a lot of studied were conducted on the applications of $scCO_2$ for textile, few investigations on the application of $scCO_2$ for the dyeing and finishing of ramie were presented at present.

2.6 Nanotechnology for textile finishing

Nanotechnology creates structures that have excellent properties by controlling atoms and molecules, functional materials, devices and systems on the nanometer scale by involving precise placement of individual atoms of the size around 0.1-100 nm. The unique and new properties of nanomaterials have attracted scientists and researchers of the textile industry also and hence the research interest for the use of nanotechnology in the textile industry has increased rapidly. Coating the surface of fabrics with nanoparticles is an approach to impart their UV blocking, antibacterial, flame retardant, water repellant and self-cleaning properties to textiles and clothing [108, 109]. A good number of studies have been made on the application of nanoparticles to textile materials in order to develop fabrics with UV protective, self-cleaning, antibacterial, flame retardant, water repellant properties [110-122]. In the following section, the application of the properties of nanoparticles including photocatalytic, antibacterial and UV protective for textiles are briefly depicted.

2.6.1 Photocatalytic self cleaning finishing

The mechanism of photocatalytic oxidation processes has been discussed extensively

in the literature [123-131]. Briefly, when a semiconductor such as TiO_2 absorbs a photon of energy equal to or greater than its band gap width (e.g. $\lambda < 390$ nm), an electron may be promoted from the valence band to the conduction band (e_{cb}^-) leaving behind an electron vacancy or ''hole'' in the valence band (h_{vb}^-). If charge separation is maintained, the electron and hole may migrate to the catalyst surface where they participate in react with absorbed species. Specially, h_{vb}^- may react with surface bound H_2O or OH^- to produce the hydroxyl radical ($OH\cdot$) and e_{cb}^- is picked up by oxygen to generate superoxide radical anion ($O^{\cdot}{}_2^-$), as indicated in Eqs. (2-1)-(2-3).

$$TiO_2 + h\square \longrightarrow e_{cb}^- + h_{vb}^- \quad (2\text{-}1)$$

$$O_2 + e_{cb}^- \longrightarrow O^{\cdot}{}_2^- \quad (2\text{-}2)$$

$$H_2O + h_{vb}^- \longrightarrow {}^{\cdot}OH^- + H^+ \quad (2\text{-}3)$$

It has been suggested that the hydroxyl radicals (${}^{\cdot}OH^-$) and superoxide radical anions ($O^{\cdot}{}_2^-$) are the primary oxidizing species in the photocatalytic oxidation processes. Since both are unstable chemical substances, when the organic compound falls on the surface of the photocatalyst it will combine with $O^{\cdot}{}_2^-$ and ${}^{\cdot}OH^-$ respectively, and turn into carbon dioxide (CO_2) and water (H_2O). They oxidate and degrade noxious organic substances such as formaldehyde and methylamine, pollutant stench and bacteria and so on to innoxious substances such as CO_2 and H_2O.

As a popular photocatalyst, nano TiO_2 has been widely used because of its various merits, such as optical and electronic properties, low cost, high photocatalytic activity, chemical stability and nontoxicity [113, 120, 121, 130-135]. Nano TiO_2 usually exists in nature with three crystal types such as anatase, rutile and brookite, especially anatase and rutile [130, 135]. As for TiO_2 as photocatalyst, photocatalysis activity of anatase is bigger than one of rutile. The cause is that more defects and dislocation exist in crystal lattice of anatase. Accordingly, anatase can produce more oxygenic empty location to capture electron, however, rutile is the most steady structure in three crystal types, so rutile has good crystallization and small defects. Cavity and electron produced is easy to complex, therefore, photocatalysis activity of rutile is affected. In addition, specific area of ratile is small and ability of adsorption oxygen is low, furthermore, simple complex

that is produced by cavity and electron is too fast. Consequently, the efficiency of photocatalysis is low. The literature shows that photocatalysis activity of single anatase is low. Mixed crystal system that a small quantity of ratile is mixed into anatase has higher photocatalysis activity [130, 135].

The photocatalytic property of nano TiO_2 has been employed in the development of self cleaning textiles via nano finishing. Bozzi et al employed nano TiO_2 to modify polyester and wool-polyamide textiles [113]. It was found that the red wine stained on the modified fabrics was degraded after exposure in sunset for 24 h. Yuranova et al finished cotton fabric with TiO_2–SiO_2 nanoparticles and proved that the wine stained on the coated fabrics disappeared after subjected to irradiation by solar light [112]. In addition, the fabrics loaded with TiO_2 nanoparticles were proved to decomposed harmful gaseous substances such as ammonia and formaldehyde in air through photocatalytic decomposition reaction [136, 137]. Most of the studies on the photocatalytic finishing fabrics were conducted on cotton or polyester. The application of photocatalytic finishing by nanoparticles on ramie fabric has less bee reported.

2.6.2 Antibacterial finishing

Neither natural nor synthetic textile fibers are resistant to bacterial or pathogenic fungi. The nanoparticles of silver (Ag), TiO_2 and zinc oxide (ZnO) exhibit high antibacterial activity [108-110, 114]. Nano-silver particles have an extremely large relative surface area, thus increasing their contact with bacteria or fungi, and vastly improving their bactericidal and fungicidal effectiveness. Nano-silver is very reactive with proteins. When contacting bacteria and fungus, it will adversely affect cellular metabolism and inhibit cell growth. It also suppresses respiration, the basal metabolism of the electron transfer system, and the transport of the substrate into the microbial cell membrane. Furthermore, it inhibits the multiplication and growth of those bacteria and fungi which cause infection, odour, itchiness and sores. Hence, nano-silver particles are widely applied to socks in order to prohibit the growth of bacteria. In addition, nano-silver can be applied to a range of other healthcare products such as dressings for

burns, scald, skin donor and recipient sites [108, 109].

Because of photocatalytic feature, nano TiO_2 are proved to show antibacterial property. Several papers have reported the use of the photocatalytic property of TiO_2 for developing antibacterial textiles [114, 132]. On the other hand, zinc oxide is also a photocatalyst, and the photocatalysis mechanism is similar to that of titanium dioxide; only the band gap is different from nano TiO_2. Nano ZnO provides effective photocatalytic properties once it is illuminated by light, and so it was employed to impart antibacterial properties to textiles [138].

2.6.3 UV protective finishing

Previously organic UV absorbers were coated on the textile material they prevent UV radiation effectively but they are less durable. Inorganic UV blockers are usually certain semiconductor oxides such as TiO_2, ZnO, SiO_2 and Al_2O_3. Among these semiconductor oxides, TiO_2 and ZnO are commonly used. It was determined that nano-sized TiO_2 and ZnO were more efficient at absorbing and scattering UV radiation than the conventional size, and were thus better able to block UV [139, 140]. This is due to the fact that nano-particles have a larger surface area per unit mass and volume than the conventional materials, leading to the increase of the effectiveness of blocking UV radiation. For small particles, light scattering predominates at approximately one-tenth of the wavelength of the scattered light. Rayleigh's scattering theory stated that the scattering was strongly dependent upon the wavelength, where the scattering was inversely proportional to the wavelength to the fourth power. This theory predicts that in order to scatter UV radiation between 200 and 400 nm, the optimum particle size will be between 20 and 40 nm

UV-blocking treatment with nanoparticles for fabrics have been extensively reported [108-110, 117, 122, 132, 139, 141]. Mihailovic et al finished polyester fabrics with nano TiO_2 colloid suspension. The treated fabrics showed that the excellent UV blocking. Paul et al used nano ZnO to finish cotton fabrics and yarn via a sol-gel process [122]. The fabrics loaded with nano ZnO demonstrated an excellent UV protective factor (UPF)

rating. Although many studies have verified that nano finishing can brought excellent UV protective properties on cotton and polyester fabrics, the successful application on ramie fabric has less been reported.

2.7 Summary

Ramie fibers have their unique molecular and morphological structure. Although all the cellulosic fibers are of identical chemical composition, there some major differences in the supramolecular structure and morphology of these fibers which will largely determine the course of modification. The high crystallinity and orientation of ramie fiber leads to some undesirable properties of ramie fabric such as low elasticity, poor wrinkle recovery and harsh handle. The advanced finishing techniques such as liquid NH_3 treatment, $scCO_2$ fluid processing and nano finishing have been successfully employed in the modification of cotton fabric. Since ramie fabric is not as extensively applied as cotton, few investigations have been made on natural dying and finishing ramie fabrics using the new technologies.

CHAPTER 3
NATURAL DYEING OF RAMIE FABRIC WITH RARE EARTH AS THE MORDANT IN THE

3.1 Introduction

Nowadays, the colorants used in commercial textile dyeing are almost exclusively synthetic. However, the synthetic dyes not only are harmful to the mankind health and but also result in a great deal of environmental pollution [41, 43, 47, 52, 54, 142]. As a result, natural dyeing in textiles is now attracting more and more attention from both academia and industry due to its environmentally friendly attributes [41-44, 46-48, 50-52, 54, 56, 59, 61, 62]. Natural dyes can exhibit better biodegradability and generally have a higher compatibility with the environment [47, 60, 142-144].

Dyeing fabrics with natural dyes often leads to problems such as lower color fastness to washing or light of the dyed textiles [44, 55, 58]. Most attempts for overcoming these problems involved the use of metallic salts (e.g., aluminum potassium sulfate, potassium dichromate, stannous chloride, ferrous sulfate and copper sulfate) as mordants [42, 49, 51, 56, 57, 64, 65]. The metal ions can act as electron donor to form coordination bonds with the dye molecules. The wastewater containing heavy metal ions from these mordants have significant impact on the environment and public health [66]. The content of heavy-metal ions in textile is limited. Therefore, nowadays selecting new mordant to replace traditional heavy-metal ions has been an important part in the development of natural dyeing of textiles.

Rare earth is ecofriendly and compatible with the environment. In general, the coordination number of rare earth can be as large as 8, 9 and even 12 [63, 145]. Additionally, the rare earth elements have large atom radius, which enable a good

number of ligands surrounding them [63, 145]. Hence the rare earth ions exhibit high capability for forming coordination compounds with natural dye molecules. As the central ions, the rare earth ions can form coordination bonds with the amino, hydroxyl or carboxyl groups, i.e., the ligands, of the natural dye molecules. When forming coordination compounds with natural dye molecules, the rare earth ions tend to exhibit electrolyte-like effect and thus quickly lower the Zeta electric potential on the surface of fibers. Therefore they are easily absorbed on the surface of fiber by static electric force. Using rare earth products as mordants can promote the formation of coordination compounds of natural dyes, rare earth and fibers and thus enhance the color fastness of the fabrics dyed with natural extracts.

This work is aimed to study the application of rare earth products as mordant for natural dyeing. The lanthanum-rich rare earth chloride was used as the mordant in the natural dyeing of ramie fabrics. The dyeing conditions including mordanting method, dyeing temperature and time, pH value of dyeing bath and concentration of mordant on the dyeing effect were investigated systematically. The color shade stability of the dyed ramie fabrics with rare earth as mordant was examined in the solutions having different pH values. The effects of using rare earth as mordant on the color fastness to washing, rubbing and light of the ramie fabrics dyed with natural dyes were studied. As compared with conventional metallic mordant Ferrous Sulfate ($FeSO_4$) and Potassium dichromate ($K_2Cr_2O_7$),

3.2 Experimental

Materials

Ramie plain fabrics (21×21s) were used in this study. The fabrics were treated with a solution containing 5g/l non-ionic detergent (Hostapal CV, Clariant) at 50^{o}C for 30 minutes prior to using. Then the fabrics were thoroughly washed with water and air dried at room temperature for usage. Caesalpinia sappan, Rhizoma coptidis, Garednia and Areca catechu were provided by the Chongqing 3533 Printing Dyeing and Clothing Co. Ltd. The lanthanum-rich rare earth chloride ($RECl_3 \cdot 6H_2O$) (REO≥50%,

La_2O_3/REO=43%, CeO_2/REO=40%, Pr_6O_{11}/REO =5.0%, Nd_2O_3/REO=18%, Sm_2O_3/REO=1.5%, Eu_2O_3/REO=0.2%, Tb_4O_7/REO=0.05%, Non-RE Impurities/REO=2.69%) and Neodymium Chloride ($NdCl_3 \cdot 6H_2O$) (REO≥50%, Nd_2O_3/REO≥99%, Non-RE Impurities/REO≤1%) were purchased from the Inner Mongolia Baotou Steel Rare-earth (Group) Hi-Tech Co., Ltd. Ferrous Sulfate ($FeSO_4 \cdot 7H_2O$)(Analytical Reagent grade, Chengdu Best Reagent Co., Ltd.) and Potassium dichromate ($K_2Cr_2O_7$) (Analytical Reagent grade, Chengdu Best Reagent Co., Ltd.) were used as received. Sodium hydroxide, acetic acid and lemon acid of chemical pure grade were purchased as from Sinopharm Chemical Reagent Co., Ltd.

Extraction of natural dyes

At first, 150g of a selected plant was precisely weighed with the analytical balance (TE1502S, Sartorius Co., Germany). After being mashed it was put into a big beaker containing 800ml of water and kept for 24 hours. Afterwards, the mixture was heated to boiling state where it was maintained till up to only 100 ml liquid being left via evaporation. Then the dissolving and evaporating processes were repeated twice. After filtration, the collected colorant liquid was distilled and condensed to 50ml. The concentrated solution containing the plant extracts was the crude natural dye liquid. The ultraviolet-visible (UV-vis) spectra of the aqueous solutions containing the natural dyes were obtained from U-3310 UV-vis spectrophotometer. As indicated in Table 3.1, the maximum absorption wave length values of the solutions containing natural dyes range from 410 nm to 460 nm, which are dependent on the different component compositions of the natural dyes. According to the maximum absorption wave length values, it is judged that the major colorant ingredients of the different natural extracts are brazilin of caesalpinia sappan, berberine of rhizoma coptidis, crocin and crocetin of gardenia, and catechin of areca catechu. Figure 3.1 shows the chemical structure of the major colorant ingredients of the different natural extracts.

Table 3.1 The maximum absorption wave lengths of the solutions containing natural dyes

	Caesalpinia sappan	Rhizoma coptidis	Gardenia	Areca catechu
Maximum absorption wave length (nm)	412	452	458	458

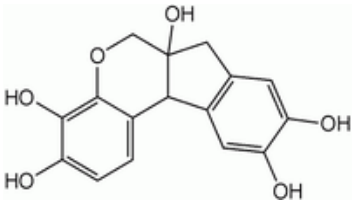

Brazilin

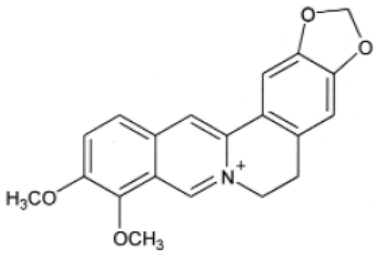

Berberine

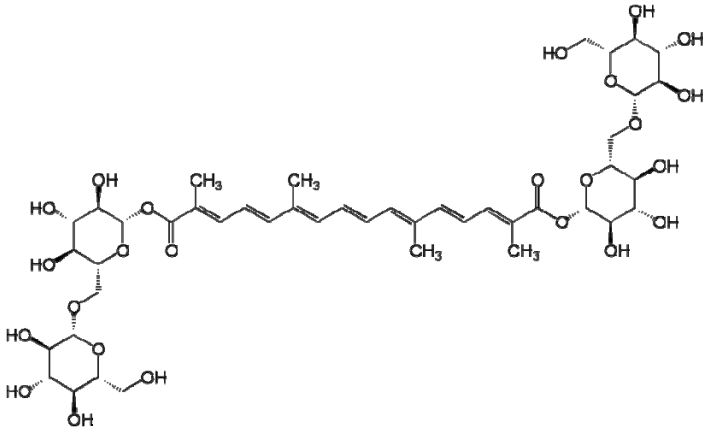

Crocin

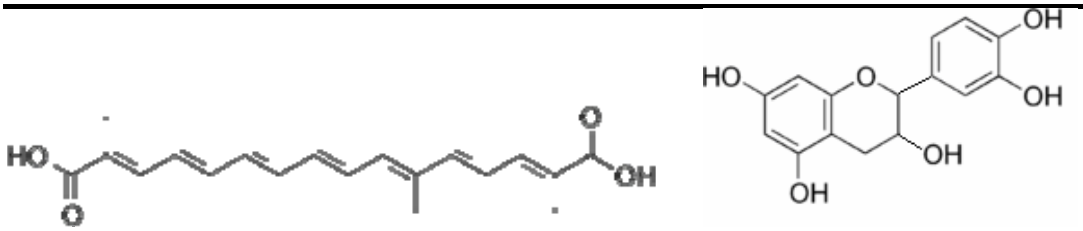

Crocetin Catechin

Figure 3.1 Chemical structure of the colorant ingredients of different natural extracts

Dyeing

In the dyeing process, a concentrated plant extract liquid was diluted by 10 times and the resultant solution was used as dyeing bath. The aqueous extracts were used as a direct dye or with the addition of a mordant. The direct dyeing was carried out by shaking the ramie fabrics with a natural dye solution in a conical flask at 90^{o}C in a thermostat shaker bath operated at 100 strokes/min. A material to liquid ratio of 1:25 was used in the dyeing experiment. The ramie fabric was then rapidly withdrawn after particular immersion times. After dyeing, the ramie fabric was rinsed with deionized water to remove the unfixed dye and then air dried. The dyeing effect of simultaneous mordanting, pre-mordanting and post-mordanting were compared. Figure 3.2 demonstrates the three mordanting methods at the dyeing temperature of 90^{o}C.

In the simultaneous mordanting process, the fabrics were immersed in a dyeing bath containing mordant, lemon acid and natural dye at 30^{o}C. They the dyeing bath was heated to 90^{o}C where it was maintained for a particular time (20-80 minutes). The fabrics were then rinsed with clean water at ambient temperature followed by being squeezed and dried. In the pre-mordanting method, the wet fabrics were first immersed in a solution of the mordant and heated up to 70^{o}C where they were kept for 30 minutes. After being added with the natural dyes the bath was heated up to 90^{o}C where the fabrics were treated for a particular time (20-80 minutes). Then the dyed samples were rinsed with clean water and dried via the similar processes mentioned above. In the post-mordanting method, the ramie fabrics were first dyed in the aqueous solution containing a natural dye at 90^{o}C for 30 minutes followed by being cooled down to 70^{o}C

where the mordant was added. Then the fabrics were kept at 70°C for another 30 minutes. Subsequently, the dyeing bath was heated

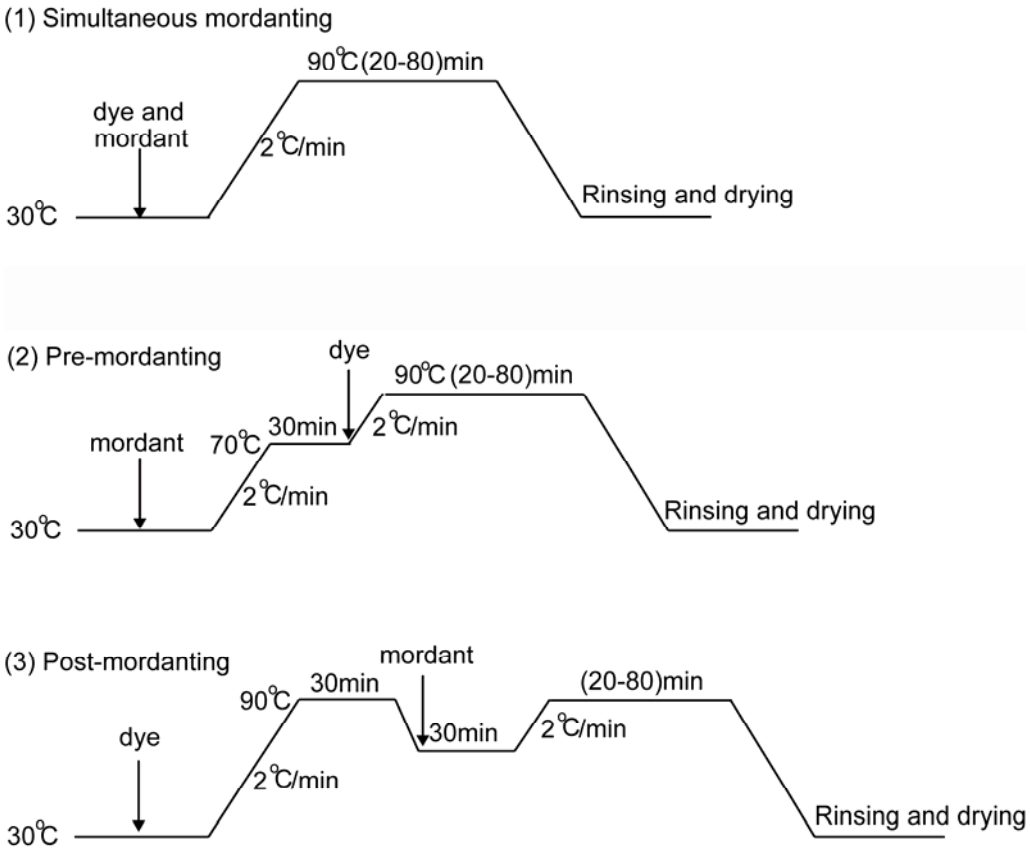

Figure 3.2 Different mordanting methods in the natural dyeing

up to 90°C again where the fabrics were dyed for a time in the range of 20-80 min. At last, the fabrics were rinsed and dried. The effects of dyeing temperature and time on the dyeing effect of ramie fabrics with the natural dyes were studied.

Measurements

The dye uptake in the dyeing of ramie fabrics was obtained through the measurement of the light absorbances at the wavelength of maximum absorption, of the dye bath before and after dyeing with a U-3310 ultraviolet-visible (UV-vis) spectrophotometer. The dye uptake was calculated with the following equation:

$$\text{Dye uptake} = \frac{A_0 - A_t}{A_0} \times 100\% \quad (1\text{-}1)$$

where A_0 and A_t refer to the absorbances of the dye solutions at the beginning and the end of dyeing, respectively.

The CIELAB colorimetric values including ΔE, L*, a*, b*, C*, and the color strength K/S of the dyed fabrics were measured by Datacolor SF600 Computer Color Matching System (Data Color International) using illuminant D_{65} and 10^o standard observer. *K*/*S* was calculated from the reflectance values using the Kubelka-Munk equation as follows:

$$K/S = \frac{(1-R)^2}{2R} \quad (1\text{-}2)$$

Where R represents the reflectance of the dyed fabric and K/S stands for the ratio of the absorption coefficient (K) to scattering coefficient (S). The higher K/S value the greater the color strength.

The color fastness to washing of the ramie fabrics was determined according to the standard ISO 105-C03. The measurement was carried out with both sample and standard ramie fabrics that were sewn together and tested under the same conditions. The sewn fabric was washed at 42^oC for 30 minutes in a standard soap solution with a material to liquid ratio of 1:50. Both fabrics were then separated and rinsed and dried. The color fastness to washing levels, observed against a grey scale, were classified as numbers ranging from 1 and 5, which corresponds to poor to excellent fastness, respectively. Color fastness to dry and wet rubbing of the dyed fabrics was tested according to ISO 105-X12 method. Color fastness to light was tested according to ISO 105-BO2 method. To examine the influence of pH change on the color shade, the fabrics dyed in presence of rare earth as mordant were immersed in the water bathes with different pH from 3, 7 to 11 at ambient temperature for 30 minutes. Then the wet fabrics were rinsed and dried for further measurement.

3.3 Results and Discussion

3.3.1 Influences of mordanting method

The effect of different mordant dyeing methods is shown in Table 3.2. It was observed that the post-mordanting gave rise to the highest color strength and dye uptake in comparison with simultaneous mordanting and pre-mordanting. In simultaneous mordanting, the colorant molecules and rare earth ions could form insoluble coordination compounds and thus precipitated from dyeing bath, resulting in the decrease of effective dye uptake and K/S value, i.e. color strength. In the case of pre-mordanting, the mordant ions absorbed on the fibers could desorb from the fibers and form insoluble coordination compounds with natural dye molecules. Likewise the pre-mordanting resulted in lower color strength. Therefore, the post-mordanting technique was employed in this study.

3.3.2 Influences of temperature and time on dye uptake

Figure 3.3 presents the influence of dyeing temperature and time on dye uptake. When the dyeing temperature was 40^{o}C, the dye uptakes of the four kinds of natural dyes increased almost monotonically as the dyeing time rose from 10 to 80 minutes. When the dyeing temperature was 70^{o}C the dye uptakes of the natural dyes increased rapidly at the beginning. With the extension of dyeing time the increasing tendency of dye uptake decreased gradually. The dye uptakes of the nature dyes were apparently enhanced as the dyeing temperature increased from 70^{o}C to 90 ^{o}C. The increase of dye uptake arises from both the increasing solubility of natural dyes and the expansion of ramie fibers with the increasing temperature. In contrast, the dye uptake of the nature colorants was slightly decreased when the dyeing temperature increased from 90^{o}C to 105^{o}C. This is caused by the different temperature dependence of absorption and diffusion of dye molecules. Dyeing takes place in three steps: absorption on the surface of fibers, diffusion to the interior of fibers and desorption from fibers into the dyeing bath [52]. On the one hand, a lower dyeing temperature is favorable to absorption of the

Table 3.2 Influence of different mordanting methods

Mordanting method	Caesalpinia sappan		Rhizoma coptidis		Gardenia		Areca catechu	
	K/S	Dye uptake	K/S	Dye uptake	K/S	Dye uptake	K/S	Dye uptake
Simultaneous mordanting	5.25	47.8	6.01	54.6	3.88	39.8	4.98	42.3
Pre-mordanting	5.86	52.2	6.58	60.1	4.23	43.5	5.45	49.8
Post-mordanting	6.12	58.0	7.29	64.1	5.07	48.4	5.96	54.6

dye molecules on fibers, but makes their diffusion inside fibers difficult. On the other hand, a high temperature leads to expansion of fibers and easy diffusion of natural dyes in fibers accordingly. However a high temperature can also intensify molecular movement resulting in desorption of more dye molecules from fibers. In a word, either excessively low or excessively high temperatures cannot give a desirable dyeing effect. The results show that 90^{o}C is a suitable temperature for dyeing ramie fabrics with the four kinds of natural dyes. As indicated by figure 3, the dye uptake rose gradually with the increase of dyeing time for all the four kinds of natural dyes. When the dyeing time increased to a certain time the dye uptake of a natural dye tent to a constant value, indicating the dye uptake equilibrium was attained [52]. It takes 70, 60, 70 and 50 minutes for the extracts of caesalpinia sappan, rhizoma coptidis, gardenia and areca catechu, respectively, to attain the dye uptake equilibrium, which relies on the molecular size and polarity of the four kinds of natural dyes.

3.3.3 Influence of pH value on dye-uptake

Figure 3.4 shows the influence of pH of dyeing bath on the dye uptake in the dyeing with the natural extracts. The figure indicates that the pH change could significantly influence the dye uptake in the dyeing with caesalpinia sappan and areca catechu. When pH value was about 2 the dye uptake of the two kinds of colorants were pretty low. With

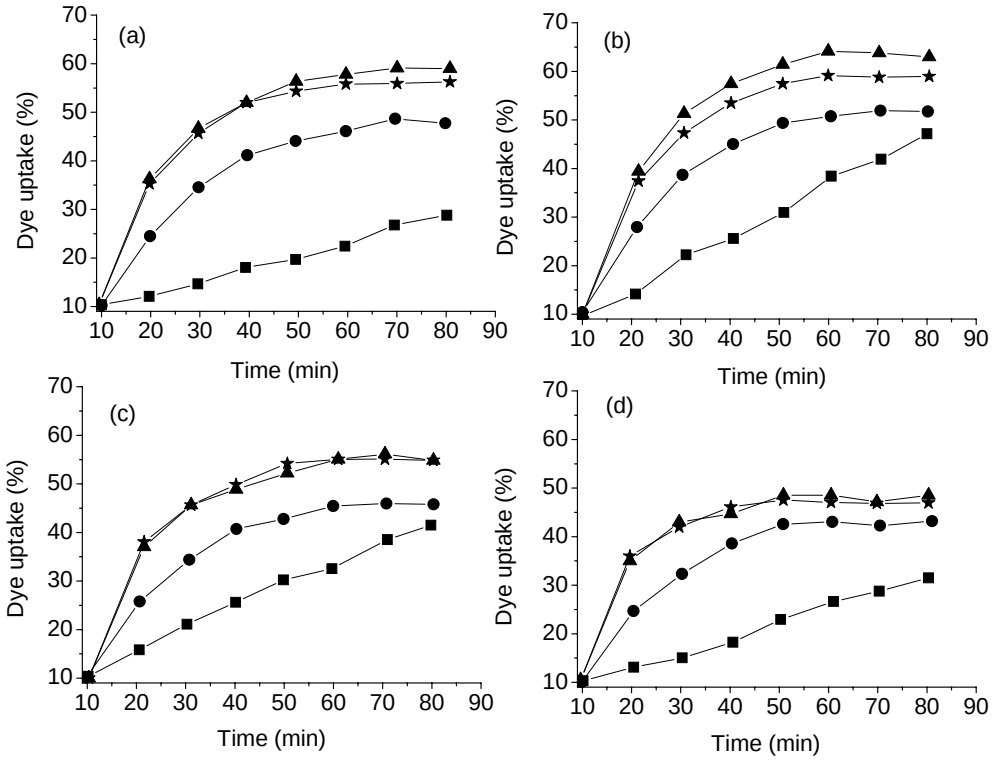

Figure 3.3 Influence of dyeing temperature and time on dye uptake: (a) Caesalpinia sappan L; (b) Rhizoma coptidis; (c) Gardenia; (d) Areca catechu. In each plot the symbols refer to different dyeing temperatures. (■) 40^{o}C; (●) 70^{o}C; (▲) 90 ^{o}C; (★) 105^{o}C.

the increase of pH, the dye uptakes of them rose gradually. When pH value increased the maximum dye uptakes of the extracts of caesalpinia sappan and areca catechu were attained at pH=7 and pH=8, respectively. Afterwards, the dye uptake of them decreased with the further increase of pH value. The effect of pH on dye uptake can be attributed to the interaction between the natural dyes and the ramie fabric. A certain number of OH and COOH groups exist in the cellulose structure. Brazilin and catechin contain polyphenols in their molecules as illustrated in Figure 3.1. Increase of pH could promote the ionization of phenolic OH groups resulting in the increase of solubility of the natural dyes in dyeing bath. Hence the dye uptakes of the two natural dyes rose with the increase of pH value. At higher pH, the hydroxyl-ion content increased, and

phenolic OH groups in the natural dye molecules and COOH groups in the cellulose fibers were transformed to phenolic oxygen anions and carboxyl anions, respectively. Phenolic oxygen anions had a repulsive interaction with OH groups and carboxyl anions which prevented the natural dye molecules being absorbed onto ramie fibers and thus reduced the dye uptakes of the two natural dyes [52]. As one of the major colorant ingredients of gardenia, crocetin contains COOH groups in its molecules. As indicated by Figure 3.4, with the increase of pH the dye uptake of the natural extract of gardenia increased resulting from the increasing solubility of the natural dyes in dye bath due to the ionization of COOH groups in crocetin. Likewise, the dye uptakes of the natural extract of gardenia decreased when pH was above 7 because of the increasing repulsion between the carboxyl anions on natural dye molecules and the carboxyl anions and OH groups on ramie fibers. In comparison with those of caesalpinia sappan and areca catechu, the extract of gardenia exhibited less dye uptake variation with the change of pH because of the relatively low content of COOH groups in the molecules of its major colorant ingredients. With the increase of pH the dye uptake of the extract rose gradually as shown in Figure 3.4. As the major colorant ingredient of rhizoma coptidis, berberine is a water soluble dye containing cationic quaternary ammonium salt [48], it would interact ionically with the carboxyl groups of cellulous fibers at higher pH via ion exchange reaction. The number of available anionic sites on ramie fibers in alkaline conditions is relatively larger than that in acidic conditions, and thus the dye uptake of berberine was increased with the dye bath pH.

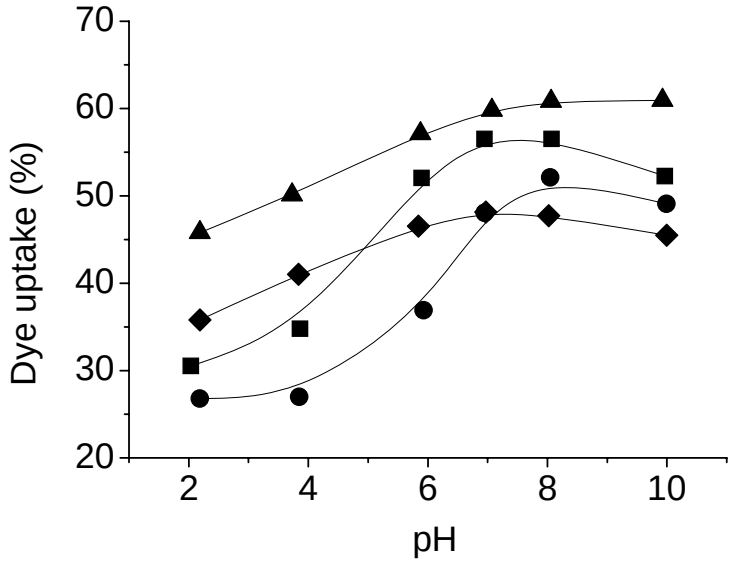

Figure 4. The influence of pH value on dye-uptake. (■) Caesalpinia sappan L.; (▲) Rhizoma coptidis; (◆) Gardenia; (●) Areca catechu.

3.3.4 Influence of the amount of rare earth on dye uptake

The electron configuration of the outer shells of rare earth ions enables them to form complex compounds with the natural dyes and ramie fibers. The influence of mordant amount on the dye uptake is shown in Figure 3.5. It can be seen that the dye uptake increased with the increase of the concentration of rare earth. However when the concentration of rare earth increased to a certain level the dye uptake tent to a constant value because the coordination among natural dye, rare earth and fiber reached to saturation state. The dye uptake of the gardenia extract was the lowest among all the four kinds of natural dyes. This should be due to the low affinity of the crocin and crocetin components in gardenia for ramie fibers. In contrast, the dye uptake of the extract of rhizoma coptidis is the highest, which can be ascribed to the ionic interaction between the cationic dyes and carboxyl anions in ramie fibers. The influence of rare earth concentration on dye uptake of the different natural colorants is determined by their complex formation from rare earth ions and natural dye molecules.

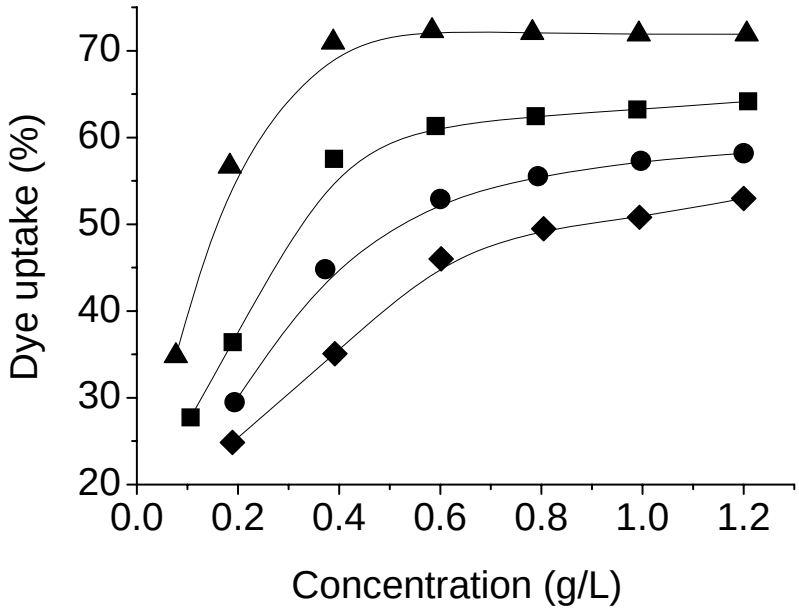

Figure 3.5 The influence of the concentration of rare earth on dye-uptake. (■) Caesalpinia sappan; (▲) Rhizoma coptidis; (◆) Gardenia; (●) Areca catechu.

3.3.5 Influence of pH on color shade of the dyed fabrics

It was found that the fabrics dyed with the natural dyes in presence of rare earth as mordant could resist the pH impact and thus change less color shade in washing. To quantify the influence of pH on color shade, the color measurements were performed on the fabrics dyed with the four kinds of natural dyes. L* represents lightness value in the CIELAB colorimetric system. Higher lightness value means lower dye uptake [45, 48, 64]. a* and b* denote the red/green value and the yellow/blue value, respectively [45, 48, 64]. The positive values of a* and b* represent redder and yellower while negative shows greener and bluer tones. C* stands for chroma or purity of colour [45, 47, 48]. ΔE refers to color difference [45, 47, 48]. As shown in table 3, the colorimetric data including ΔE, L*, a*, b*, and C* of the dyed fabrics did not change much when pH of the bath changed from 3 to 7 and 11. This is ascribed to the formation of stable complexes among rare earth ions, natural dye molecules,

Table 3.3 Influence of pH on the colorimetric data of the dyed fabrics

	ΔE	L*	a*	b*	C*
Caesalpinia sappan (pH=3)	49.89	61.64	3.93	56.98	57.11
Caesalpinia sappan (pH=7)	50.15	60.15	4.26	56.78	56.94
Caesalpinia sappan (pH=11)	51.68	61.38	3.89	55.89	52.03
Rhizoma coptidis (pH=3)	58.98	50.89	5.98	48.61	48.97
Rhizoma coptidis (pH=7)	60.65	50.48	7.03	46.18	46.71
Rhizoma coptidis (pH=11)	59.08	50.90	6.45	49.06	49.48
Gardenia (pH=3)	48.89	82.89	5.58	30.34	30.34
Gardenia (pH=7)	50.15	79.15	5.83	30.86	30.34
Gardenia (pH=11)	54.68	83.68	5.21	32.78	32.78
Areca catechu (pH=3)	38.58	68.08	10.93	41.78	43.19
Areca catechu (pH=7)	40.63	66.65	11.56	40.89	42.49
Areca catechu (pH=11)	39.28	66.98	12.89	40.23	42.24

ramie fibers. The formation of the coordination bonds is irreversible. The resultant coordination compounds are highly stable in acidic, neutral and alkaline baths. In addition, the multiple complexes formed by rare earth ions and natural dyes can interact with each other, which can result in the dissociation of the electron pairs on the both sides of the complex conjugating system. The dissociated electrons can drift among the complexes and thus generate the so called ultrasensitive transition effect which changes the characteristic absorption spectrum. Thus the dyed fabrics can resist the pH fluctuation and maintain stable color shade in either acidic or alkaline bath. This is a significant advantage of for using rare earth as mordant in natural dyeing.

3.3.6 Color fastness of the dyed fabrics

Table 3.4 shows the color fastnesses ratings to washing, rubbing and light of the fabrics dyed with the four kinds of natural dyes in presence and in absence of rare earth

as mordant. In comparison with the fabrics colored via direct dyeing, the fabrics dyed having rare earth as mordant exhibited much better color fastness to washing and rubbing. The ratings of color fastness to washing and rubbing of all the dyed fabrics having rare earth as mordant were found to be grade 4-5. The fastness to washing and fastness to rubbing of the fabrics dyed with the natural extracts depend on the type of mordants, mordanting method and mordant concentrations as well as molecular size and chemical structure of the dye, the dye-fiber or dye-fiber-mordant interaction or bonds [44]. The most important factor for determining the color fastness to washing and rubbing is the dye-fiber-mordant interaction, which relies on the formation of stable coordination bonds among rare earth ions and natural dyes and fibers. The ratings of color fastness to light of the dyed fabrics using rare earth as mordant were in the range 3-4 grade. However, the ratings of fastness to light of the dyed fabrics without mordanting were found to be grade 1-2. The color fastness to light of a natural dye is influenced by: the chemical structure of dye, physicochemical interaction between natural dye and fiber, physical state of the dye inside the fiber, dye concentration, chemical structure and physical characteristics of the fiber itself, types of mordant, mordant concentrations and mordanting method used[44, 56, 57]. Generally, it is well known that the color fastness to light of natural dyes was poor [44, 56, 57]. In this sense, the light fastness of dyed fabrics with rare earth as mordant is considerably good. The formation of stable coordination bonds between rare earth ions and dye molecules and ramie fibers accounts for the improvement of fastness to light of the dyed fabrics.

3.3.7 Comparison of different metallic mordants

As mentioned above, the lanthanum-rich rare earth chloride was proved to greatly improve the color fastness, color strength and dye uptake. Hence it is possible to replace the commonly used heavy metallic salts with the rare earth chloride as the ecofriendly mordant. The authors compared the rare earth mordants with the conventional metallic

Table 3.4 Ratings of color fastness of the ramie fabrics dyed with rare earth as mordant

	Washing		Wet rubbing		Dry rubbing		Light
	Fade	Strain	Fade	Strain	Fade	Strain	
Caesalpinia sappan (mordanted)	5	4	3-4	3-4	4-5	4	3-4
Caesalpinia sappan (direct)	3	2-3	2-3	2	3	3	2
Rhizoma coptidis (mordante)	4	4	3-4	4	4	4	3
Rhizoma coptidis (direct)	3	3	2	2	2-3	3	1-2
Gardenia (mordanted)	4-5	4-5	4	3-4	4	5	3-4
Gardenia (direct)	2	2-3	2	2	3	3	2
Areca catechu (mordanted)	4	4-5	4	3-4	4	4-5	3
Areca catechu (direct)	2	3	3	2	3	3	2

mordants $FeSO_4$ and $K_2Cr_2O_7$. The efficiency of the different mordants was explored by using $RECl_3{\cdot}6H_2O$, $NdCl_3{\cdot}6H_2O$, $FeSO_4{\cdot}7H_2O$ and $K_2Cr_2O_7$, respectively, as mordants in the natural dyeing of ramie fabrics with Caesalpinia Sappan colorant. Figure 3.6 shows the influence of mordant concentration on dye uptake and K/S values in presence of the different mordants. As expected, with the increase of mordant concentration the dye uptake and color strength increased dramatically at lower concentrations, suggesting that all of the mordants can enhance dyeing effect significantly. After a certain mordant concentration level, both the color strength and dye uptake tend to a constant level for all the tests. Combining the dyeing effect together with the consideration of using less metallic mordant, the optimal concentration of $RECl_3{\cdot}6H_2O$, $NdCl_3{\cdot}6H_2O$, $FeSO_4{\cdot}7H_2O$ and $K_2Cr_2O_7$ was determined as 0.6g/L, 0.6 g/L, 4.0g/L and 1.6g/L, respectively. As a result, the ionic concentration employed for deriving optimal dyeing effect was $[Nd^{3+}]$=0.24mg/L, $[Fe^{2+}]$=0.81mg/L and $[Cr^{6+}]$=0.57mg/L. The total rare earth ionic concentration $[RE^{3+}]$ in the $RECl_3$ solution should be close to $[Nd^{3+}]$. Apparently, employing rare earth mordent can greatly reduce the ionic concentration

employed in natural dyeing. The coordination number of rare earth elements is larger that that of the Fe^{2+} and Cr^{6+}. The coordination number of d-block transition metals is usually 4 or 6. In contrast, the most common coordination number of rare earth ions is 8 or 9 because when a rare earth ion is coordinated to ligands its 6s, 6p and 5d orbits usually participate in the formation of coordination bonds [63, 145]. In addition, the larger ionic radius of lanthanide elements accounts of the larger coordination number of rare earth complex. Hence using rare earth chlorides as mordants in natural dyeing can avoid heavy metal pollution. In addition, the presence of metallic mordant usually changes the color shade of dyed fabrics in natural dyeing. For example, Fe^{2+} usually results in the darkening of the dyed fabrics. Using rare earth as mordants can also enlarge the design flexibility in the dyeing process to derive the desired color shade.

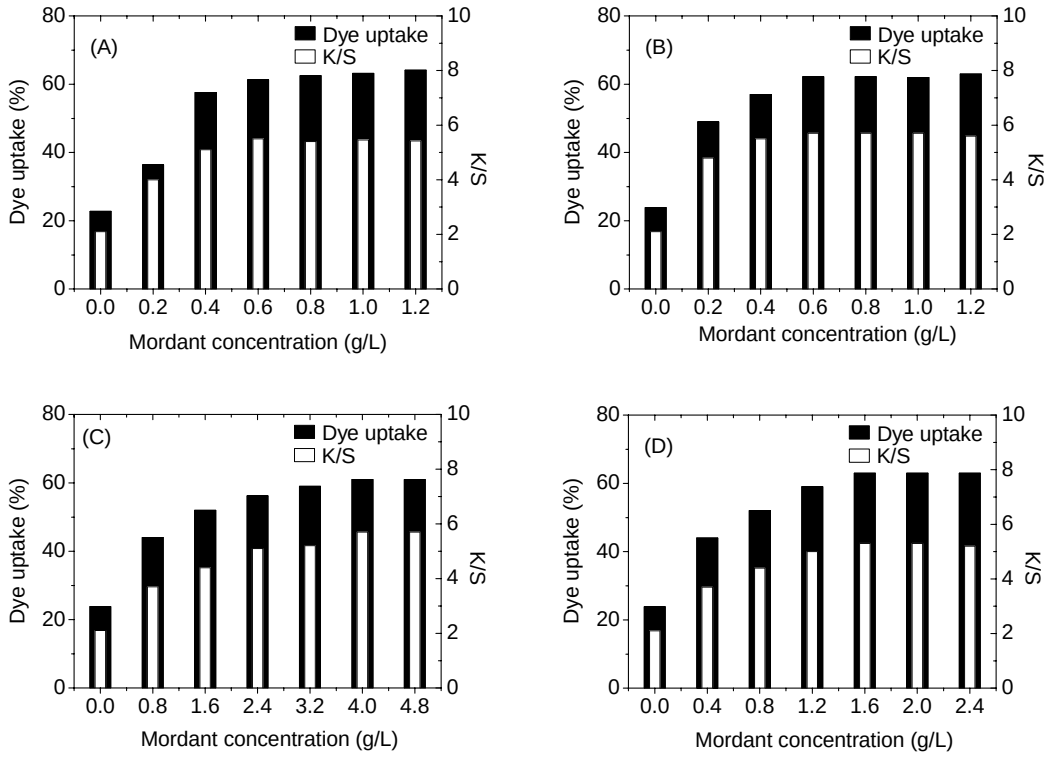

Figure 3.6 Influence of mordant concentration of dye uptake and K/S values of the different mordants in the dyeing with Caesalpinia Sappan colorant. (A) $RECl_3 \cdot 6H_2O$; (B) $NdCl_3 \cdot 6H_2O$; (C) $FeSO_4 \cdot 7H_2O$; (D) $K_2Cr_2O_7$.

3.4 Conclusion

In this study, the rare earth was employed as mordant for the dyeing of ramie fabrics with the natural extracts of caesalpinia sappan, rhizoma coptidis, gardenia and areca catechu. The effect of pre-mordanting, simultaneous mordanting, and post-mordanting on the dyeing effect were compared. The dyeing temperature of 90oC was determined as the best dyeing temperature while the optimal dyeing time for the four kinds of natural dyes was in the range 50-70 minutes. It was found that the highest dye uptake was obtained when the dyeing bath pH was 7 or 8. The fabrics dyed in presence of rare earth as mordant exhibited higher color shade stability. On one hand, this is owing to the stable coordination bonds among the rare earth, natural dye and fiber. On the other hand, it is ascribed to the interaction of the multiple complexes formed by rare earth ions and natural dyes which enable the dyed fabrics to resist pH impact maintaining the constant color shade. It was proved that using rare earth as mordant apparently enhanced the color fastness to washing, rubbing and light of the fabrics dyed with the natural extracts. As compared with the mordants containing Fe2+ and Cr6+, the rare earth mordants can greatly reduce the ionic concentration employed in natural dyeing. This study proved that rare earth is promising in the application for mordant in the dyeing with natural colorants.

CHAPTER 4
WRINKLE RESISTANT TREATMENT OF RAMIE FABRIC USING LIQUID AMMONIA TECHNOLOGY

4.1 Introduction

Advantages and disadvantages of ramie fibers

As a class of natural textile material, ramie fabric is popular due to their several advantageous features like excellent tensile properties, high tenacity, "cool-handle" attribute, good comfort and appearance [1, 10]. However, the crystallinity of ramie fiber is much higher than that of cotton fiber [11, 72, 74, 75, 146]. Moreover the cellulose molecules of ramie fibers are highly oriented. As a result, ramie fabrics are characterized by a low degree of wrinkle recovery, poor abrasion resistance, dimensional stability, harsh hand and low resilience, which prevent their extensive applications [71-75, 147]. A major challenge for the industry is to improve the wrinkle resistance of ramie fabrics, particularly when ramie fabrics are used in apparel and in household textiles.

A variety of finishing techniques have been investigated over the past decades to achieve the wrinkle-free appearance in cotton fabrics [73, 76, 148, 149]. Resin treatment is generally employed to give wrinkle resistant feature, but this method has the drawback of making cotton fiber weak and hard [71-73, 147]. However, using liquid NH_3 treatment makes cotton strong and soft prior to resin treatment and will offset this drawback. Liquid NH_3 treatment is known to improve the soft hand of cotton fabrics [23-25, 30-32, 34, 36-38]. The surface tension and viscosity of liquid NH_3 is lower than water [26-29, 31-35, 38, 150, 151]. Therefore, when soaked in liquid NH_3, cotton fiber instantaneously swells, forms a circular shape and becomes twist-free. As a result, cotton fabrics become harder to shrink and wrinkle. The cotton fabrics exhibit increased resilience become soft and strong. Moreover, the changes in crystallinity, accessibility and surface properties were followed [25, 31, 34, 37]. The commercial liquid ammonia

treatment is generally applied to cotton products and the advantages of liquid ammonia on the strength, abrasion resistance, dye absorption and color yield of cotton fabric have been well documented [23-25, 30-32, 34, 36-38]. But only a few investigations have been made on the liquid NH_3 treatment of ramie fabrics [26, 27].

In this study, the liquid NH_3 technique was employed for the wrinkle resistant treatment of ramie fabrics. The influences of liquid NH_3 treatment on the structure of ramie fibers were studied by scanning electron microscopy (SEM) and x-ray diffraction (XRD). The swelling effect and decrease of crystallinity of the ramie fibers caused by the liquid NH_3 treatment were observed. The liquid NH_3 pretreatment prior to resin finishing were proved to reduce strength loss without sacrificing wrinkle resistant effect. In addition to the liquid NH_3 pretreatment, a kind of reactive polyurethane (PU) emulsion was also employed as strength protector in the wrinkle resistant finishing, which have never reported. The influences on the treatment conditions including curing temperature, curing time, resin content and reactive PU emulsion content on the wrinkle resistant effect and mechanical properties were investigated systematically and the optimal treatment conditions were achieved thereof. It was proved that application of liquid NH_3 pretreatment as well as reactive PU emulsion is rather favorable for the wrinkle resistant treatment of ramie fabrics.

4.2 Experimental

Materials

The ramie fabric (21×21s) was desized, scoured and bleached prior to using. The cross-linking agent Arkofix NETM which was modified from the typical cross-linking agent Dimethyloldihydroxyethyleneurea (DMDHEU) resin was provided by the Clariant Chemical Co., Ltd. C. I. Direct Red 23 was supplied by Dalian Dyechem International Co. The thermally reactive polyurethane (PU) emulsion DM-3911 (solid content 33%) was purchased from the DYMATIC Chemicals Inc. (Foshan, Guangdong, China). Silicon softener AV-910 was produced by Advanced Chem. & Fabrics Inc. The chemicals including magnesium chloride ($MgCl_2.6H_2O$), Ammonium Chloride (NH_4Cl),

Sodium Chloride (NaCl) and Barium Chloride ($BaCl_2$) were purchased from Aldrich Co.

Liquid NH_3 treatment

The ramie fabrics were treated in patented (patent number ZL02289238. 9) batch-type liquid NH_3 equipment as illustrated in Figure 4.1. The equipment comprises the liquid NH_3 reaction tank, circulation bump, NH_3 compressor, laundry system, safety controlling system and liquid NH_3 recycling system. The ramie fabrics were warp into hollow rollers and placed into the liquid NH_3 reaction tank. Afterwards, the liquid NH_3 reaction tank was sealed by tank cover and was then filled with liquid NH_3 via opening the valve attached to the tank. The ramie fabrics were treated for another 5 min in the liquid NH_3 after the tank was fulfilled totally with liquid NH_3 indicated by the pressure. At the end of the treatment, the liquid NH_3 transferred into the balance tank and the residual NH_3 was removed via the NH_3 compressor. Then the fabrics were washed with diluted sulfuric acid (1-2g/L) in the tank and were rinsed with water till to pH=7. Then the treated fabrics were dried for use.

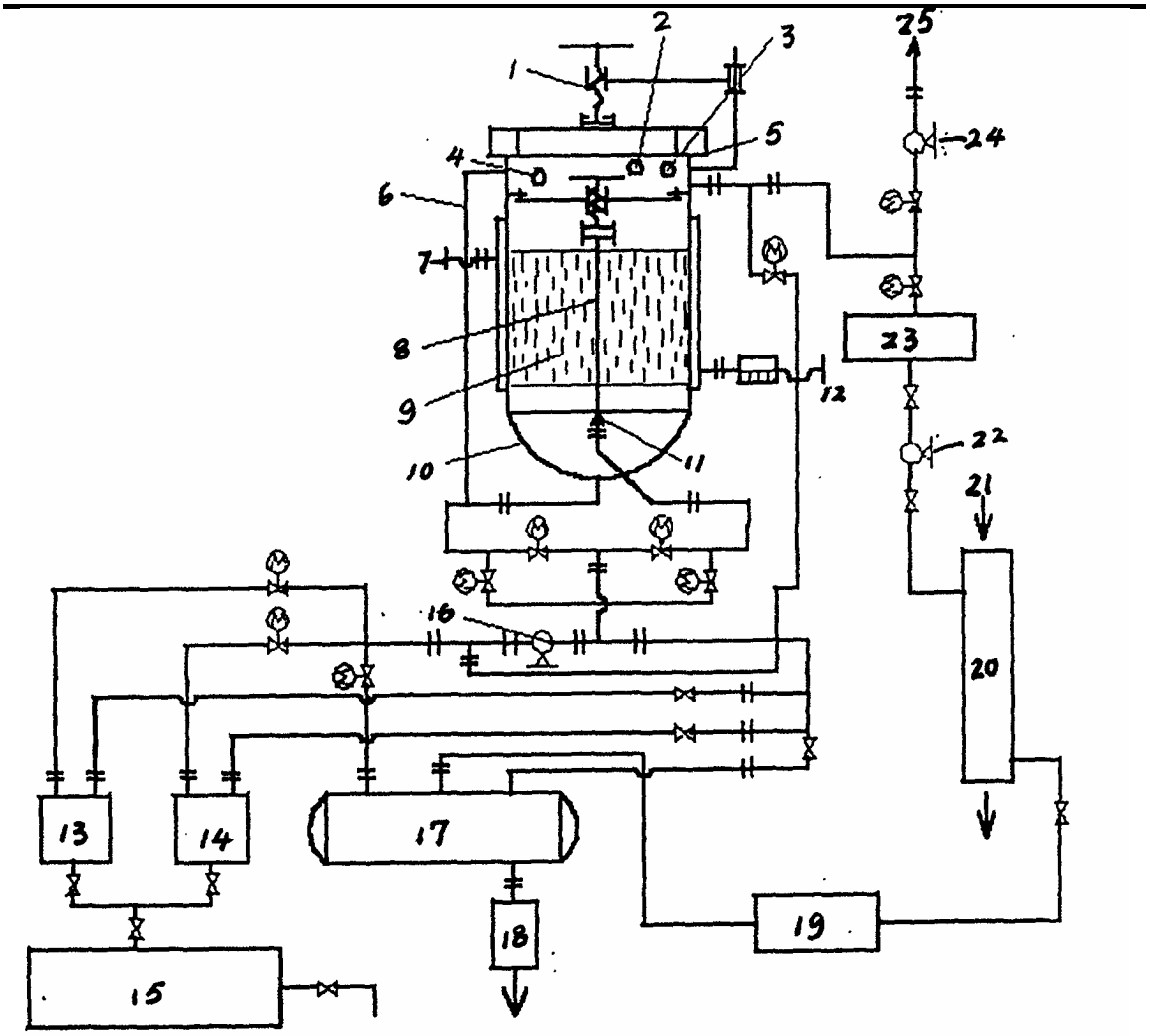

Figure 4.1 The illustration of the batch-type liquid ammonia treatment equipment.
1 Tank cover pressure holder; 2 Pressure gauge; 3 Thermometer; 4 Safety valve; 5 Tank cover; 6 Liquid level indicator; 7 NH_3 inlet; 8 Warp beam; 9 Fabric; 10 Liquid ammonia reaction tank; 11 Warp beam connector; 12 NH_3 outlet; 13 Water; 14 Diluted acid; 15 Waste water treatment unit; 16 Circulation bump; 17 Liquid ammonia preservation tank; 18 Emergency outlet; 19 Oil remover; 20 Condenser; 21 Water; 22, NH_3 compressor; 23 Oil remover; 24vacuum bump; 25 Air.

Dyeing

Untreated and liquid NH_3 treated ramie fabrics were dyed with an acid dye C. I. Direct Red 23 and the apparent dyeing rate and equilibrium dye uptake were measured. The dyeing bath was adjusted to an initial dye concentration of 2% (owf) while the

concentration of NaCl was 4g/L. The dyeing was carried out for at 70°C and the liquor ratio of 30:1 with the dyeing time varying from 5 min, 10 min, 20 min, 40 min, 60 min, 80 min to 100 min.

Wrinkle resistant treatment

The wrinkle resistant treatment was performed via the conventional dip-pad-dry-cure process with the Rapid 354 padding machine, WernerMathis AG drying machine, Maag & Schenk Ironing Machine and Mathis Lab dryer. The ramie fabrics treated by liquid NH3 were treated with varying content of Arkofix NETM, catalyst and softener in order to find out the optimal conditions combination to attain the best comprehensive wrinkle resistant treatment effect and strength. To ensure that the fabrics absorb the treatment liquid fully and evenly, the liquid pick up was controlled in the range 60-70% after the padding process which the padding pressure was set at 0.25MPa. The drying temperature was 80^{o}C and drying time was 3 min. The curing of the treated fabrics was conducted at 150^{o}C for 2min. After twice padding-drying-curing treatments, the treated ramie fabric samples and the untreated ramie fabric samples were washed different times in a domestic electric washing machine according to the AATCC-135 test method. Each kind of fabric was tested with 5 pieces of fabric samples for averaging. After drying, the wrinkle resistant effect and strength of the ramie fabric sample were evaluated.

Measurements

To view the swelling effect of liquid ammonia on the ramie fibers, fiber samples were were embedded in cured epoxy resin and were cut with a microtome in advance. Then the cross sectional morphology of the fiber sample was observed by the Hitachi S-2600HS scanning electron microscope (SEM).

The crystallinity of cotton fabric untreated and treated with liquid ammonia was measured using a powder reflection method with CuK_{α} monochromatic x-ray on a Rigaku x-ray diffractometer, model 111-DMAX. The degree of crystallinity (C_x) was obtained by:

$$C_x = \frac{I_c}{I_a + I_c} \times 100 \quad (4\text{-}1)$$

where I_c refers to the integrated diffraction intensity of the crystalline region, and I_a stands for the integrated diffraction intensity of the amorphous region based on 20 = 18°.

Ramie fabric was immersed in water for 24 hours and then centrifuged for 20 minutes at 3000 rpm (w_1), kept 48 hours at 65% RH (w_2), and finally dried for 3 hours at 105°C (w_0). Moisture regain and water absorbency were calculated by 48 hours at 65% RH (w2), and finally dried for 3 hours at 105°C (w_0). Moisture regain and water absorbency were calculated by:

$$\text{Moisture regain} = \frac{w_2 - w_0}{w_0} \times 100 \quad (4\text{-}2)$$

$$\text{Water absorbency} = \frac{w_1 - w_0}{w_0} \times 100 \quad (4\text{-}3)$$

The average degree of polymerization ($\overline{DP}$) of ramie fibers was determined by the method of viscosity using copper diethyleneamine (Cuene) as the cellulose solvent according to the following equation:

$$\overline{DP} = \frac{156 \times \eta_{sp}}{c \times \left(1 + 0.29 \times \eta_{sp}\right)} \quad (4\text{-}4)$$

where c is the concentration of the cellulose Cuene solution equal to 0.1 g/100 ml, and η_{sp} is the specific viscosity of the cellulose Cuene solution calculated according to:

$$\eta_{sp} = \frac{t - t_0}{t_0} \quad (4\text{-}5)$$

where t is the fluid time of the cellulose solution, and t_o is the fluid time of the solvent. All the results were the average of three measurements. The viscosity was determined using an Ostwald viscosimeter at 20°C.

The capillary effect of the ramie fabrics was measured on the LY-MX Capillary Effect

Tester (Dongguan Lili Test Equipment Co., Ltd.) according the standard FZ/T01071.

The barium activity number of untreated and treated by liquid NH_3 ramie fabrics was measured according to AATCC 89-1998 test method. The mercerized and un-mercerized cotton fabrics were cut into small lengths, weighing 1 g were treated with 30 mL of 0.25 N barium hydroxide solutions in 100 mL flasks. After 2 h, 10 mL of the solution was titrated with 0.1 N hydrochloric acid. A blank was also run in without any fabric sample. If A, B and C are the titration reading for the blank, mercerized sample and unmercerized sample respectively, then the barium activity number is given by:

$$\text{Barium activity number} = \frac{A-B}{A-C} \times 100 \quad (4\text{-}6)$$

The dye uptake in the dyeing of ramie fabrics was obtained through the measurement of the light absorbances at the wavelength of maximum absorption, of the dye bath before and after dyeing with a U-3310 ultraviolet-visible (UV-vis) spectrophotometer. The dye uptake was calculated with the following equation:

$$\text{Dye uptake} = \frac{A_0 - A_t}{A_0} \times 100\% \quad (4\text{-}6)$$

where A_0 and A_t refer to the absorbances of the dye solutions at the beginning and the end of dyeing, respectively. The color strength K/S of the ramie fabrics were measured by DatacolorSF600 Computer Color Matching System (Data Color International) using illuminant D_{65} and 10^o standard observer. K/S was calculated from the reflectance values using the Kubelka-Munk equation as follows:

$$K/S = \frac{(1-R)^2}{2R} \quad (4\text{-}7)$$

Where R represents the reflectance of the dyed fabric and K/S stands for the ratio of the absorption coefficient (K) to scattering coefficient (S). The higher K/S value the greater the color strength.

The tensile strength and elongation at break of the ramie fabrics were tested by an Instron 4411 according the standard ASTM D 5034-1995. The tearing strength of the ramie fabrics was measured by an Elmendorf tearing tester according the standard

ASTM D 1424-1996. The flat appearance and the crease retention of the ramie fabrics were evaluated in accordance with the method AATCC 124-2001 and AATCC 88C-2003, respectively. For a given untreated or treated fabric, all the mechanical property and wrinkle resistant evaluation tests were performed on 5 samples for averaging.

4.3 Results and Discussion

4.3.1 Influences of liquid NH_3 on structure of ramie fibers

Scanning electron microscopy has proved to be very useful for studying the surface characteristics of textile materials and establishing the mechanism of failure in fibers, yarns, and fabrics. Figure 4.1 presents the cross sectional SEM images of the ramie fibers untreated and treated by liquid NH_3. The shape of untreated ramie fiber's cross section is usually ellipse with some crevices on it (as shown in Figure 4.2 (a)), while the shape of that treated by liquid NH_3 became rounder and thicker with much less crevices (see Figure 4.2 (b)). In addition, the lumen decreased with increasing cell wall area. This indicates that the liquid NH_3 treatment resulted in apparent fiber swelling indeed.

The crystallinities of ramie fibers untreated and treated by liquid ammonia were determined by XRD, and the results are shown in Figure 4.3 and Table 4.1. It was found that not only the crystallinity but also the crystalline form changed greatly. In Figure 4.3, the untreated ramie fibers exhibited these three peaks at 2θ= 14.6°, 16.1°and 22.2°, which means the crystalline form of the untreated ramie fibers was cellulose I type. While for treated ramie fabric, there were another two peaks besides these three ones, which corresponded to 2θ=12.1° and 20.9°. Those two peaks belong to the characteristic peaks of cellulose III. Therefore, it can be drawn that liquid ammonia treatment resulted in some crystals of ramie fiber changing from cellulose I to cellulose III. In comparison with those of untreated fabric, the diffraction peaks of the XRD profile of ramie fiber were broader in width and lower in intensity, suggesting that the liquid ammonia treatment resulted in the increase of the amount of amorphous region and the decrease

of crystalline region. Table 4.1 showed that the liquid NH_3 treatment gave rise to the crystallinity decrease of 13.8%. It is also noted that the diffraction of 2θ=22.2° slightly shift to lower angle, indicating the cellulose I type crystallites in the ramie fibers treated by liquid NH_3 were less perfect as compared with those of the untreated fibers.

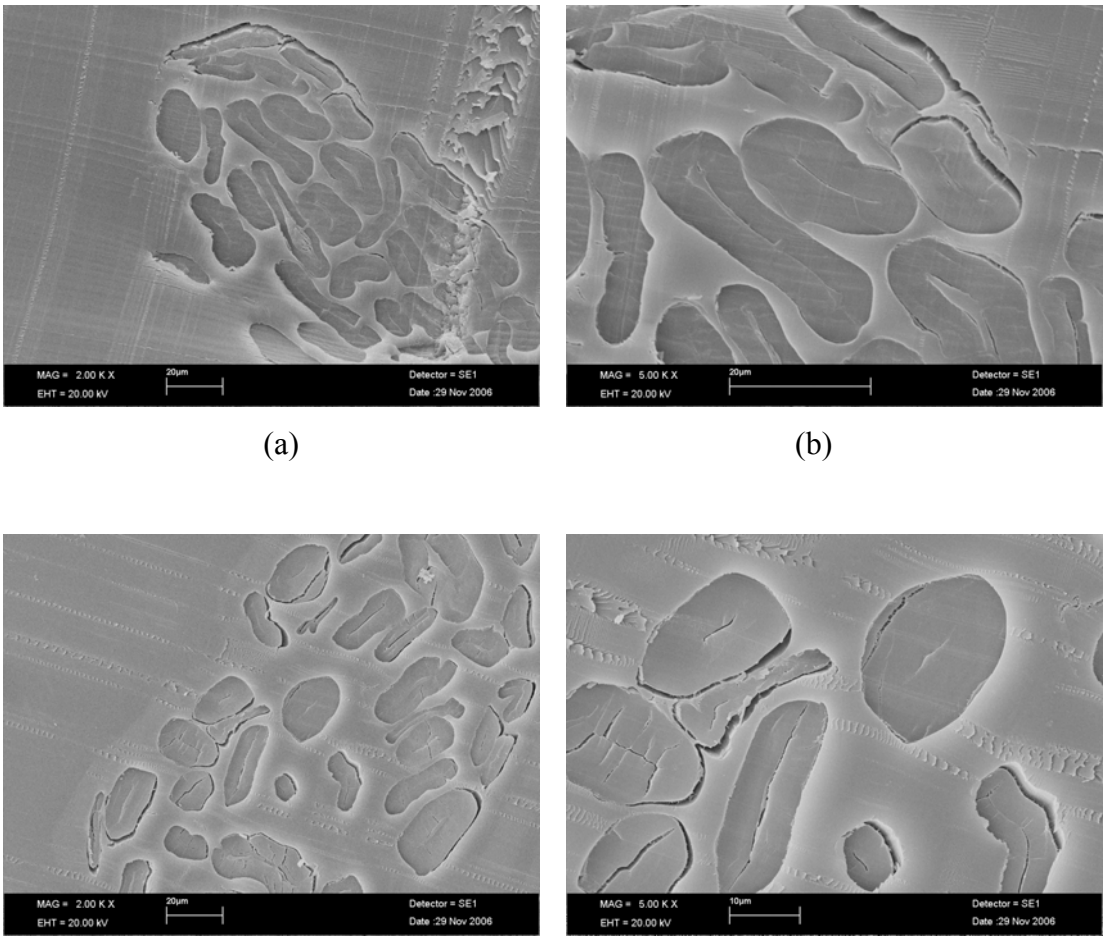

(a) (b)

(c) (d)

Figure 4.2 The cross sectional SEM images of the ramie fibers: (a) untreated fibers with a magnification of ×2000 times; (b) untreated fibers with a magnification of ×5000 times; (c) fibers treated by liquid NH_3 with a magnification of ×2000 times; (d) fibers treated by liquid NH_3 with a magnification of ×5000 times.

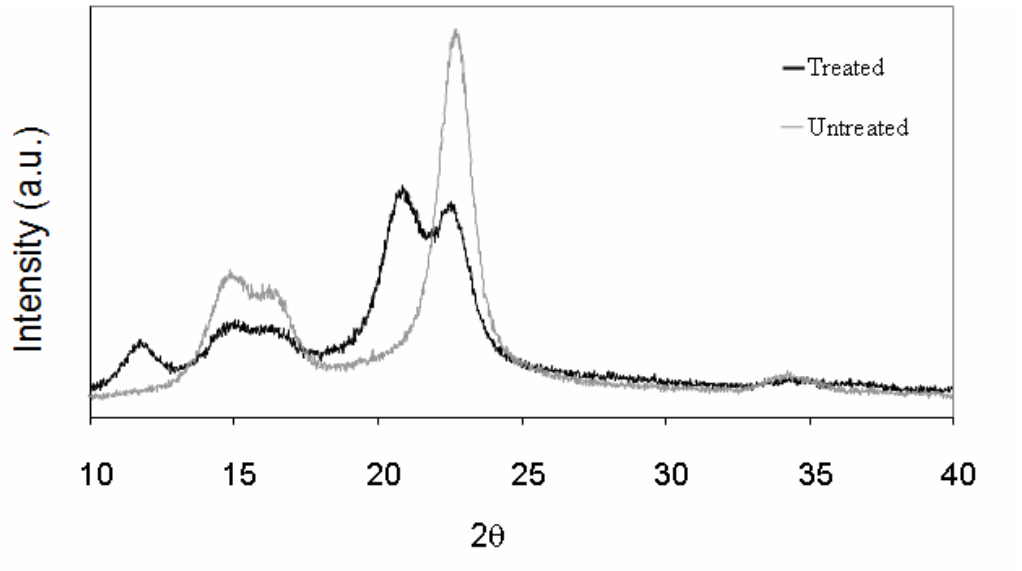

Figure 4.3 XRD profiles of the ramie fibers untreated and treated with liquid NH_3.

Table 4.1 Crystallinity and crystal type of untreated and liquid NH_3 treated ramie fibers.

Ramie fabrics	Crystallinity (%)	Crystal type
Untreated	78.4	Cellulose I
Treated by liquid NH_3	59.6	Cellulose I and Cellulose III

Table 4.2 Influence of liquid NH_3 treatment on the degree of polymerization and characteristic viscosity of ramie fibers.

Fabrics	Degree of polymerization	Characteristic viscosity
Untreated	1645	10.5
Treated by liquid NH_3	1603	10.32

Table 4.2 presents the influence of liquid NH_3 treatment on degree of polymerization and characteristic viscosity of ramie fibers. As shown in Table 4.2, the degree of polymerization and characteristic viscosity of the ramie fibers

treated by liquid NH_3 were almost similar to those of the untreated fibers. This suggests that the cellulose macromolecule in the ramie fibers did not degrade after the liquid NH_3 treatment.

Moisture regain is a property related to the accessible internal surface in the conditioned fiber, which increase with decreasing crystallinity of the cellulose structure. As indicated by Table 4.3, the moisture regain of fabric treated by liquid NH_3 was higher than that of untreated fabric due to the decrease of crystallinity caused by the liquid NH_3 treatment. In contrast, the water absorbency of the fabric treated by liquid NH_3 was lower than that of untreated fabric regardless the remarkable decrease in crystallinity. Capillary effect is a sensitive indicator of the degree of water affinity and accessibility of fabrics. Table 4.3 shows that the capillary effect values of the liquid NH_3 treated ramie fabric were higher than those of the untreated ramie fabric. It was reported that cotton or linen fabrics also showed increased accessibility after ammonia treatment. The barium activity number is widely used to express the degree of mercerization. The higher the barium activity number, the better the mercerization effect. The barium activity number of mercerized fabrics is inversely proportional to the crystallinity of fabrics. Table 4.3 reveals that the barium activity number was raised after liquid NH_3 treatment.

Table 4.3 Effect of liquid NH_3 treatments on some physical properties of untreated and liquid NH_3 treated ramie fabrics.

Fabrics	Moisture regain (%)	Water absorbency (%)	Capillary effect		Barium activity number
			W	F	
Untreated	6.18	24.8	7.1	6.8	114
Treated by liquid NH_3	7.05	20.7	8.3	7.5	123

All the property changes of the ramie fabrics after liquid NH_3 treatment were caused by the internal structural changes of the ramie fibers. The NH_3 treatment is known to change the internal structure of the cellulose fibers and leads to the crystalline phase

from cellulose I to cellulose III. Also, the orientation of the amorphous region is higher than that of the untreated fiber, despite a considerable decrease in crystallinity. That is to say, the arrangement of cellulose molecular chains in amorphous region got more regular. In addition, it was proved that liquid ammonia treatment had significant effect on the pore structure of cellulose fibers. A significant decrease in total pore volume was observed as a consequence of the loss of large pores and the increase in small pores [16]. As a result, after liquid ammonia treatment, the size distribution of micropores became narrow and the micropores distribution became more uniform. In addition, some accessible micropores have appeared in the places where no micropores ever existed.

4.3.2 Influences of liquid NH_3 on dyeing properties of ramie fabrics

Table 4.4 shows the influences liquid NH_3 treatment on the dyeing properties of ramie fabrics. It can be seen that after the liquid NH_3 treatment both the half time of dyeing of and equilibrium dye uptake of ramie fabric were raised. This is due the internal structural changes occurred to the ramie fibers after liquid NH_3 treatment. Although the amount of amorphous region increased with the liquid NH_3 treatment, the orientation of the cellulose molecular chain in amorphous region was enhanced and the cellulose molecules in amorphous region were packed more tightly. Moreover, a great fraction of larger pores disappeared while the fraction of small pores rose due to the swelling effect brought but liquid NH_3 treatment. The larger direct dye molecules have difficulty penetrating into the fiber because of the high orientation of the cellulose molecular chain in the amorphous region. However because the total crystallinity of the ramie fibers decreased greatly after all, the affinity and accessibility of the ramie fibers were proved to rise as mentioned above. Therefore, the equilibrium dye uptake of ramie fabric was raised in long dyeing time. Accordingly, the color strength K/S of the ramie fabric pretreated by liquid NH_3 was higher than that of the untreated fabric when the equilibrium dye uptake was attained.

4.3.3 Influences of liquid NH_3 on wrinkle resistant and mechanical properties

In this study, the mixture of $MgCl_2 \cdot 6H_2O$ and NH_4Cl (in weight ratio of 15:1) was

Table 4.4 Dyeing properties of ramie fabrics untreated and treated by liquid NH_3.

	Equilibrium dye uptake (%)	Half time of dyeing $t_{1/2}$ (min)	*K*/*S*
Untreated	73.56	36.04	7.79
Pretreated by liquid NH_3	82.84	76.00	9.0

used as the cooperative catalyst in the wrinkle resistant treatment. The ion Mg^{2+} and H^+ generated in the cross-linking reaction have catalytic activity for the cross-linking reaction between $–CH_2OH$ group of Arkofix NETM resin and the –OH on cellulose molecules. The chemical NH_4Cl is the potential acid catalyst and can release acid and NH_3 which can react with the free formaldehyde to form hexamethylenetetramine and H^+, and thus can reduce the free formaldehyde. However NH_4Cl can result in the depression of mechanical properties of the fabrics due to the presence of Cl^-. Hence the fraction of NH_4Cl in the mixed catalyst should be controlled and small. In addition, the content of the mixed catalyst should also be selected carefully. Lower content of catalyst can efficiently catalyze the cross-linking reaction of ramie fibers. On the contrary, higher content of catalyst can lead to decomposition of cellulose fibers and destroy of cross-linking resin. In this study, the content mixed catalyst was set as 11g/L.

To examine the influences of liquid NH_3 treatment on the wrinkle resistant and mechanical properties, the ramie fabric pretreated by liquid NH_3 and the fabric untreated were used to carry out wrinkle resistant treatment via the same conditions, i.e., Arkofix NETM resin content of 80g/L, curing temperature of 140^{o}C and curing time of 2 min. As well known, the wrinkle resistant treatment of cellulose fabrics can result in significant depression of mechanical strength of fabrics. In this study, a kind of polyurethane emulsion bearing blocked isocyanate groups was employed as the strength protector. The wrinkle resistant treatment was also performed on the ramie fabric pretreated by liquid NH_3 with both the Arkofix NETM resin with content of 80g/L and the PU emulsion with the content of 80g/L. In the identical conditions, the wrinkle resistant effect tests including flat appearance and crease retention and the tensile and

tearing tests were performed on the original ramie fabric experienced not any treatment, the ramie fabric pretreated by liquid NH_3, the original ramie fabric finished by Arkofix NETM resin, the ramie fabric pretreated by liquid NH_3 and subsequently treated by Arkofix NETM resin as well as the ramie fabric pretreated by liquid NH_3 and subsequently finished by both Arkofix NETM resin and PU emulsion. For convenience, the five kinds of fabric samples were designated as "Untreated", NH_3, "Resin", "NH_3+Resin" and "NH_3+Resin+PU", respectively.

Figure 4.4 presents the comparisons of the flat appearance and crease recovery of the five kind ramie fabric samples after 1 washing. As expected, the "Untreated" ramie fabric exhibit only 1 grade of flat appearance and crease recovery, namely, the original ramie fabric experienced not any treatment did not exhibit any wrinkle resistant effect. The flat appearance and the crease recovery of "NH_3" sample were all over grade 2. This is because the liquid NH_3 treatment resulted in the swelling ramie fibers and gave rise to the increase of elasticity and strength of the fibers. As a consequence, the wrinkle resistant of the ramie fabric pretreated by liquid NH_3 rose somehow. The flat appearance and the crease recovery of "Resin" sample were all over grade 3 due to increase of elasticity caused by the cross-linking of the cellulose molecules. The "NH_3+Resin" and "NH_3+Resin+PU" samples exhibited highest flat appearance and crease recovery, suggesting NH_3 pretreatment was favorable for the improvement of wrinkle resistant effect in resin finishing since the swelling effect brought by the NH_3 treatment could not only raise the elasticity of ramie fibers but also enhance the accessibility for the cross-linking resin molecules in the wrinkle resistant treatment. In addition, the presence of PU emulsion in the resin finishing basically did not affect the wrinkle resistant effect. In the other word, PU emulsion did not reduce at lease or even increase the wrinkle resistant effect slightly.

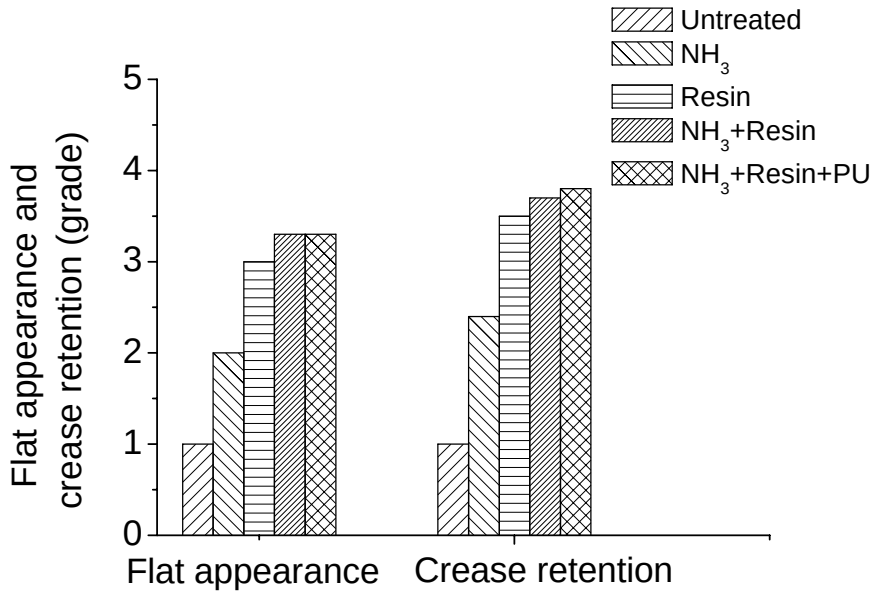

Figure 4.4 Flat appearance and crease retention of the original ramie fabric and those subjected to different treatments after 1 washing.

Figure 4.5 shows the tensile strength retention rates of the original ramie fabric and those experienced different treatments. After the pretreatment by liquid NH_3, the tensile strength of ramie fabric was raised by 10% in warp direction but decreased by 8% in filling direction. In some previous reports, the cotton and linen fabrics treated by liquid NH_3 showed the similar different tensile strength change in different directions. The increase of tensile strength in warp direction should be ascribed the swelling effect, which increased the elasticity of ramie fibers and reduced the uneven distribution of the stress. The different tensile strength should result from the tension difference between warp yarn and filling yarn in the liquid NH_3 treatment. The tensile strength retention of "Resin" sample was only 60-70%. The tensile strength loss was ascribed to two aspects: one is the fiber degradation caused by the acid catalyst at high temperature, the other one is the restriction of the stress distribution within the fibers due to the cross-linking sites. As compared with that of "Resin" sample, the tensile strength retention of "NH_3+Resin" fabric rose to above 70%. This is because the liquid NH_3 on one hand raised the elasticity and strength of the ramie fabric and on the other hand the even swelling effect reduced the internal stress, which enabled the stress to distribute evenly

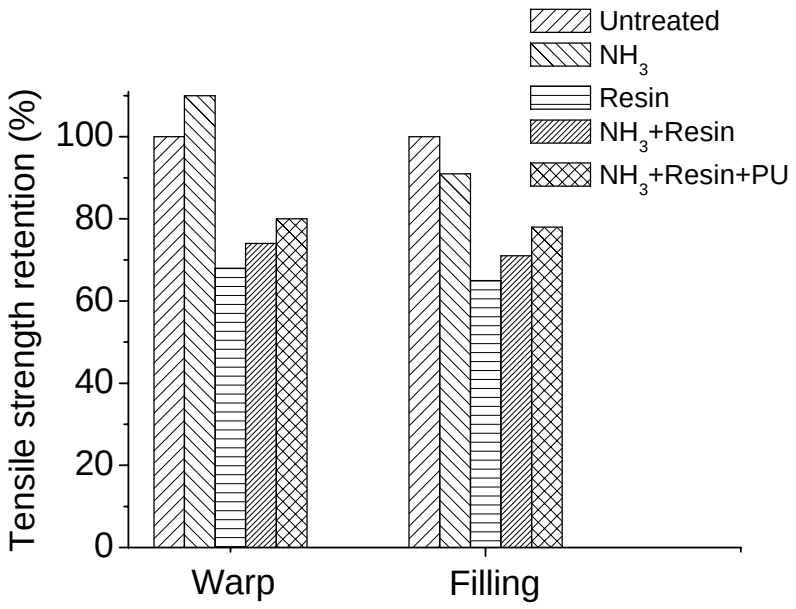

Figure 4.5 Tensile strength retention rates of the original ramie fabric and those subjected to different treatments.

along the ramie fibers. The "NH_3+Resin+PU" fabric exhibited the highest tensile strength retention (~80%). Besides the tensile strength enhancement brought by the liquid NH_3 pretreatment the PU molecules also gave rise to the increase of tensile strength for the ramie fabric. The molecular mechanism of the strength protection rendered by the PU emulsion is demonstrated in Figure 4.6 in which R refers to the blocking agent. The PU emulsion DM-3911 was a kind of low-molecular-weight reactive polyurethane bearing blocked isocyanate groups. The isocyanate groups could be unblocked and released by the elevated temperature in the course of curing. The free isocyanate groups thus could react with the –OH groups on the surface of the ramie fibers and form cross-linking networks on the ramie fibers. The ramie fabrics were thus reinforced further. Since the polyurethane molecules are larger than the cross-linking resin molecules, they hardly penetrated into the internal parts of the ramie fibers and thus contributed less to wrinkle resistant effect.

Figure 4.7 presents the elongation at break of the untreated ramie fabric and those

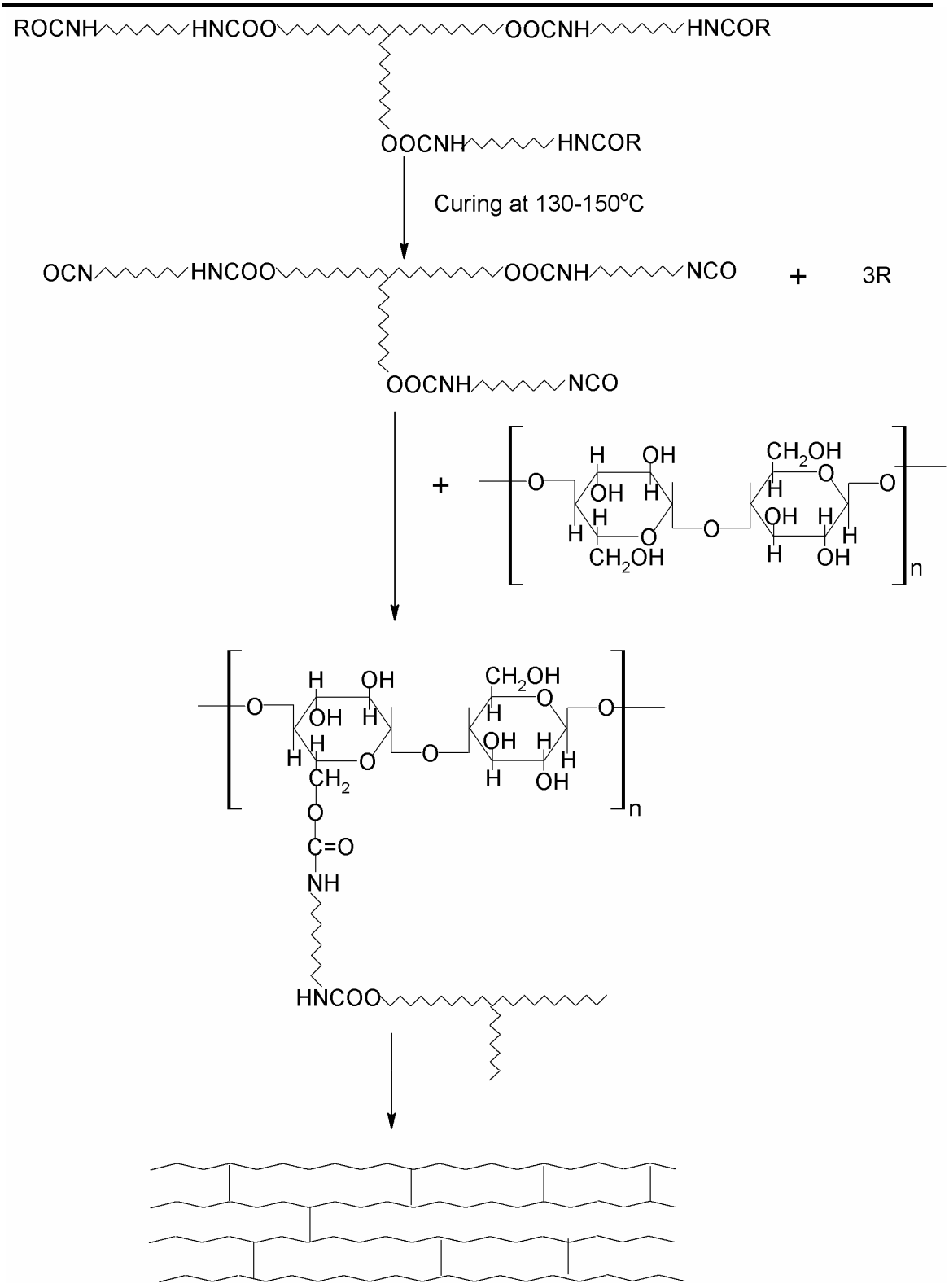

Figure 4.6 Reaction between blocked PU and cellulose.

were finished differently. It can be seen that the elongation at break of the ramie fabric was greatly raised prominently by the liquid NH_3 pretreatment. This is because the even swelling effect rendered by the liquid NH_3 pretreatment increased the elasticity and reduced the internal stress and stress concentration, resulting in the increase of extensibility of the ramie fibers. The elongation at break of the "resin" fabric was similar to that of the original ramie fabric. The "NH_3+resin" fabric gave rise to lower elongation at break as compared with the "NH_3" fabric, suggesting the resin finishing increased the rigidity of the fibers and thus reduced the elongation at break. The elongation at break of the "NH_3+resin+PU" ramie fabric was similar to that of the "NH_3+resin" fabric.

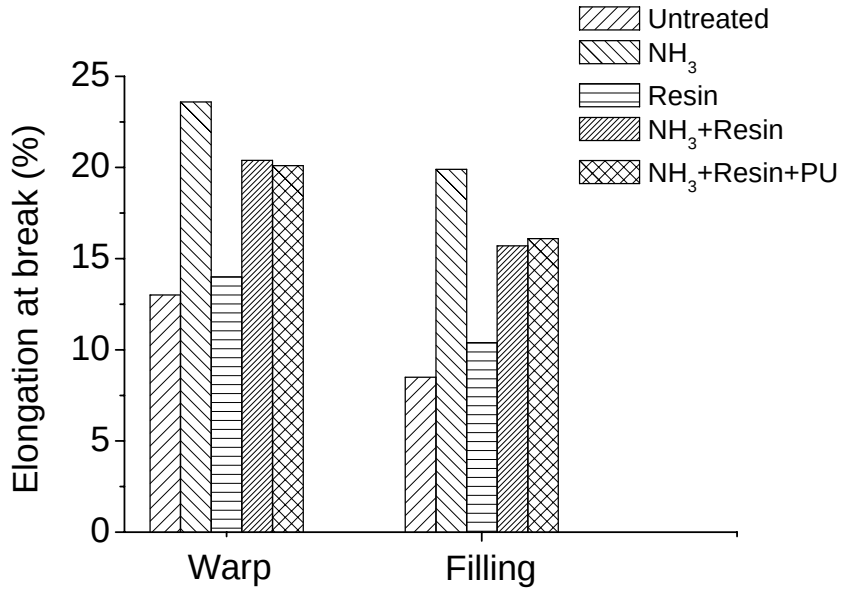

Figure 4.7 Elongation at break of the original ramie fabric and those subjected to different treatments.

Figure 4.8 shows the tearing strength retention rates of the original ramie fabrics and those subjected to different treatments. As compared with the "Untreated" ramie fabric, the "NH_3" fabric has its tearing strength decreased by over 10% in both warp and filling directions. After resin finishing, the tearing strength retention decreased to below 70%. If the liquid NH_3 treatment was performed prior to resin finishing, the tearing strength retention rates were elevated to over 70%. When the reactive PU emulsion was involved

in the resin finishing, the tearing strength retentions in warp and filling directions were all increased further by 2-8%.

It thus can be drawn that the liquid NH_3 pretreatment on ramie fabric prior to the resin finishing was favorable for enhancing wrinkle resistant effect and reducing strength loss. The application of the reactive polyurethane emulsion in resin finishing could raise the strength retention without influencing wrinkle resistant effect. Therefore performing liquid NH_3 pretreatment prior to resin finishing and employing reactive PU emulsion as strength protector were used for the subsequent studies.

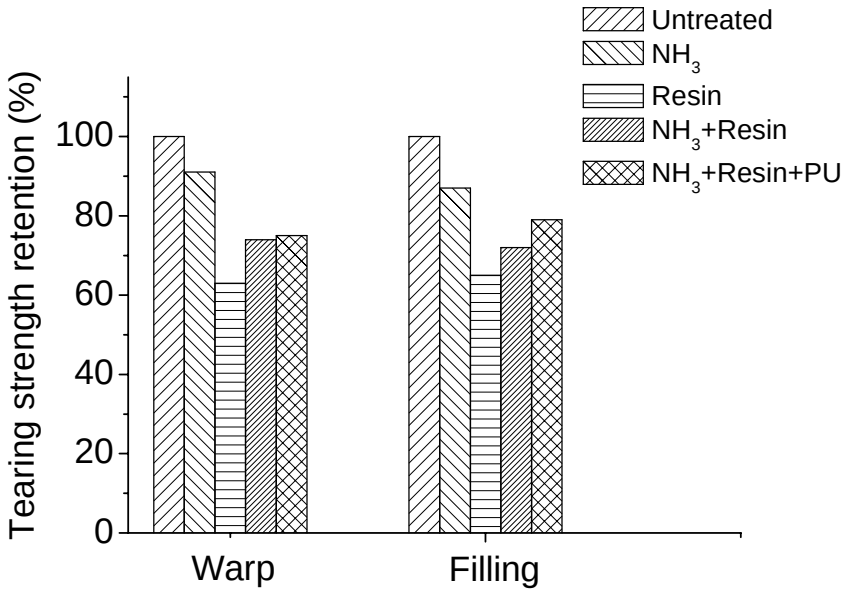

Figure 4.8 Tearing strength retention rates of the original ramie fabrics and those subjected to different treatments.

4.3.4 Influences of varying treatment conditions

To achieve the optimal treatment conditions in resin finishing, the influences of curing temperature, curing time, content of cross-linking resin and content of reactive PU emulsion on the wrinkle resistant effect and mechanical properties were investigated.

The ramie fabrics pretreated by liquid NH_3 were finished with Arkofix NETM resin by keeping the other conditions identical to those employed in the above resin finishing

tests but just varying curing temperature from 120 °C to 160°C with a 10 °C interval. In the resin finishing, the reactive PU emulsion was utilized as strength protector. The influences of the curing temperature were shown in Table 4.5. It can be seen that with the increase of curing temperature the tensile strength, elongation at break as well as tearing strength all decreased, suggesting that the cross-linking density of the ramie fibers increased. As a result, the flat appearance and crease retention rose with the increasing curing temperature. But above the increasing tendency of the wrinkle resistant effect was rather slow when the curing temperature was above 140°C. Too low curing temperature would not achieve the satisfied wrinkle resistant effect while too high curing temperature would result in significant strength loss and could give rise to color change. To balance the different requirements of strength loss and wrinkle resistant effect, the optimal curing temperature was determined to be 140°C where the tensile strength retention was close to 80% while the flat appearance and crease retention were above grade 3.5.

Likewise, the influences of curing time was studied by keeping the other conditions identical to those employed in the previous resin finishing tests but varying curing time from 1min to 4 min. As indicated in Table 4.6, with the increase of curing time the mechanical properties including tensile strength, elongation at break and tearing strength all depressed. In contrast, the wrinkle resistant got better with the increasing curing time. Similar to the case of curing temperature, the rising tendency of wrinkle resistant effect was very slow. The optimal curing time for the wrinkle resistant treatment of ramie fabrics was determined to be 3 min.

Table 4.5 Effect of curing temperature on the physical properties of ramie fabrics

Curing temperature (°C)	Tensile strength retention (%)		Elongation at break (%)		Tearing strength retention (%)		Flat appearance (grade)	Crease retention (grade)
	W	F	W	F	W	F		
120	88	89	26.9	19.4	86	84	3.0	3.2

130	85	80	25.5	18.1	83	82	3.4	3.7
140	80	79	24.5	17.1	78	74	3.5	4.0
150	76	74	25.0	15.9	76	70	3.5	4.0
160	70	68	23.5	16.2	70	63	3.6	4.0

Tabke 4.6 Effect of curing time on the physical properties of ramie fabrics

Curing time (min)	Tensile strength retention (%)		Elongation at break (%)		Tearing strength retention (%)		Flat appearance (grade)	Crease retention (grade)
	W	F	W	F	W	F		
1	90	90	26.9	19.4	87	85	2.9	3.2
2	83	81	24.5	17.1	83	83	3.2	4.0
3	80	79	23.5	16.0	80	79	3.6	4.2
4	77	74	22.9	15.8	75	72	3.6	4.3

Similarly, the influences of resin content on the wrinkle resistant effect and tensile strength were investigated. As indicated in Figure 4.9, both the flat appearance and crease retention rose as the resin content gradually increased from 30g/L to 130g/L. However the increasing

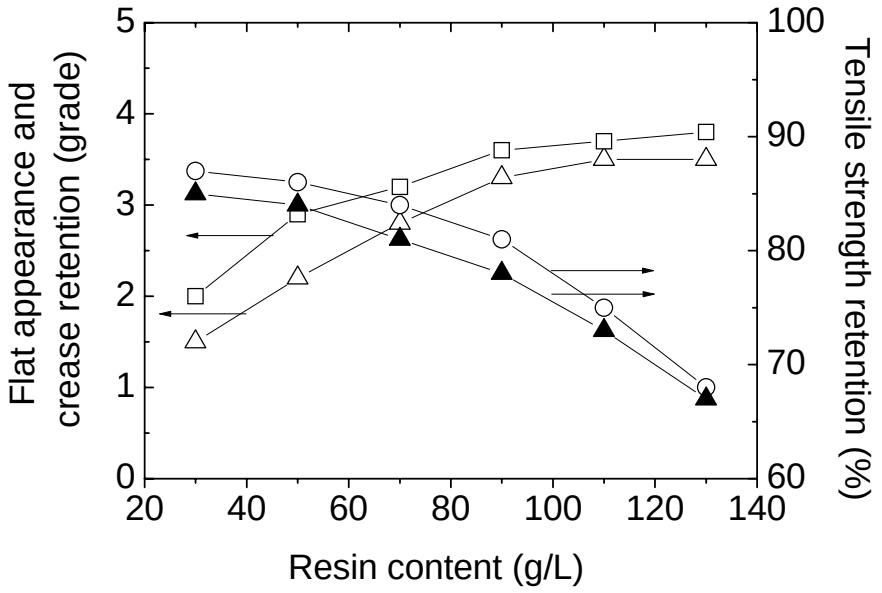

Figure 4.9 Effect of resin content on (Δ) flat appearance, (□) crease retention, (○) tensile strength retention in warp direction and (▲) tensile strength retention in filling direction.

tendency was obviously slowed down when the resin content was above 100g/L. In contrast, the tensile strength retention continuously decreased with the increase of resin content. To balance the wrinkle resistant effect and the tensile strength retention, the optimal resin content was determined as 90g/L where the tensile strength retentions in warp and filling directions were close to 80% in this study.

The influences of reactive PU content on the wrinkle resistant effect and tensile strength were also explored in the same way. As shown in Figure 4.10, the flat appearance and crease retention almost did not change with the PU content variation, which further proved that the presence of PU molecules on the ramie fibers contribute less to wrinkle resistant effect. But the tensile strength retention in warp and filling directions rose with the increase of the PU content. To balance the wrinkle resistant effect and the tensile strength retention, the optimal resin content was determined as 90g/L where the tensile strength retentions in warp and filling directions were close to 80% in this study. However with increase of the PU content the handle of the ramie fabrics got worse gradually. By considering both strength protection effect and soft hand

of ramie fabric, the optimal PU content was 100g/L in this study.

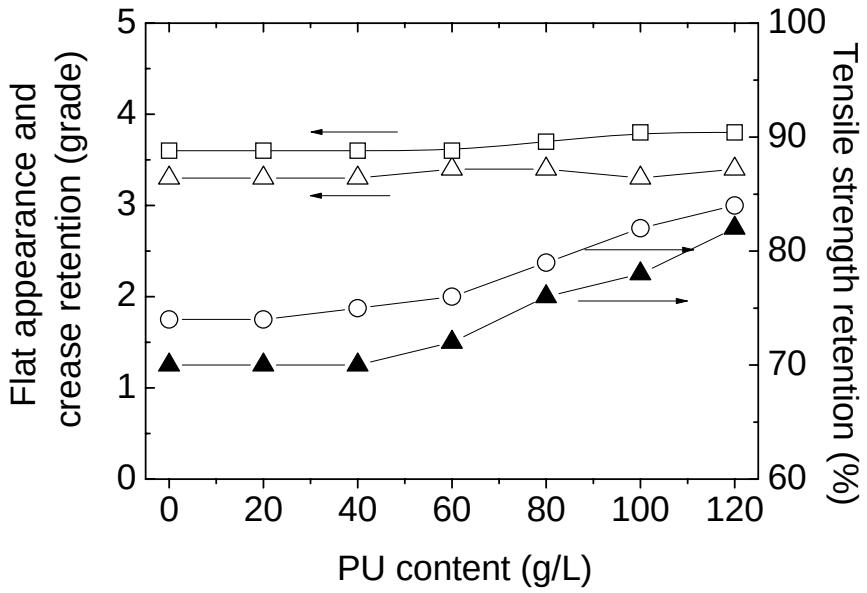

Figure 4.10 Effect of PU content on (Δ) flat appearance, (□) crease retention, (○) tensile strength retention in warp direction and (▲) tensile strength retention in filling direction.

4.3.5 Wrinkle resistant durability after repeated washings

To examine the wrinkle resistant durability after many cycles of laundry, all the ramie fabrics were treated in the optimal conditions. The flat appearance and crease retention evaluations were performed on the ramie fabrics subjected to different washings. The wrinkle resistant durability were compared among the ramie fabrics untreated, treated by liquid NH_3, finished by resin, pretreated by liquid NH_3 and then finished with resin as well as pretreated by liquid NH_3 and finished by resin with PU as protector. For each kind of fabrics, five fabric samples were evaluated for averaging and the experimental results are summarized in Table 4.7.

Table 4.7 Wrinkle resistant durability after repeated laundry cycles.

Fabrics	Flat appearance after repeated washings (grade)			Crease retention after repeated washings (grade)		
	1	5	10	1	5	10
Untreated	1.0	1.0	1.0	1.0	1.0	1.0
Treated with liquid NH_3	2.0	1.5	1.0	3.0	2.5	1.5
Treated with Resin	3.0	3.0	2.0	3.5	3.0	2.5
Treated with liquid NH_3 + Resin	3.5	3.3	3.0	4.0	3.8	3.5
Treated with liquid NH_3 + Resin + PU	3.5	3.5	3.0	4.1	3.7	3.5

As would be expected, the flat appearance and crease retention decreased with the increase of washing times. The wrinkle resistant effect of the ramie fabrics experienced liquid NH_3 pretreatment prior to resin finishing was higher than that of the fabric treated only with resin by 0.5-1 grade, which is consistent with the experimental results mentioned above. It is also noted that the flat appearance and crease retention of the ramie fabrics subjected to liquid NH_3 treatment before resin finishing were decreased by only 0.5 grade. The flat appearance and crease retention of these ramie fabrics were all above 3.0 grade, which is better than those the ramie fabric finished only with resin. This should be ascribed to the swelling effect of ramie fibers caused by liquid NH_3 treatment, and as a consequence the elasticity of the ramie fibers was raised greatly. The increased elasticity was favorable for the wrinkle resistant durability in repeated washings.

4.4 Conclusions

In this study, the application of batch type liquid NH_3 technique for wrinkle resistant treatment of ramie fabric was studied. The liquid NH_3 treatment was proved to decrease the crystallinity of ramie fibers and bring about apparent swelling effect to the fibers. As a result, the accessibility of the ramie fabrics treated by liquid NH_3 was elevated. The liquid NH_3 treatment gave rise to the decrease of dyeing rate but resulted in the increase

of equilibrium dye uptake. The liquid NH_3 pretreatment prior to wrinkle resistant resin finishing could enhance the wrinkle resistant effect and also reduce the strength loss. Employing reactive PU emulsion in resin finishing could raise the strength retention of the ramie fabric without influencing wrinkle resistant effect since the reactive PU molecule could react with ramie fibers and thus played the role of strength protector. The influences of wrinkle resistant treatment conditions were explored systematically. The optimal conditions was thus determined in which the curing temperature was 140^{o}C, curing time 3 min, cross-linking resin content 90 g/L and reactive PU content 100 g/L. After 10 laundry cycles, the flat appearance and crease retention of these ramie fabrics pretreated by liquid NH_3 prior to resin finishing were all above grade 3.0 which is better that those the ramie fabric finished only with resin. The increased elasticity brought by the liquid NH_3 treatment was favorable for the keeping the wrinkle resistant durability in repeated washings. Therefore the liquid NH_3 pretreatment and the reactive PU protector were much helpful for elevating wrinkle resistant effect of ramie fabrics but reducing strength loss.

CHAPTER 5
ELECTROMAGNETIC SHIELDING FINISHING OF RAMIE FABRIC USING SUPERCRITICAL CO_2 TECHNOLOGY

5.1 Introduction

With the development of science and technology, people are exposed to the increasing pollution of electromagnetic (EM) radiation. EM waves have harmful effects on mankind health [152, 153]. To solve EM interference problems, the development of EM shielding (EMS) fabrics has attracted increasing attention, and many novel technologies have been applied to date [105, 152-155]. However, most of investigations on the EM shielding (EMS) fabrics were based on the synthetic fibers. Fewer attempts have been made on the development of EMS fabrics with natural fibers. This study is aimed to develop EMS ramie fabrics via electroless copper plating process.

Ramie fiber has many unique properties, including a high Young's modulus, a high degree of the polymerization, orientation, and crystallinity [78, 91]. Therefore, it has some disadvantages in the fabrication process, such as poor spinning ability, easy corrugation, and poor dyeing ability. Moreover, it causes disgusting feelings of stinging or itching when it is used as a textile and in contact with human skin. Thus, ramie fibers must be pretreated before dyeing and finishing. In general, the pretreatment procedure through chemical modification of the ramie fibers is rather long and causes heavy pollution to the environment. Therefore, it is important to develop a new and effective treatment for ramie fiber and fabric.

Recently, the supercritical fluid technique has been attracting much attention as an environmentally benign process [106, 107, 156, 157]. Supercritical fluids have a higher diffusion rate and a lower viscosity than liquids. Supercritical fluids are widely used in chemical extraction, polymerization of polymers, textile dyeing and impregnation of

desired additives into the matrices [77, 80, 83, 85, 87-90, 105, 156, 158-160]. Supercritical carbon dioxide ($scCO_2$) is inexpensive, essentially nontoxic, and nonflammable, has easily accessible critical conditions (T_c = 31°C and P_c= 7.37 MPa) and can be recycled. Many efforts have been made on the applications of $scCO_2$ in textile processing in the past two decades. But the treatment of ramie fabric with $scCO_2$ has been rarely reported.

In this study, the $scCO_2$ was employed in the pretreatment of ramie fabrics. It is found that the impurities, especially lignin of ramie fibers could be removed apparently by $scCO_2$ under appropriate conditions. Meanwhile, the microstructure of the ramie fiber also changed, which could give rise to the increase of the absorbency of the ramie fibers to additives. The impregnation of Palladium (II)-hexafluoroacetylacetonate ($Pd(hfa)_2$) into the ramie fibers was accomplished in $scCO_2$ fluid at 150°C whereby the surface was coated with a film of Palladium as catalyst. Afterwards, the pretreated ramie fabrics were coated with copper (Cu) via an electroless plating process. It was proved that the Cu plated ramie fabrics exhibited high electrical conductivity and good EMS effect.

5.2 Experimental

Materials

The ramie fabrics were dried in a vacuum oven for 24h and weighed before using. The carbon dioxide (purity: 99.99%) was purchased from the Uno Oxygen Co., and used as received. $Pd(hfa)_2$ and ethanol (EtOH) were purchased from the Aldrich Chemical Co., and used without further purification. Swelling agent was provided by Clariant Co. Electroless copper plating solution containing ATS-ADDCOPPER IW-A, ATS-ADDCOPPER IW-M, ATS-ADDCOPPER C was bought from the Okuno Chemical Industry Co., Ltd.

Pretreatment in $scCO_2$

All experiments were performed on a batch-type supercritical extractor (SFE System

2200, ISCO, USA). The illustration of the apparatus is demonstrated in Figure 1. The pretreatment of the ramie fabrics was conducted in a $10cm^3$ sample cartridge, which could be inserted or extracted from a high-pressure stainless-steel vessel being sealed with a plug at one end and with a high-pressure needle valve at the other end. After heating the sample to a specific temperature, the $scCO_2$ was injected into the stainless-steel vessel via the high-pressure syringe pump to the desired pressure. The testing sample was then treated for a certain time at a certain constant temperature and pressure. In order to enhance the swelling effect of $scCO_2$ for the ramie fabrics, a certain amount of swelling agent was added into the $scCO_2$ treating system. After the supercritical process, the sample was taken out after decompression. Finally, the pretreated fabric samples were dried and weighed individually so as to assess the weight losses of the ramie fabrics.

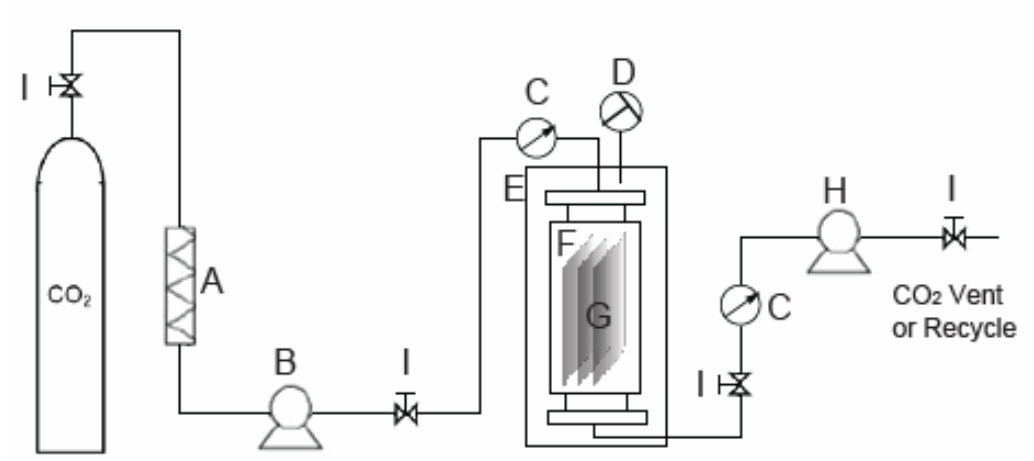

Figure 5.1 Illustration of the $scCO_2$ equipment. (A) cooling unit. (B) high-pressure pump. (C) pressure gauges. (D) thermometer. (E) heater and high-pressure stainless-steel vessel. (F) sample cartridge. (G) sample. (H) cleaning pump. (I) valves.

2.3 Electroless Cu plating

The impregnation of $Pd(hfa)_2$ into ramie fabrics was conducted in the $scCO_2$ fluid at 150 °C. Before sealing the sample cartridge, a glass filter was placed over the ramie fabrics without mutual contact. A certain amount of organometallic complex powder,

calculated in 1% of the weight of the ramie sample, was placed on the glass filter. After the desired temperature (150 °C) was reached, the sealed sample cartridge was placed in the stainless-steel vessel, and then carbon dioxide was added via the high-pressure syringe pump to the desired pressure. The impregnation was carried out for 15 or 60 min. The Cu plating was finished via an electroless Cu plating way in which the electroless Cu plating solution was made from ATS-ADDCOPPER IW-A ATS-ADDCOPPER IW-M ATS-ADDCOPPER C and deionized water under well mixing. The ramie fabrics coated with Pd catalyst were dipped into the electroless copper plating solution at 42°C for some tine under magnet stirring or ultrasonic irradiation. Eventually, the fabrics were kept in a vacuum oven for 24 h for eliminating any moisture in the fibers.

Characterization

Thermogravimetric analysis (TGA) was used to analyze the thermal decomposition of the Pd complex by TG/DTA32 (Seiko Instruments, Inc.). The TGA experiments were carried out at a heating rate of 10 °C/min under the protection of argon purging. The content of lignin in the ramie fabrics was measured according to the Chinese standard GB5889-86. The surface of the treated and untreated ramie fibers were observed by a Hitachi S-2600HS scanning electron microscope (SEM). The sectional morphology of the treated and untreated ramie fibers was viewed by a Nikon Microscope. The ramie fabrics impregnated with $Pd(hfa)_2$ were analyzed by X-ray photoelectron spectroscopy (XPS) to verify the presence of Pd on the fiber surface. For the XPS, an ULVAC Φ5500 spectrometer with Mg-Kα excitation (15.0 kV, 300 W, φ=100 μm) under a vacuum pressure of 1×10^{-8} Pa was used. Also, the plated surface morphology of the sample was examined by the Hitachi S-2600HS SEM. The surface resistivity of the plated fabric was measured by the four point probe method using a Roresta AP MCP-T400 (Mitsubishi Petrochemical Co., Ltd.). The electromagnetic shielding effectiveness was measured by the KEC (Kansai Electronic Industry Development Center) method.

5.3 Result and discussion

5.3.1 Influences of $scCO_2$ pretreatment

The chemical compositions of the ramie fiber are usually divided into two parts: cellulose and non-cellulose compounds. Cellulose compounds form the fibrillar cell of the ramie fiber and are the dominant component of the fiber. Non-cellulose compounds including hemicellulose, pectin, oil, wax, lignin and other impurities exist between the fibrillar cells or adhere on the surface of the fibrils. When the ramie fibers are treated with $scCO_2$, due to the high dissolving capacity of the $scCO_2$, the organic impurities adhered on the fiber surface can be dissolved and eliminated from the fiber surface. Meanwhile the tacky materials of the ramie fabrics can also be removed. Figure 5.2 shows the SEM images of the pretreated and untreated ramie fibers. It can be seen that a large amount of impurities exists on the surface of the untreated fibers. But after being pretreated with the $scCO_2$, the surfaces of the ramie fibers become apparently smoother, suggesting that the impurities existing naturally in the ramie fibers and the processing auxiliaries such as spinning oil, lubricant, size, etc, adhering on the ramie fabric in spinning and weaving process dissolved in the $scCO_2$ fluid and were removed from the ramie fabrics.

Figure 5.3 presents the influence of temperature and time on the weight loss of ramie fabric during the $scCO_2$ process conducted under the constant pressure of 25MPa. It can be seen as the temperature increases from 80^oC to 120^oC the weight loss of the ramie fabric increases. This is because on one hand the increase of temperature raises the diffusiveness of CO_2 molecules. On the other hand, higher temperature promotes the thermal expansion of ramie fibers, resulting in the increase of their free volume. Therefore the CO_2 molecules can more easily diffuse into the ramie fibers and extract the impurities.

(A)

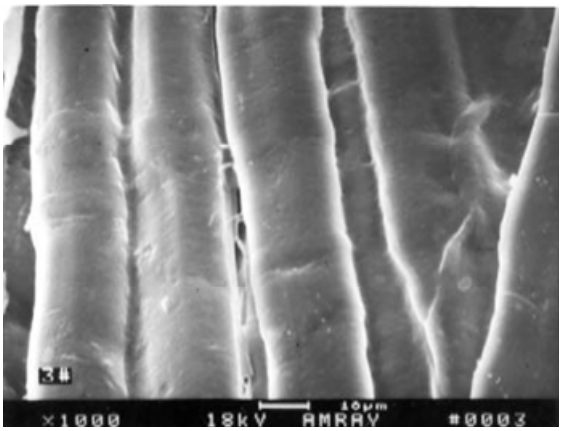

(B)

Figure 5.2 SEM of the treated and untreated ramie fibers. A：before pretreatment B: after pretreatment.

Figure 5.4 presents the influence of temperature and time on the weight loss of ramie fabric when the temperature was set at 150^{o}C. It is evident that the weight loss increases with the increase of pressure due to the increase of the density of $scCO_2$ at the certain temperature. This is because the intermolecular distance of the CO_2 molecules decreases and thus the interaction between solvent and solute increases leading to the solubility increase of the impurities in $scCO_2$ fluid.

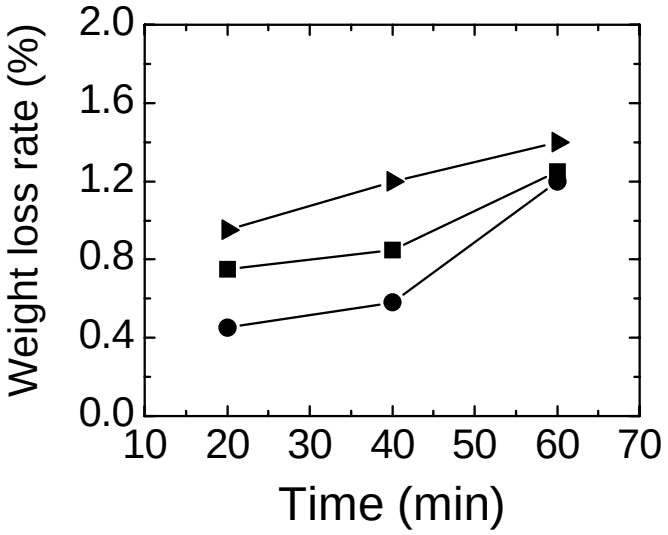

Figure 5.3 Influences of temperature and time on weight loss under the pressure of 25MPa. (●) 80°C; (■) 100°C; (►) 120°C.

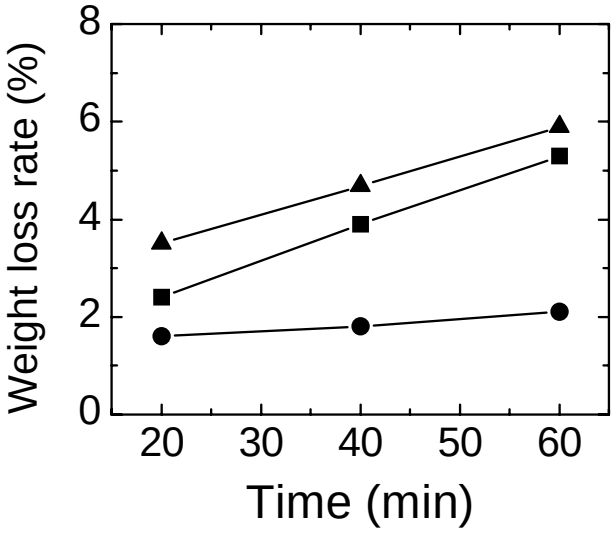

Figure 5.4 Influences of pressure and time on weight loss at the temperature of 150°C. (●) 20MPa; (■) 25MPa; (▲) 30MPa.

Figure 5.5 shows the TGA thermograms of the untreated and treated ramie fabrics. It can be seen that the initial decomposition temperatures of the pretreated ramie fabrics are obviously higher than that of the untreated fabric. Moreover, the thermal stability of

the ramie fabric pretreated under 100°C is slightly higher than that of the one pretreated at 80 °C. It is supposed that for the untreated ramie fibers the decomposition at lower temperatures is mainly ascribed to the decomposition of impurities. The testing results prove that the $scCO_2$ pretreatment indeed removed the impurities and resulted in the rise of initial decomposition temperature. In addition, higher treatment temperature gives rise to better thermal stability, i.e., higher removal ratio of impurities.

It is well known that ramie fibers contain a large amount of lignin which results in bad spinning ability and lower absorbency to other additives. In general, the lignin in ramie fibers has to be removed in the strong alkaline solutions, resulting in heavy environmental pollution. The authors studied the removal of the lignin when the ramie fabrics were pretreated at 150°C in $scCO_2$ fluid. Table 5.1 presents the removal of lignin under different conditions. It can be seen that the removal ratio of lignin in ramie fabrics varies in the range ~48-69% under the different treatment conditions. In general, the removal of lignin increases with the increase of treatment temperature, pressure and time.

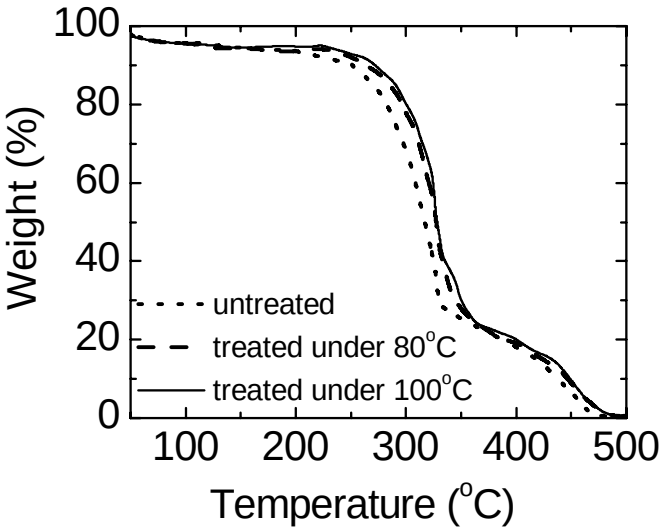

Figure 5.5 TGA tests of the treated and untreated ramie fibers.

In order to raise the lignin removal further, a certain sort of swelling agent was employed in the $scCO_2$ pretreatment when the temperature was set at 150°C, pressure was 30MPa and treatment time was 60min. As a result, the lignin removal was raised to

over 80%. Therefore it is possible to replace the traditional chemical process for the elimination of the lignin in ramie fibers with $scCO_2$ fluid technique by selecting appropriate conditions.

In order to examine the swelling effect of $scCO_2$ pretreatment on the ramie fibers, the cross sectional morphology of the pretreated and untreated ramie fibers were observed via microscopy. As shown in Figure 5.6, the pretreated fibers are mostly larger than that of the untreated fibers in diameter. Most of the untreated ramie fibers have their lumens close. In contrast, those of the treated ramie fibers apparently open. This suggests that

Table 5.1 Effect of the $scCO_2$ pretreatment upon lignin removal of ramie fibers

Pressure (MPa)	Treatment temperature (^oC)	Time (min)	Lignin removal (%)
20	100	40	58.4
	120	20	56.6
	150	60	69.1
25	100	20	48. 3
	120	60	66.8
	150	40	65.9
30	100	60	65.3
	120	40	62.1
	150	20	62.6

$scCO_2$ can result in the swelling of the ramie fibers, which may increase their absorption for other additives in dying or finishing.

Table 5.2 shows the influences of $scCO_2$ pretreatment on the warp density, pick density and capillary effect of the ramie fabrics. It can be seen that the swelling of the ramie fiber led to the increase of pick density but the decrease of warp density. Meanwhile, and the wetting time of the ramie fabrics was shortened greatly (see Table

5), indicating the absorbency of the ramie fabric was increased significantly. The increase of the absorbency of the ramie fibers resulted from the elimination of the hydrophobic organic impurities by $scCO_2$ fluid and the expansion of the lumens in the ramie fibers. Thereby the pretreatment by $scCO_2$ fluid favors the following processes such as dyeing, printing and finishing of the ramie fabrics.

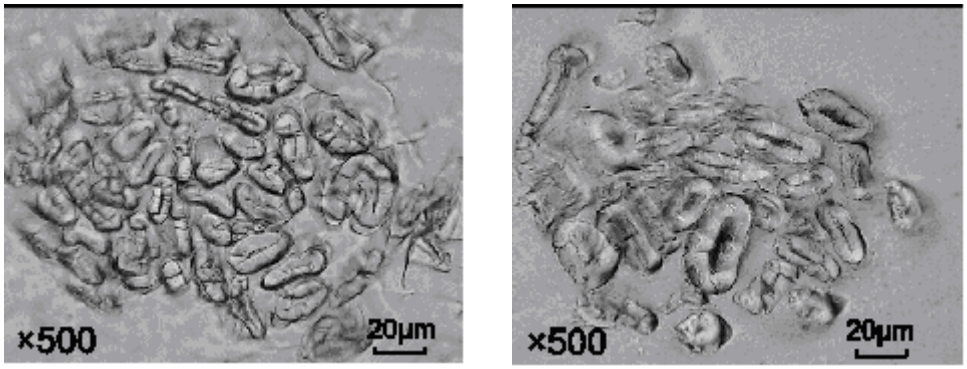

(A) **(B)**

Figure 5.6. Cross sectional view of the treated and untreated ramie fibers multiplied by 500 times A：before treatment B: after treatment

5.3.2 Electroless copper plating

$Pd(hfa)_2$ can be easily dissolved in $scCO_2$ due to its hydrophobic feature. Because of low viscosity and high diffusiveness of $scCO_2$, the $Pd(hfa)_2$ contained in the $scCO_2$ fluid can be impregnated into the polymers [105]. Thermal analysis proved that the thermal decomposition of $Pd(hfa)_2$ occurred in the temperature range 90-154°C [105]. After being heated to the temperature range, the $Pd(hfa)_2$ has its ligands removed, which results in a layer of Pd catalyst coating on the surface of polymer fibers. When a fabric coated with palladium was immersed in a copper plating solution a copper film could form on the surface of the fabric because of the reduction reaction of copper ions. In addition, CO_2 is non-polar and thus is difficult to diffuse into hydrophilic natural fibers such as cotton and ramie. Some polar co-solvents such as methanol (MeOH), ethanol (EtOH), acetone, etc., were reported to be effective for increasing the solubility of polar

substance in scCO2 fluid [161, 162]. In this study, the impregnation of Pd(hfa)2 into ramie fabrics were conducted at 150oC and 20MPa for 15min or 60min in scCO2 fluid. In some experiments, some EtOH calculated in 5.6% of the weight of scCO2 fluid was employed.

Table 5.2 The swelling effect of the scCO2 pretreatment on the ramie fabrics

Pressure (MPa)	Temperature (^oC)	Time (min)	Warp density	Pick density	Capillary Effect (sec)
Untreated fabric			227.3	193.6	56.8
20	60	40	181.8	204.3	33.4
	80	20	184.8	204.3	39.4
	100	30	184.8	206.5	45.7
25	60	30	163.6	204.3	36.5
	80	40	193.9	206.4	25.5
	100	20	193.9	204.3	25.4
30	60	20	184.8	202.1	23.5
	80	30	190.9	204.2	19.5
	100	40	193.9	206.4	29.8

Figure 5.7 shows the appearance changes of a ramie fabric in the electroless copper plating. When the ramie fabric was kept in the $scCO_2$ fluid containing $Pd(hfa)_2$ for 15min or 60 min at 150 °C the sample changed from original light gray (see Figure 5.7 (A)) to dark gray in color (see Figure 5.7 (B)), suggesting some Pd catalyst deposited on the surface of the ramie fibers. When a ramie fabric coated with Pd catalyst was placed into the Cu plating solution, it turned into brown yellow color in 5 min (see Figure 5.7 (A)), indicating formation of the copper film on the ramie fabric.

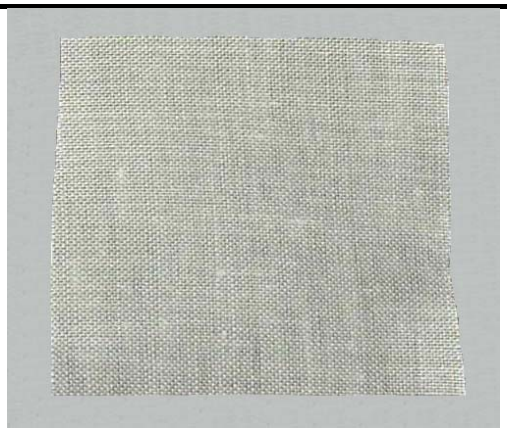

(A)

(B)

(C)

Figure 5.7 Appearance changes of a ramie fabric in the electoless copper plating. (A) Original ramie fabric; (B) After impregnation with $Pd(hfa)_2$; (C) After Cu plating.

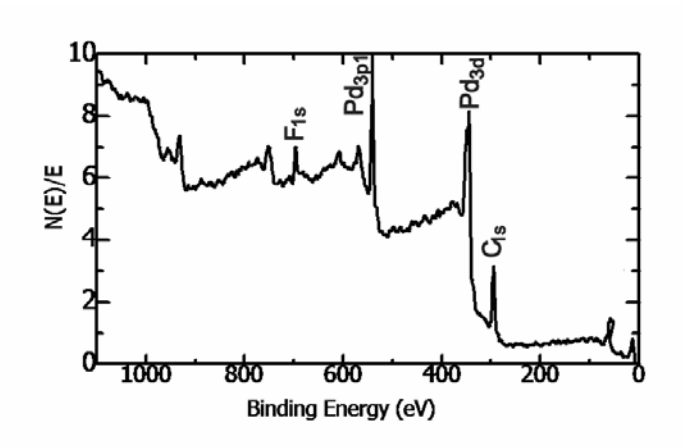

(A)

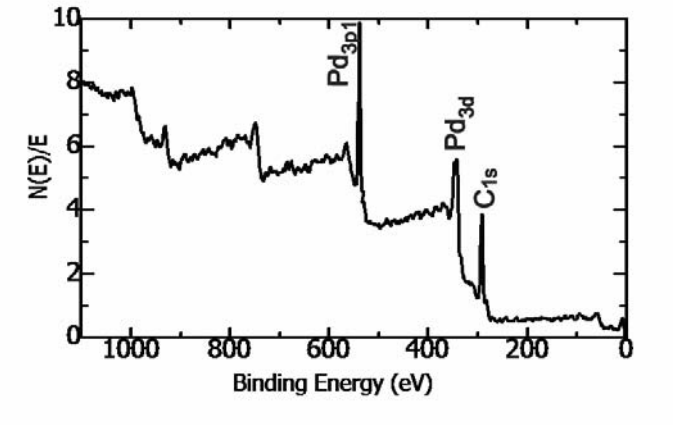

(B)

Figure 5.8 XPS spectra of the ramie fabrics impregnated with $Pd(hfa)_2$. (A) Treated for 15min without ethanol being employed; (B) Treated for 60 min with ethanol being employed.

The atomic compositions of the surface of the ramie fabrics impregnated with $Pd(hfa)_2$ under different conditions were investigated by XPS. Figure 5.8 (A) shows the XPS spectrum of the ramie fabric impregnated with $Pd(hfa)_2$ for 15min without EtOH as co-solvent while Figure 5.8 (B) presents that of the sample impregnated with $Pd(hfa)_2$ for 60min with EtOH as co-solvent. As shown in Figure 5.8 (A) and (B), the intense peak at ca. 288eV is caused by the emission of the 1s level electrons of C atoms. Another two intense peaks at ca. 561eV and ca. 335eV are ascribed to the emission from

the 3p1 level and 3d level electrons of the Pd atoms, indicating the presence of Pt catalyst on both of the two samples. In Figure 5.8 (A), the peak at ca. 686eV is ascribed to the emission from the 1s level electrons of F Original ramie fabric; (B) After impregnation with $Pd(hfa)_2$; (C) After Cu plating. atoms whereas the peak disappears in Figure 5.8 (B). The atomic compositions of the ramie fabrics treated under different conditions were summarized in Table 5.3. It can be seen that as the impregnation time increases from 15min to 60min the Pd content on the surface of the ramie fibers increases while the F content decreases, suggesting that with the increase of impregnation time more $Pd(hfa)_2$ was impregnated into the ramie fibers and gradually transformed into Pd film at this high temperature. In addition, it is found that the presence of EtOH in the scCO2 greatly raised the Pd content and reduced the F content. This suggests that EtOH promoted the impregnation of $Pd(hfa)_2$ into ramie fibers since EtOH enhanced the compatibility of ramie fibers and scCO2.

Table 5.3. Atomic compositions of ramie fabrics treated with $Pd(hfa)_2$ and Cu plating effect.

Impregnation conditions		Atomic composition of the fabric impregnated with $Pd(hfa)_2$		Cu plating effect	
Time (min)	EtOH (wt%)	Pd/C ($\times10^{-2}$)	F/C ($\times10^{-2}$)	Cu content (g/m^2)	Surface resistance (Ω/cm^2)
15	-	3.78	1.37	17.9	0.72
15	5.6	5.42	0.38	19.6	0.59
60	5.6	7.27	0	20.2	0.51

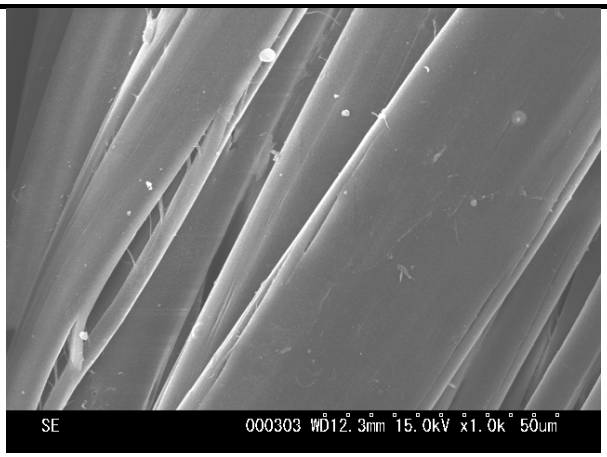

(A)

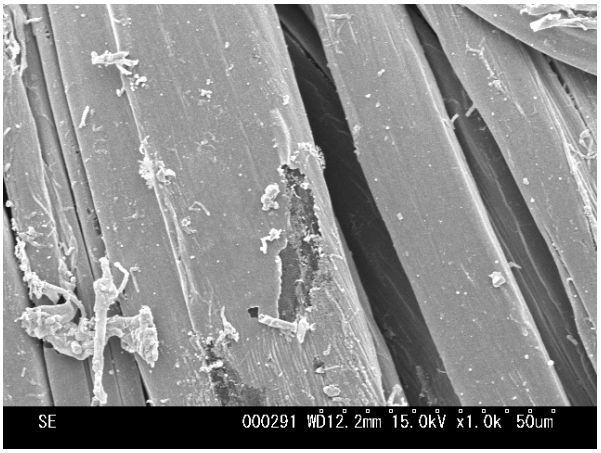

(B)

Figure 5.9 SEM images of the ramie fibers before and after Cu plating. (A) After being pretreated with $scCO_2$ (B) after Cu plating.

Figure 5.9 shows the SEM images of the ramie fibers before and after Cu Plating. Before Cu plating the surface of the ramie fabric is very smooth, thanking to the pretreatment of scCO2 after which most of the impurities of the ramie fibers was removed (see Figure 9 (A)). After Cu plating for 5min the surface of the ramie fibers became rather coarse, suggesting Cu atoms depositing on the surface of the ramie fibers (see Figure 9 (B)). The Cu plating effects of the ramie fabrics are summarized in Table 5.3. As would be expected, with the increase of impregnation time the Cu content increased and the surface electric resistance decreased. If the impregnation of $Pd(hfa)_2$

was conducted with EtOH as co-solvent the resultant Cu plating fabrics exhibited higher Cu content and lower surface electric resistance.

5.3.3 Shielding effect of the Cu plated ramie fabrics

The shielding effect tests were performed on two fabrics: the one prepared via the impregnation for 60 min with EtOH as co-solvent and the other one produced by the impregnation for 15 min without EtOH as co-solvent. As shown in Figure 5.10, the electromagnetic shielding effectiveness of the ramie fabric treated with EtOH as co-solvent in $Pd(hfa)_2$ impregnation reached 92–67 dB in the frequency range of 10–1000 MHz. In contrast, without EtOH as co-solvent in $Pd(hfa)_2$ impregnation the resultant Cu plated ramie fabric exhibited lower electromagnetic shielding effectiveness of 89–63 dB in the same frequency range. Both of the two kinds of Cu plated ramie fabrics exhibited good electromagnetic shielding effect. Therefore this study presents an effective method to develop electromagnetic shielding fabrics from hydrophilic natural fibers.

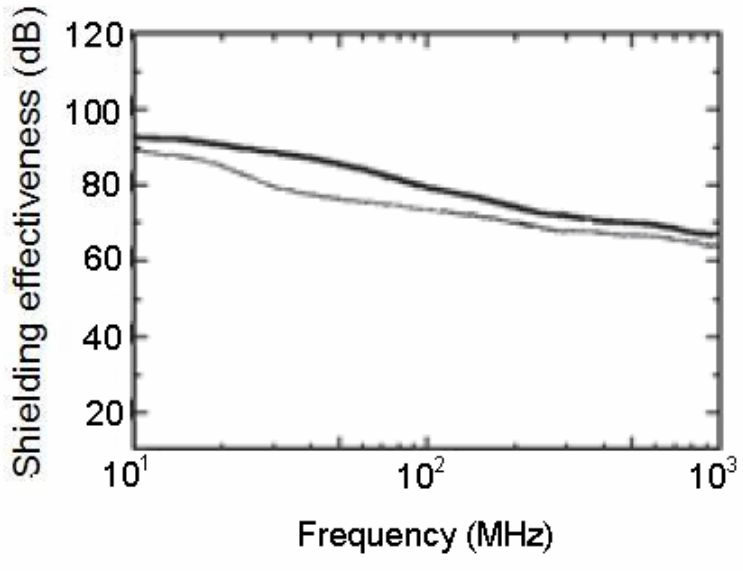

Figure 5.10 Electromagnetic shielding effect of the ramie fabrics coated with copper. Thick line impregnation for 60 min with ethanol as co-solvent; thin line impregnation for 15 min without ethanol.

5.4 Conclusions

This study is concerned with the application of $scCO_2$ fluid technology for the electroless Cu plating on ramie fabrics. It was found that the $scCO_2$ fluid could remove the impurities of the ramie fibers, especially at higher temperature, higher pressure and in longer treatment time. In comparison with the conventionally method where a large amount of strong alkaline solutions is employed, the $scCO_2$ fluid is a better way to eliminate lignin from the ramie fibers. In particular, the removal of lignin in $scCO_2$ fluid could be raised to over 80% in presence of some swelling agent. The $scCO_2$ fluid could result in the swelling and expansion of ramie fibers, which increases the absorbency of the ramie fibers to additives. By using $scCO_2$ fluid, the $Pd(hfa)_2$ could be impregnated into the ramie fibers under appropriate conditions. As co-solvent, ethanol could promote the impregnation of Palladium complex into ramie fibers. After the Cu plating, the ramie fabrics deposited with Palladium were plated by a Cu film whose content was ca. 18-20g/m^2. The Cu plated ramie fabrics exhibited good shielding effect. Their electromagnetic shielding effectiveness was ca. 63-92 dB in the frequency range 1-1000 MHz. This study is supposed to explore a new way for the application of $scCO_2$ fluid in the textile industry regarding the hydrophilic natural fibers.

CHAPTER 6

MULTIFUNCTIONAL FINISHING OF RAMIE FABRIC USING TITANIUM DIOXIDE NANOPARTICLES

6.1 Introduction

Nowadays, global trends in textile industry are oriented towards development and manufacturing of high-added value products with multifunctional properties. In addition to fashion and comfort demands, the garments today are desired to render multiple functions [132]. With the advent of nanotechnology, a new area has developed in the realm of textile finishing. Through coating nanoparticles on fabric, the high quality textile and clothing with functions such as self cleaning, water repellence, antibacterial property, UV protection and photocatalytic feature were developed. The multifunctional properties give rise to added value to textile and clothing and raise their competiveness.

Among all the nanoparticles, titanium dioxide (TiO_2) nanoparticles drew the most attention from academia and industry due to their excellent properties, nontoxic feature and low cost [163]. The application of TiO_2 nanoparticles to textile materials has been the object of a good number of studies aimed at producing finished fabrics with multifunctional properties. The TiO_2 loaded fabrics showing the characteristics such as UV protection [110, 117], self cleaning [110, 112, 113, 119, 128, 133], antibacterial property [114], harmful gas removing [136, 137] and even wrinkle resistance [164] have been reported. However, most of the investigations on finishing with TiO_2 nanoparticles were conducted with cotton or polyester fabric. Few attempts have been made on the nano finishing of ramie fabric. This study is aimed to develop multifunctional ramie fabrics through finishing with TiO_2 nanoparticles.

Various techniques have been developed and employed to produce nano TiO_2 coated fabrics, such as the sol-gel method, vacuum evaporation, sputtering, and dip-coating. [163] The sol-gel method is one of the most widely used techniques because of its simple process. This kind of method, however, does not adapt to preparing uniform and

compact functional films in a large area. The bad adhesive force between the fabric and the function films also cannot satisfy the need for lengthy and repeated usage. In addition, the chemical pollution caused by a wet process is another serious disadvantage. Chemical vapor deposition and magnetron sputtering can offer better adhesion between the fabric and the function films. But these techniques require some high-temperature complicated equipment and are specific to the surface to be coated [163]. Coating of TiO_2 by dip-coating is most widely used by most researchers because the technique is easy and does not require any complicated equipment. [136]

There are two major technical challenges when using TiO_2 nanoparticles for textile finishing via dip-coating. At first, it is difficult to produce stable and uniformly dispersed TiO_2 aqueous suspension because of the intense aggregation tendency TiO_2 nanoparticles. This solution is dependent on appropriate selection of dispersant and optimization of dispersion condition. Secondly, the interaction between the TiO_2 nanoparticles and the fabric substrate is relatively weak and therefore the finishing durability would normally be interfered [115, 117] . In most cases, in order to achieve optimum adhesion of the nanoparticles to the textile substrates, modification of either the nanoparticles or fabric surface is necessary before nano finishing. For instance, before nano finishing the cotton fabrics were activated by radiofrequency (RF) plasma, microwave (MW) plasma or UV irradiation for introducing negatively charged functional groups to anchor TiO_2 to the textile surface [122] . In another previous study, Meilert *et. al.* used chemical spacers (succinic acid, 1,2,3-propanetricarboxylic acid, and 1,2,3,4-butanetetracarboxylic acid) to attach TiO2 particles to cotton fabric surfaces [128]. In this process, the spacers were attached on the cotton by the formation of ester bonds, which are then used to anchor TiO2 particles. The results showed that TiO_2 coated cotton fabric possessed stable self-cleaning properties. Apart from modification of nanoparticles and fabrics, nanoparticles can also be fixed to the substrate by the use of functional polymers.

In this study, in order to produce multifunctional ramie fabric with nano TiO_2, aqueous dispersion containing TiO_2 nanoparticles was prepared for making up working bath. A kind of hydrophilic silica aerogel was used as dispersant. The conditions of the

dispersion of nanoparticles were optimized. To enhance the nano finishing durability, the ramie fabric samples were pretreated by citric acid before coating TiO_2. A kind of thermal reactive polyurethane (PU) emulsion was employed as the binder of TiO_2 nanoparticles. The photocatalytic and antibacterial properties as well as the UV protective capability of the TiO_2 loaded ramie fabrics were examined. The citric acid pretreatment and the PU emulsion were compared with respect to enhancing the washing durability. This study proved the newly developed TiO_2 coated ramie fabrics exhibited excellent UV protection, good antibacterial property and high capability for decomposing formaldehyde. Formaldehyde is a common indoor pollutant and irritant and is often used in adhesives, resins, textiles, and consumer products. It is supposed that when the newly developed TiO_2 coated ramie fabrics are used in decorative things, such as bedding, coat of seat and indoor curtain, through catalysis of ultraviolet lamp-house of daylight or lamplight, they can result in the degradation of harmful gases such as formaldehyde and purify the indoor air, providing comfortable and healthy living environment for mankind.

6.2 Experimental

Materials

The ramie fabric (21×21s) (provided by Huling Jindi Group, Chongqin, China) was desized, scoured and bleached prior to using. The TiO_2 nanoparticles were provided by PENZHIHUA Iron & Steel (Group) Co. (Penzhihua, China). The particle size of the nano TiO_2 is about 10-20 nm. The chemicals including sodium dodecyl sulfonate (SDS), trimeric sodium phosphate, sodium hexameta phosphate, sodium silicate, sodium hypophosphate and citric acid of chemical pure grade were purchased from Sinopharm Chemical Reagent Co., Ltd. A hydrophilic silica aerogel powder was provided by Nano High-tech Co., Ltd. (Shaoxing, Zhejiang, China). This white powder product own low density, high specific surface area, high porosity ratio. The PU emulsion DM-3541 was purchased from the DYMATIC Chemicals Inc. (Foshan, Guangdong, China). The water used in our experiments was distilled for three times in our laboratory prior to using.

Preparing aqueous suspension of TiO_2 nanoparticles

The TiO_2 nanoparticle suspension was prepared under the agitation via an ultrasonic homogenizer (Ningbo Scientific Biotechnology Co., Ltd., Ningbo, Zhejiang, China) for a certain time at a given temperature. Then a certain amount of dispersant was added into the TiO_2 nanoparticle suspension. The mixed liquid was further agitated by the ultrasonic waves for another 30 min. The pH of the nanoparticle suspensions were adjusted using HCl or NaOH. After 24 h, some sediment appeared at the bottom of the suspensions prepared with different dispersants under different conditions. Removing the upper suspension, the sediment at the bottom was dried and weighed. Thereof the weight fraction of the dispersed TiO_2 nanoparticles was calculated. The dispersion effect was also evaluated by analyzing the absorbance of the suspensions. At first, the suspensions were subjected to centrifugal operation at 4000 r/min for 40 min. Some of the upper clear liquid was extracting after centrifugal operation and was diluted by 10 times. The light absorbance and transmission of the diluted liquid were measured with the 7200 visible spectrophotometer (UNICO (Shanghai) Instruments Co., Ltd.) at λ=360 nm. According to Beer–Lambert law:

$$A = \varepsilon_m b c_s \tag{6-1}$$

$$A = -\log T \tag{6-2}$$

where A and T refer to light absorbance and transmission, respectively. The parameters ε_m, b and c_s stand for molar absorbance coefficient, the path length of light and the concentration of the solution examined. Higher absorbance means the larger concentration of the solution, i.e, the better dispersion effect. By investigating the influences of dispersants, ultrasonic dispersion time, dispersion temperature and pH value of aqueous suspension, the optimal conditions of the dispersion of TiO_2 nanoparticles were determined. Under the optimal conditions, the TiO_2 aqueous suspension with concentration of 1 wt% was prepared and used as the master TiO_2 suspension for preparing different working baths.

Fabric coating

In order to introduce -COOH groups to ramie fibers, an series of aqueous solution of citric acid in presence of sodium hypophosphate as catalyst (4 wt%) was prepared in

advance. The content of citric acid varied from 2% owf to 7% owf and 10% owf. The ramie fabric samples were immersed in the treatment solution for 1 h. After drying at 90^{o}C for 3 min in a preheated oven, the ramie fabric samples were cured at 150^{o}C for 2min in another preheated oven. These fabrics were then thoroughly washed with cold water and dried at ambient temperature.

The TiO_2 coating of the ramie fabric samples modified by citric acid as well as the untreated original ramie fabric samples were performed via a conventional dip-pad-dry-cure process. At first, a series of working baths were prepared with the TiO_2 aqueous suspension produced under the optimal dispersion conditions and distilled water. In the working baths, the content of TiO_2 varied from 0.2g/L to 0.4g/L, 0.6g/L and 0.8g/L. In order to enhance the washing durability of the coated ramie fabrics the PU emulsion DM-3541 was employed in the working baths. In the working baths, the content of PU emulsion DM-3541varied from 2 g/L to 5 g/L, 10 g/L and 20 g/L. The ramie fabric samples were immersed into a working bath prepared thereof and padded once or twice by the Rapid 354 padding machine Then the wet ramie fabrics were dried in the preheated Werner Mathis AG drying machine at 90 ^{o}C for 3 min and cured in the preheated Mathis Lab dryer at 150 ^{o}C for 2 min. After curing, the cured fabric was ultrasonically washed for 10 min in order to remove TiO_2 nanoparticles having no bonding reaction with ramie fibers. The ramie fabric samples coated with TiO_2 nanoparticles and original untreated ramie fabric samples were washed different times in a domestic electric washing machine according to the AATCC 124 test method.

Evaluation of photocatalytic degradation of formaldehyde

As shown in Figure 6.1, the evaluation of the photocatalytic degradation of formaldehyde by the fabrics coated with TiO_2 nanoparticles was accomplished in a specially designed closure reactive cabinet. The cabinet was equipped with a UV lamp obtained from Shanghai Philips-Yaming Company (light centered at 366 nm). The cabinet was cooled with a cross-flow ventilator to ensure constant temperature for the formaldehyde degradation reaction. A ramie fabric sample was placed in the cabinet. Then the formaldehyde sample with known concentration was injected into the chamber. Afterwards, the fabric sample was exposed to the constant UV irradiation. The

concentration of the formaldehyde was examined after a certain time interval with gas chromatography (Clarus 480 GC, Perkin Elmer). The effect of photocatalytic degradation of formaldehyde is represented by $C/C_0 \times 100\%$ where C_0 is the initial concentration of formaldehyde, and C is the residual concentration of formaldehyde after photocatalytic reaction.

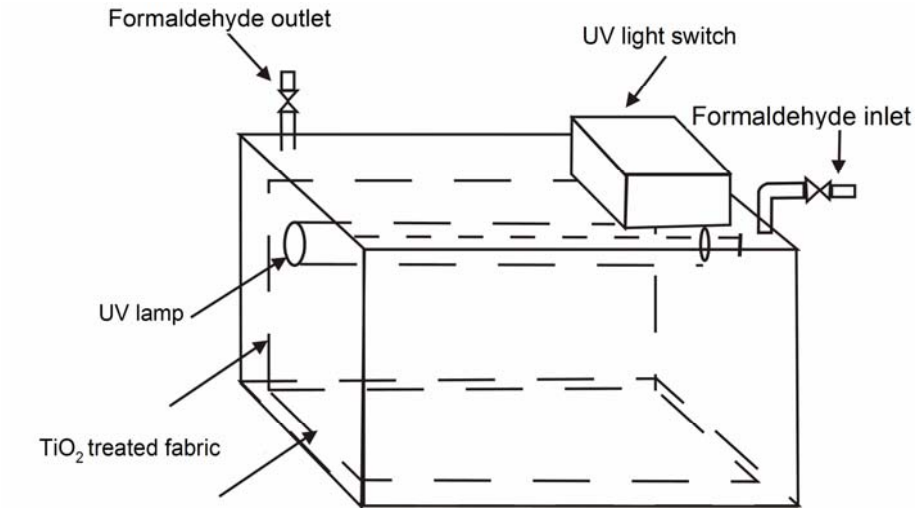

Figure 6.1 Illustration of the evaluation of photocatalytic degradation of formaldehyde.

UV-resistant tests

The UV protection of the fabric specimens was measured in accordance with the Australian/New Zealand Standard AS/NZS 2604 (1998) using the Cary 300 UV-visible spectrophotometer (Varian, USA) with the scope of wavelength ranging from 280nm to 400nm. The value of ultraviolet protection factor (UPF) was recorded and the result of sun protective clothing was classified according to the rated ultraviolet protection factor. The UPF (average of 12 scans) was computed using the following formula:

$$UPF = \frac{\int_{290}^{400} E_\lambda S_\lambda d\lambda}{\int_{290}^{400} E_\lambda S_\lambda \tau_\lambda d\lambda} \tag{6-3}$$

where E_λ corresponds to the relative Erythemal effectiveness, S_λ is the solar spectral irradiance, T_λ is the average spectral transmittance, and $d\lambda$ is the measured wavelength

interval in nanometers (290 nm≤ λ≤400 nm).

Antibacterial tests

The antibacterial effect of ramie fabrics was evaluated on two kinds of bacteria Escherichia coli and Staphylococcus aureus. The microorganisms used in the antibacterial test were obtained from College of Life Science of Sichuan University. Escherichia coli and Staphylococcus aureus were all cultured on Tryptic Soy Broth (TSB) for 24 h at 35-37^{o}C and 200 rev. /min. The potassium hydrogen phosphate buffer solution (0.5M, pH=7.2) was used as the testing medium. Afterwards, 50 mL of sterile potassium hydrogen phosphate buffer solution was added to sterile Erlenmeyer flask (300 mL), which was then inoculated with 0.5 mL of the bacterial inoculum. The zero counts were made by removing 1 ml aliquots from the flask with inoculum, and making 1:10 and 1:100 dilutions in physiological saline solution. 0.1 ml of the 1:100 solution was placed onto a tripton soy agar and after 24 h of incubation at 37 ^{o}C, the zero time counts (initial number of bacterial colonies) of viable bacteria were recorded. Prior to antibacterial test, one gram of a ramie fabric loaded with TiO_2 was weighed and cut into small precise were put into flask with autoclave and sterilized at 120^{o}C for 20 min. Likewise the ramie fabric untreated with TiO_2 was subjected to the same sterilization. The sterilized fabric was put in the flask where 50 ml of sterile potassium hydrogen phosphate buffer solution was inoculated with 0.5 ml of the bacterial inoculum. Then the flask was shaken for 1 h. One hour counts were recorded in accordance with the procedure describe above. The percentage of bacteria reduction (R%) was calculated using the following equation:

$$R = \frac{W - Q}{W} \times 100\% \qquad (6\text{-}4)$$

Where W is the number of bacteria colonies on the control fabric and Q is the number of bacteria colonies on the fabric loaded with TiO_2.

Measurement of tearing strength

The tearing strength of the ramie fabrics loaded with TiO_2 nanoparticles and the untreated ramie fabrics was measured by an Elmendorf tearing tester according the standard ASTM D 1424-1996. Five samples were prepared in the warp direction of each

ramie fabric. Consequently, the tearing strength was separately recorded for each sample and the average results were then reported. Before and after exposure to UV light for a certain time, the tearing strength change of a ramie fabric loaded with TiO_2 was thus investigated.

6.3 Results and discussion

6.3.1 Dispersion of TiO_2 nanoparticles

Influence of dispersants

In this study, the dispersion effect of five kinds of dispersants sodium dodecyl sulfonate (SDS), trimeric sodium phosphate, sodium hexametaphosphate, triethylolamine and hydrophilic silica aerogel was studied. As shown in Figure 6.3, all the five kinds of dispersants exhibited a maximum fraction of dispersed TiO_2 at an optimal dose (wt% of amount of TiO_2) value above and below which the fraction of dispersed TiO_2 decreased dramatically. The hydrophilic silica aerogel exhibited the best dispersion effect. The highest fraction of dispersed TiO_2 was above 65% when the dose of hydrophilic silica aerogel was 0.06 wt% of the amount of TiO_2 nanoparticles. The highest fraction of dispersed TiO_2 was about 35% when SDS was used as the dispersant. According to the maximum fraction of dispersed TiO_2 of the dispersant, the dispersion capability increased in the order SDS, sodium hexametaphosphate, sodium silicate, trimeric sodium phosphate and hydrophilic silica aerogel.

The aqueous solutions of sodium hexametaphosphate, sodium silicate and trimeric sodium phosphate are electrolytes. In the dispersion of TiO_2 nanoparticles using the three kinds of chemicals as dispersants, the static repulsive force dominates the dispersion behaviors. TiO_2 nanoparticles absorb opposite ions from the electrolytes and form electric double layer on the surface of TiO_2 nanoparticles with the presence of electrolytes in water. With the increase of the content of dispersant, the thickness of electric double layer on the surface of TiO_2 nanoparticles increased and raised the static

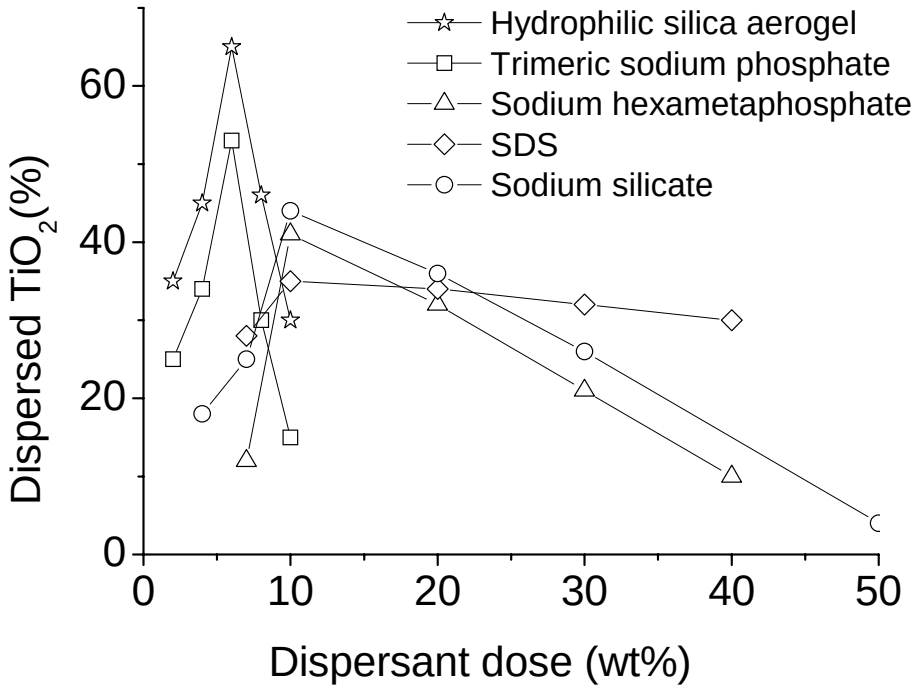

Figure 6.2 Influence of different dispersants on the dispersion effect of TiO_2

repulsive force among the nanoparticles, which favor the dispersion of TiO_2 nanoparticles. But with the further increase of these electrolyte dispersants, the thickness of electric double layer reduced, resulting in the decrease of dispersion of TiO_2 nanoparticles. It can be seen that the optimal contents of sodium hexametaphosphate, sodium silicate and trimeric sodium phosphate for achieving the best dispersion of TiO_2 nanoparticles were 10%, 10% and 6% (wt% of the dose of TiO_2 nanoparticles).

SDS is a kind of typical anionic surfactant which is composed of a highly hydrophilic sulfonic group on one side and a hydrophobic dodecyl chain on the other side in its molecule. The presence of long alkyl chain in SDS molecules results in the steric hindrance effect is more significant while the role of static repulsive force is weakened. In the dispersion of TiO_2 nanoparticles, the anionic groups of SDS were absorbed on the surface of TiO2 nanoparticles because of the Van Der Waals force. It is noted that the dispersion effect of TiO_2 nanoparticles varied less with the change of SDS dose. In contrast, the variation of the three electrolyte dispersants mentioned above results in

great change of dispersion effect. This implies that in the dispersion of the hydrophilic TiO_2 nanoparticles the static repulsive force should be an important influencing factor.

Silica aerogel, also known as "Blue Smoke" or "Frozen Smoke", is the lightest known solid material. As illustrated in Figure 6.3, silica aerogel is highly porous and contains a great amount of nano-sized pores. It has high specific surface area and thus strong adsorptive ability. It contains a good number of free hydroxyl (-OH) groups as well as hydrogen bonded –OH groups inside and outside. In this study, the hydrophilic silica aerogel powder has specific surface area of 600 m^2/g and density of 40-80kg/m^3. Its porosity is as high as 90-98% and its pore capacity is 3.0-6.0 cm^3/g. The pore diameter is in the range 20-80 nm. Because of the high specific surface area and strong adsorptive ability of the hydrophilic silica aerogel, the TiO_2 nanoparticles tent to be easily absorbed onto the surface of the hydrophilic silica aerogel particles in the aqueous suspension. The presence of abundant –OH groups on hydrophilic silica aerogel surface not only favor the dispersion of silica aerogel itself in water but also help the absorbance of TiO_2 nanoparticles. The presence of hydrophilic silica aerogel prevented the aggregation of TiO_2 nanoparticles with each other. It thus favored the dispersion of nanoparticles on one hand and helped retain the small size feature of TiO_2 nanoparticles on the other hand. In addition, some fraction of TiO_2 nanoparticles maybe also were enclosed by internal pores of hydrophilic silica aerogel since its pore size is larger than that of TiO_2 nanoparticles because the internal pores of the hydrophilic silica aerogel are larger than the nanoparticles. This can reduce the direct contact between TiO_2 nanoparticles with ramie fibers. It should be favorable for reducing the destruction of ramie fibers brought by the photocatalytic reaction. Using the hydrophilic silica aerogel as dispersant represents a new method for preparing nanoparticle suspension, which has never been reported.

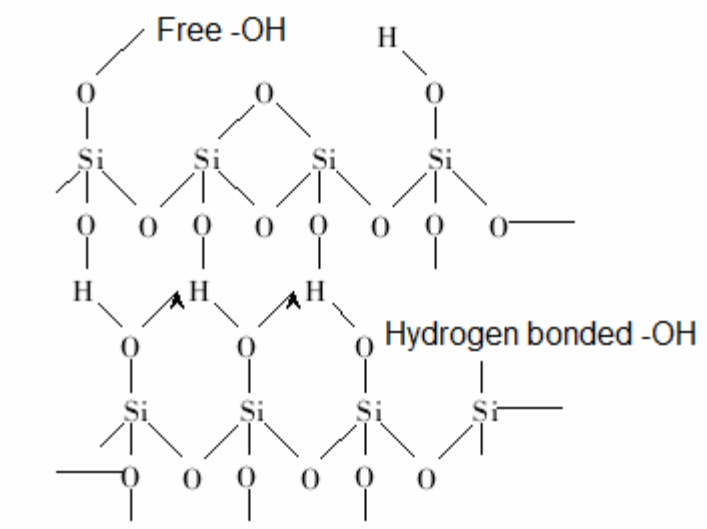

Figure 6.3 Illustration of structure of silica areogel

In the following dispersion experiments, hydrophilic silica aerogel was used as dispersant and its optimal dose was 6% (wt% of amount of TiO_2).

Influence of pH

The influence of pH on dispersion effect of TiO_2 nanoparticles was investigated by varying the pH value from 2 to 12. As shown in Figure 6.4, the light absorbance of the suspension decreased from 0.8 to 0.23 as pH rose from 2 to 4, suggesting the depression of the dispersion effect of TiO_2 nanoparticles. In the pH range 4-5, the absorbance was very low indication that the dispersion effect was the worst in this case. As rose from 5 to 7, the absorbance increased prominently, namely, the dispersion effect increased as well. In the pH range 9-10, the absorbance reached the highest level, implying the dispersion effect was the best in this range. When pH further grew up to 12, the dispersion effect depressed dramatically again. This is because the isoelectric point of TiO_2 nanoparticles was situated at about pH=4.0. When pH was below its isoelectric point, the TiO_2 nanoparticles were positively charged. As the decrease of pH, the H^+ ions absorbed on the surface of TiO_2 nanoparticles reduced, resulting in the decrease of static repulsive force among the nanoparticles which was unfavorable for the dispersion

of nanoparticles. In the vicinity of isoelectric point, the static repulsive force among nanoparticles reduced to the minimum level and the TiO_2 nanoparticles tent to aggregate. As a result, the dispersion effect was lower in this range. When pH was above its isoelectric point, the TiO_2 nanoparticles were negatively charged. With the increase of pH, the negative ions increasingly aggregated on the surface of TiO_2 nanoparticles, leading to the increase of static repulsive force among nanoparticles. Therefore the dispersion effect rose as pH increased when pH>5. But as pH increased to over 10, the concentration of Na^+ in the suspension reached to rather high level. The Na^+ could reduce the thickness of electric double layer on the surface of nanoparticles, resulting in prominent depression of dispersion effect. Hence pH=9 was the employed in the following experiments for producing aqueous of suspensions of TiO_2 nanoparticles.

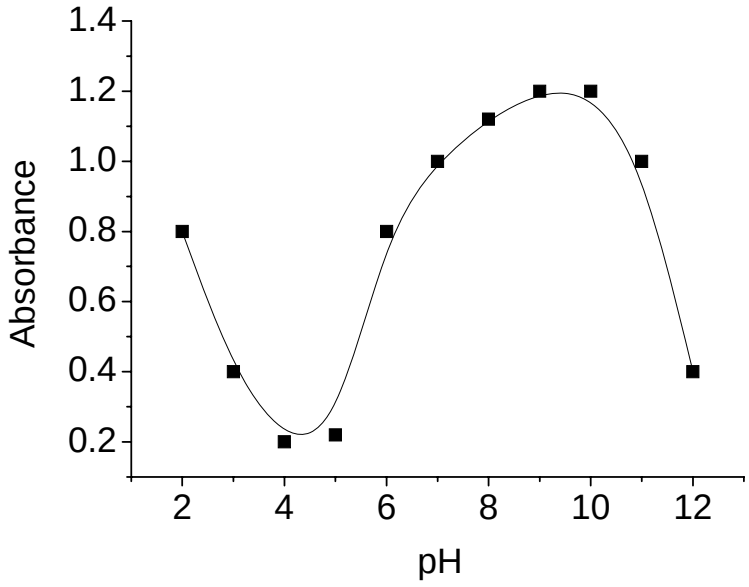

Figure 6.4 Influence of pH

Influence of dispersion temperature

Figure 6.5 presents the influence of dispersion temperature on the dispersion of TiO_2 nanoparticles. As can be seen, the light absorbance rose steadily as dispersion temperature increased from 25^{o}C to 50^{o}C, suggesting the dispersion effect increased. But absorbance decreased when dispersion temperature further increased from 50^{o}C to 80^{o}C, indicating the reduction of the dispersion effect. This because increasing

temperature could raise the molecular mobility of dispersants and enable them to be easily absorbed by TiO_2 nanoparticles, forming compact electric double layer on the surface of TiO_2 nanoparticles. But too high temperature could result in rather high molecular mobility of dispersants and give rise to the difficulty of covering TiO_2 nanoparticles by dispersants. Moreover, higher temperature could raise the probability of collisions among nanoparticles and reduce the dispersion effect. Hence the optimal dispersion temperature was determined at 50 ^{o}C.

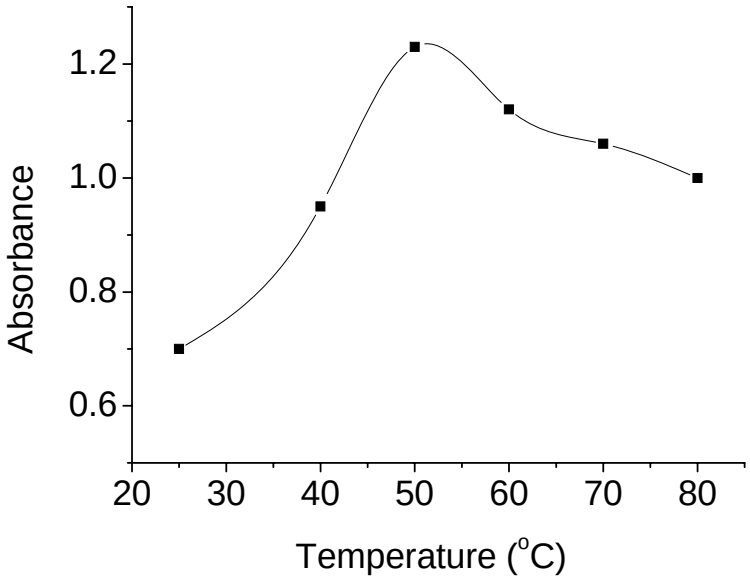

Figure 6.5 Influence of dispersion temperature

Influence of ultrasonic treatment time

As well established, ultrasound is a very effective processing method in the generation and application of nano materials. During the low pressure cycle, high-intensity ultrasonic waves create small vacuum bubbles or voids in the liquid. When the bubbles attain a volume at which they can no longer absorb energy, they collapse violently during a high pressure cycle. This phenomenon is termed as cavitation. In general, ultrasonic cavitation in liquids may cause fast and complete degassing and is favor of producing uniform dispersions of nanoparticles. Figure 6.6 indicates the influence of time of ultrasonic treatment in the dispersion of TiO_2 nanoparticles. When the dispersion time increased from 10 min to 30 min the absorbance rose apparently. However, after 30 min the dispersion effect depressed with

the extension of ultrasonic time. This is because ultrasonic wave also gives rise to Bemoulli force via non-linear vibration besides the cavitation effect. The Bemoulli force results in the TiO_2 nanoparticles to approach with each other and tend to aggregate thereby. In addition, long-time ultrasonic treatment could raise the temperature of the suspension and enhance the collisions among nanoparticles. The separated nanoparticles could thus reunion. Therefore the optimal ultrasonic time was determined as 30 min in this study.

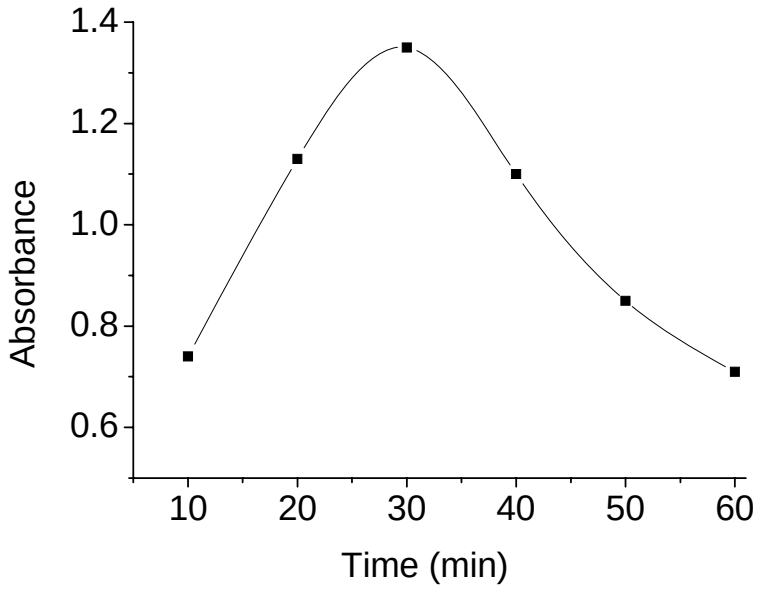

Figure 6.6 Influence of time of ultrasonic treatment

The dispersion effect of the TiO_2 nanoparticles in aqueous suspensions were observed by a Nikon SMZ645 Microscope. Figure 6.7 the views of aqueous suspension prepared using the optimal conditions and the conditions before optimization under microscope with a magnification of ×1000. It can be seen that the dispersion effect of TiO_2 nanoparticles were improved prominently. Under inappropriate conditions, larger clusters of TiO_2 nanoparticle aggregation could be viewed. In contrast, the TiO_2 nanoparticles were evenly distributed when the suspension was prepared using the optimal condition combination.

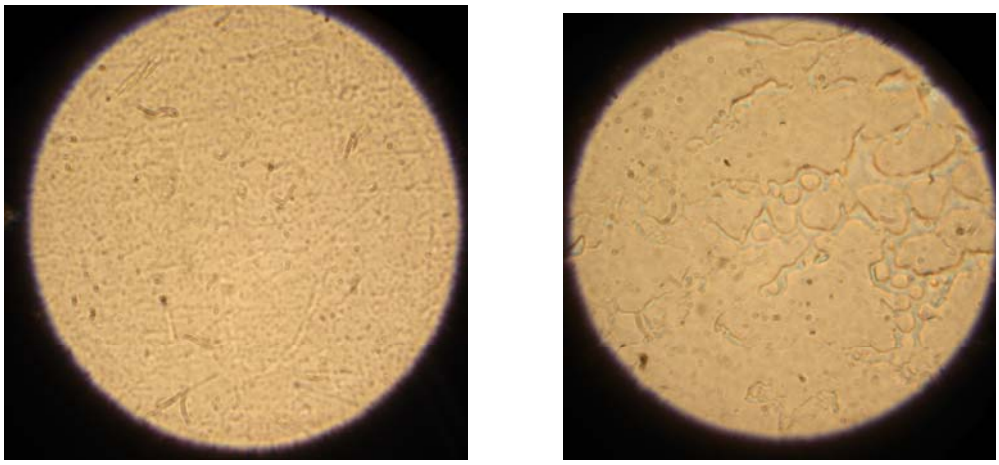

(a) **(b)**

Figure 6.7 Views of dispersion effect under microscope with a magnification of ×1000: (a) suspension prepared under the optimal condition combination; (b) suspension prepared using the conditions before optimization.

6.3.2 Photocatalytic degradation of formaldehyde

Influence of content of TiO_2

Figure 6.8 presents the effect of photocatalytic degradation of formaldehyde by the ramie fabrics treated by the working baths in which the content of TiO_2 varied from 0.2g/L to 0.8g/L. As shown in Figure 6.8, for the untreated ramie fabric, the concentration of formaldehyde changed only slightly due to exposure of UV light. In contrast, the concentration of residual formaldehyde dramatically decreased with the extension of UV exposure time when the tests were performed on the ramie fabrics coated with TiO_2, suggesting the occurrence of prominent photocatalytic degradation of formaldehyde upon exposed to UV light. For the ramie fabrics coated with TiO_2, the formaldehyde concentration reduced dramatically at the beginning of photocatalytic reaction, especially for the ramie fabrics with higher loading of TiO_2, suggesting the rapid photocatalytic degradation rate. With the elapse of time, the photocatalytic degradation rate declined. This is because the probability of the collision between TiO_2

nanoparticles and formaldehyde molecules reduced with the decrease of formaldehyde concentration. This means that most of formaldehyde in reactor could be destroyed by the ramie fabrics loaded with TiO_2 nanoparticles in a short time after being exposed to UV light. It is also viewed that as the content of TiO_2 increased from 0.2 g/L to 0.8g/L in the working bath the effect of photocatalytic degradation of formaldehyde increased gradually. Apparently, this is ascribed to increased amount of TiO_2 nanoparticles loaded on the ramie fiber surface, which improved the decomposition efficiency of formaldehyde. For the ramie fabric treated with working bath in which the content of TiO_2 was 0.8g/L, the residual formaldehyde percentage reduced to 45% when it was exposed to UV light for 200 min. It is apparent that the photocatalytic degradation efficiency of formaldehyde was dependent on many factors. Besides the nature of TiO_2 nanoparticles, the loading of TiO_2 on ramie fabric, the UV light intensity and UV exposure time, the atmosphere environment and humidity, the interaction area of formaldehyde and fabric coated with TiO_2 nanoparticles, the cabinet capacity, and the ratio of fabric area to formaldehyde amount also play important roles in determining the photocatalytic efficiency.

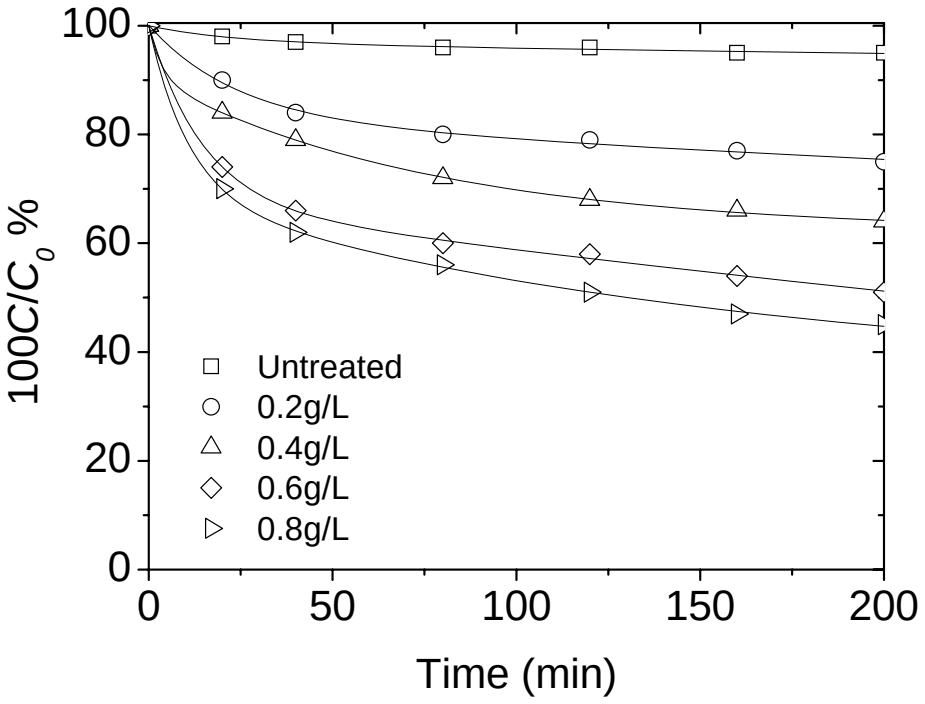

Figure 6.8 Influence of content of TiO_2 nanoparticles

Influence of PU emulsion

For the ramie fabrics treated with the working baths made up only by TiO_2 aqueous dispersion and distilled water, the TiO_2 nanoparticles were only attached to the ramie fibers due to the physical interactions, such as Van Der Waals force, which can not stand repeated laundry cycles. In order to enhance the washing durability, polymer adhesives such as the self cross-linking acrylic emulsions were frequently employed in the textile finishing with nanoparticles. But using the self cross-linking acrylic emulsions can result in hard handle of the treated fabrics. In this study, a kind of PU emulsion was employed as the binder of TiO_2 nanoparticles. Polyurethane is well known for its outstanding elasticity, which is supposed to avoid the depression of soft handle of ramie fabric in this study. Moreover, the PU emulsion employed in this study was also thermally reactive, similar to that described in Chapter 4. The blocked –NCO groups can be released at higher temperatures and react with the –OH groups on ramie fibers. As a result, the washing resistance of TiO_2 loaded fabrics is supposed to enhance.

In this study, the ramie fabric without citric acid pretreatment were finished by the series of working baths made up of TiO_2 aqueous suspension and PU emulsion in which the dose of PU emulsion DM-3541varied from 2 g/L to 5 g/L, 10 g/L and 20 g/L. Figure 6.9 shows the influence of PU emulsion on the residual formaldehyde percentage after 200 min photocatalytic reaction. As can be seen, the residual formaldehyde percentage greatly increased with the increase of washings if PU emulsion was absence in the working bath. This proved that the photocatalytic effect of ramie fabric dramatically decreased because TiO_2 nanoparticles lost in repeated washing cycles. In contrast, the residual formaldehyde percentage increased slowly with the increase of washings when the PU emulsion was employed in working baths. In particular, with the increase of content PU emulsion employed in working baths the tendency of residual formaldehyde percentage rising with the increase of washings was gradually weakened. This suggested that the presence of PU emulsion in working baths indeed enhanced the washing durability of the TiO_2 coated ramie fabrics. However, with the increase of PU content in working baths the residual percentage of formaldehyde before washing increased, suggesting the photocatalytic effect reduced. When the PU emulsion content

was 20g/L, the residual percentage of formaldehyde was above 70% before washing. This is because PU emulsion formed a layer of thin film on ramie fibers after finishing. The TiO_2 nanoparticles were mostly embedded in the polymer film and could not contact with air and formaldehyde when higher content of PU emulsion was used. Moreover the UV light could be greatly blocked. The photocatalytic effect was greatly weakened. Therefore the content of PU emulsion in working bath must be strictly controlled in order to balance the washing resistance and depression of photocatalytic effect. Therefore the content of PU emulsion in working bath was determined as 5g/L.

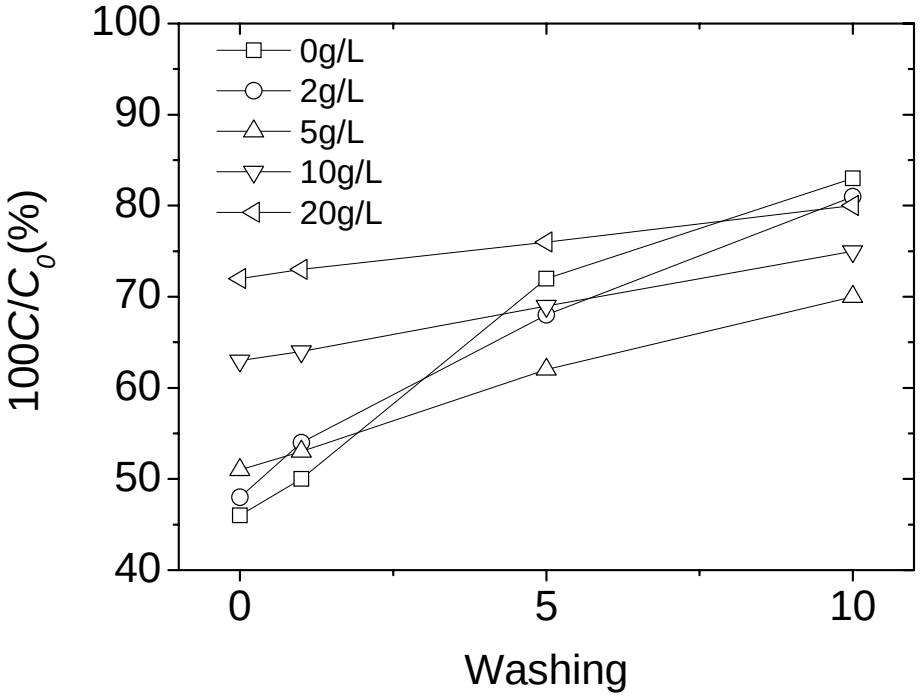

Figure 6.9 Influence of PU emulsion on photocatalytic degradation of formaldehyde.

Influence of pretreatment by citric acid

Apart from polymer adhesive, chemical modification on fabric or nanoparticles were also employed to fix nanoparticles on fabrics. One way to graft nanoparticles onto cellulose fabrics is attained by using cross-linking agents. The cross-linking agents have at least two free carboxylic groups to be able to bind both fiber and nanoparticles. The cross-linking agents such as succinic acid, 1,2,3-propanetricarboxylic acid and 1,2,3,4-butanetetracarboxylic acid have been used for the purpose in previous reports. In

this study, citric acid was used as the cross-linking agent. As illustrated in Scheme 6.1, the carboxyl (-COOH) groups citric acid can either form a covalent ester bond with a cellulose macromolecule or react with two hydroxyl (-OH) groups resulting in the cross-linking of ramie fibers. Through reactions the cross-linking agent citric acid is

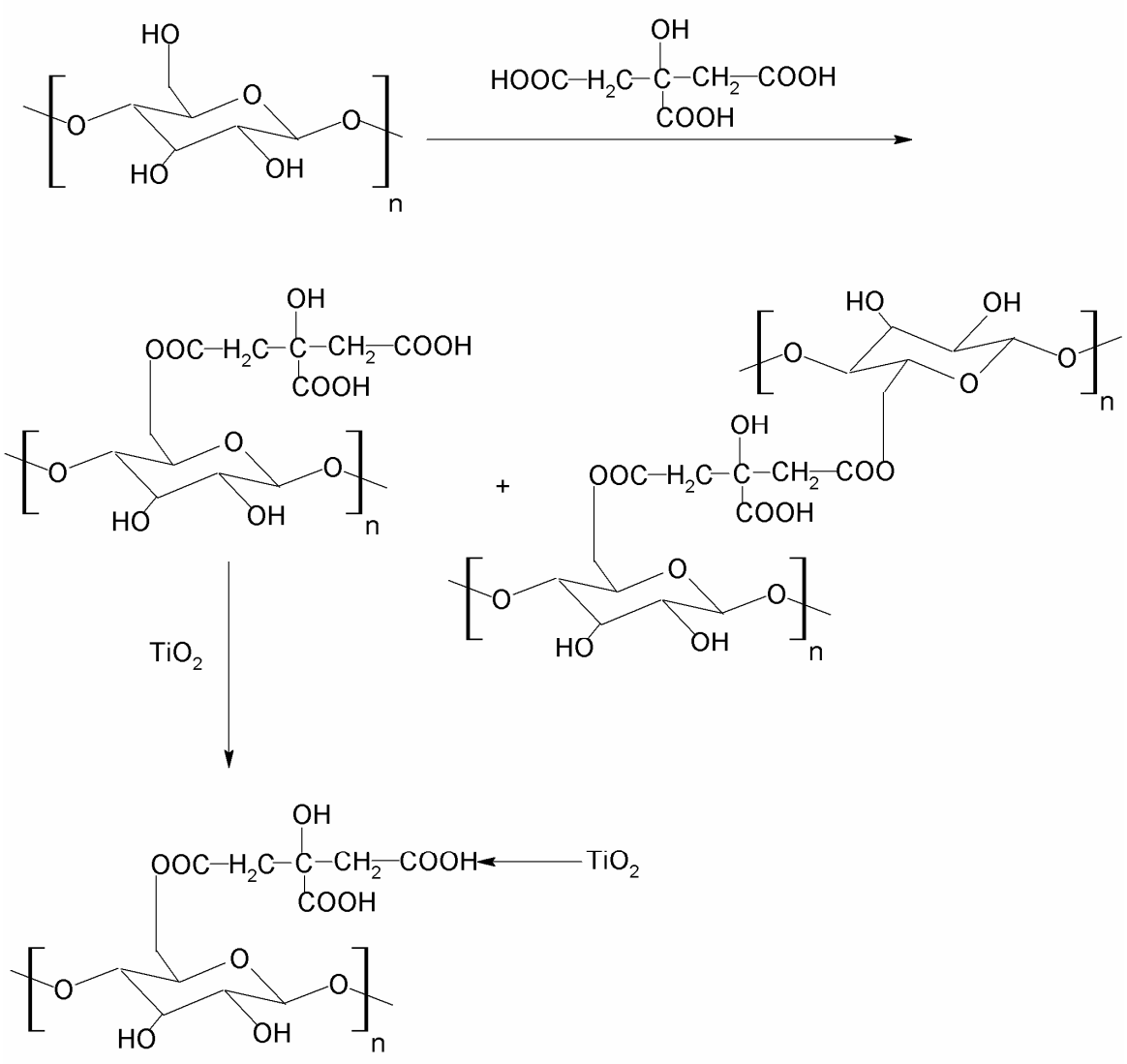

Scheme 6.1 Reaction with cellulose and interaction with TiO_2 of citric acid.

grafted onto ramie fibers. The residual –COOH groups are meant to anchor TiO_2 on ramie fibers by an electrostatic interaction. Previous studies have shown that TiO_2 presents a strong electrostatic interaction with carboxylic group. Of course, the three –COOH groups of citric acid can all react with –OH groups of ramie fibers under

appropriate conditions. Therefore it is essential to control the curing temperature and time in the pretreatment of ramie fabrics with citric acid so that a proper content of free –COOH groups left for fixing TiO_2 nanoparticles on ramie fibers in the following TiO_2 coating process.

Figure 6.10 shows the influence of pretreatment by citric acid on washing durability. As can be seen, the residual formaldehyde percentage increased significantly with the increase of washing time when the ramie fabric was pretreated by citric acid. This means that the photocatalytic effect of ramie fabric greatly decreased. In contrast, the residual formaldehyde percentage increased more slowly with the increase of washing time if the ramie fabric was subjected to pretreatment by citric acid. This suggests that after cross-linking pretreatment the washing resistant of the ramie fabric coated with TiO_2 was enhanced greatly. Moreover, the washing resistant was significantly enhanced as the concentration of citric acid increased from 2% owf to 7% owf in the pretreatment of ramie fabrics. But when the citric acid concentration increased from 7% owf to 10% owf the washing resistant effect increased little. This might be because with the increase of citric acid concentration the free –OH groups on the surface of ramie fibers mostly react with –COOH. This means the amount of –OH groups available for reacting decreased. In addition, with the increase of citric acid concentration the amount of -COOH groups on ramie fibers rose, resulting in the increase of grafting TiO_2 nanoparticles. However, with the increasing amount of TiO_2 nanoparticles on ramie fibers the steric hindrance rose as well, which prevented more TiO_2 nanoparticles to attach to ramie fibers. In the other word, with the increase of citric acid concentration the reaction sites on ramie fibers tent to saturation state. Hence the washing durability could not be raised by further increasing the citric acid concentration in ramie pretreatment. Hence the optimal citric acid concentration in ramie pretreatment was determined as 7% owf in this study.

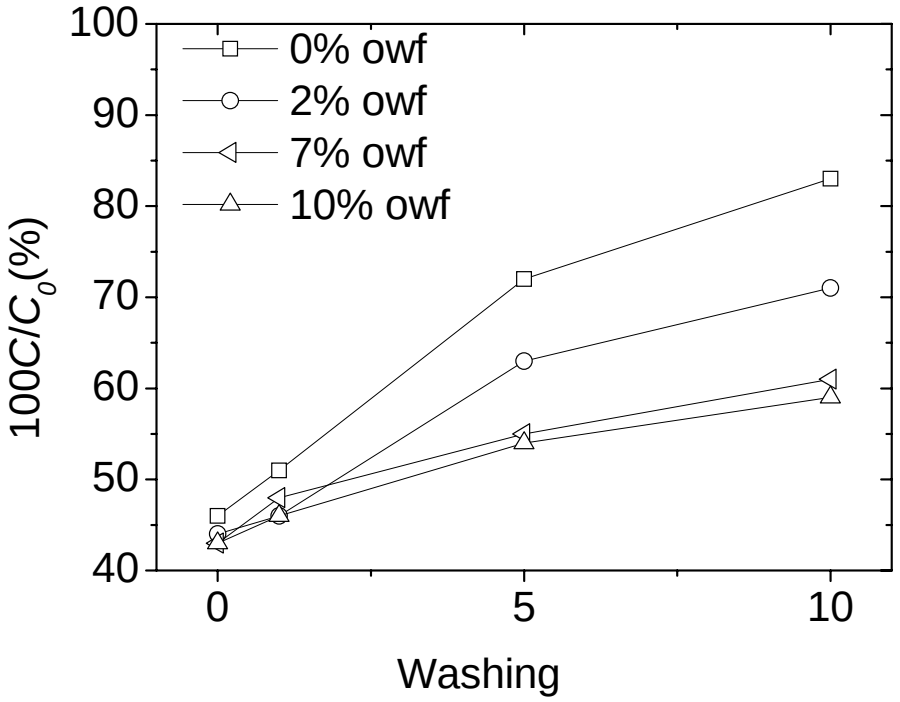

Figure 6.10 Influence of pretreatment by citric acid on washing durability

6.3.3 Antibacterial effect

In this study, the antibacterial property against of Escherichia Coli and Staphylococcus Aureus of the ramie fabrics loaded TiO_2. Table 6.1 presents the antibacterial property of the TiO_2 loaded ramie fabrics prepared differently. As would be expected, the antibacterial property the TiO_2 loaded ramie fabrics rose with the increasing content of aqueous suspension of TiO_2 nanoparticles in working bath. Moreover, the antibacterial property against Escherichia Coli of a TiO_2 loaded ramie fabric was close to its antibacterial property against Staphylococcus Aureus. When the content of TiO_2 in the working bath increased to 0.8g/L, the percentage of bacteria reduction approached to 100%.

Table 6.1 Antibacterial property of the TiO_2 loaded ramie fabrics prepared differently.

Sample	Number of bacteria colony (cfu/ml)		*R*%	
	A	B	A	B
Control (not coated with TiO_2)	1.38×10^5	1.65×10^5	-	-
0.2g/L TiO_2 in working bath	1.43×10^4	1.85×10^4	89.6	88.8
0.4g/L TiO_2 in working bath	8.97×10^3	1.30×10^4	93.5	92.1
0.6g/L TiO_2 in working bath	4.69×10^3	6.27×10^3	96.6	97.2
0.8g/L TiO_2 in working bath	1.93×10^3	1.98×10^3	98.9	99.2
0.8g/L TiO_2 and 5g/L PU emulsion in working bath	6.62×10^3	9.08×10^3	97.0	96.5
7% owf citric acid pretreatment + 0.8g/L TiO_2 working bath	2.07×10^3	1.65×10^3	98.5	99.0

Note: A represents Escherichia Coli;
B refers to Staphylococcus Aureus.

Figure 6.11 presents the comparison of antibacterial performance of untreated ramie fabric and that finished by the working bath containing 0.8g/L TiO_2 suspension. A lot of bacteria colonies can be viewed in the untreated ramie samples. On the contrary, most of the bacteria were killed by the TiO_2 loaded ramie fabric. Only very few bacteria colonies can be seen for both the antibacterial tests against Escherichia Coli and Staphylococcus Aureus.

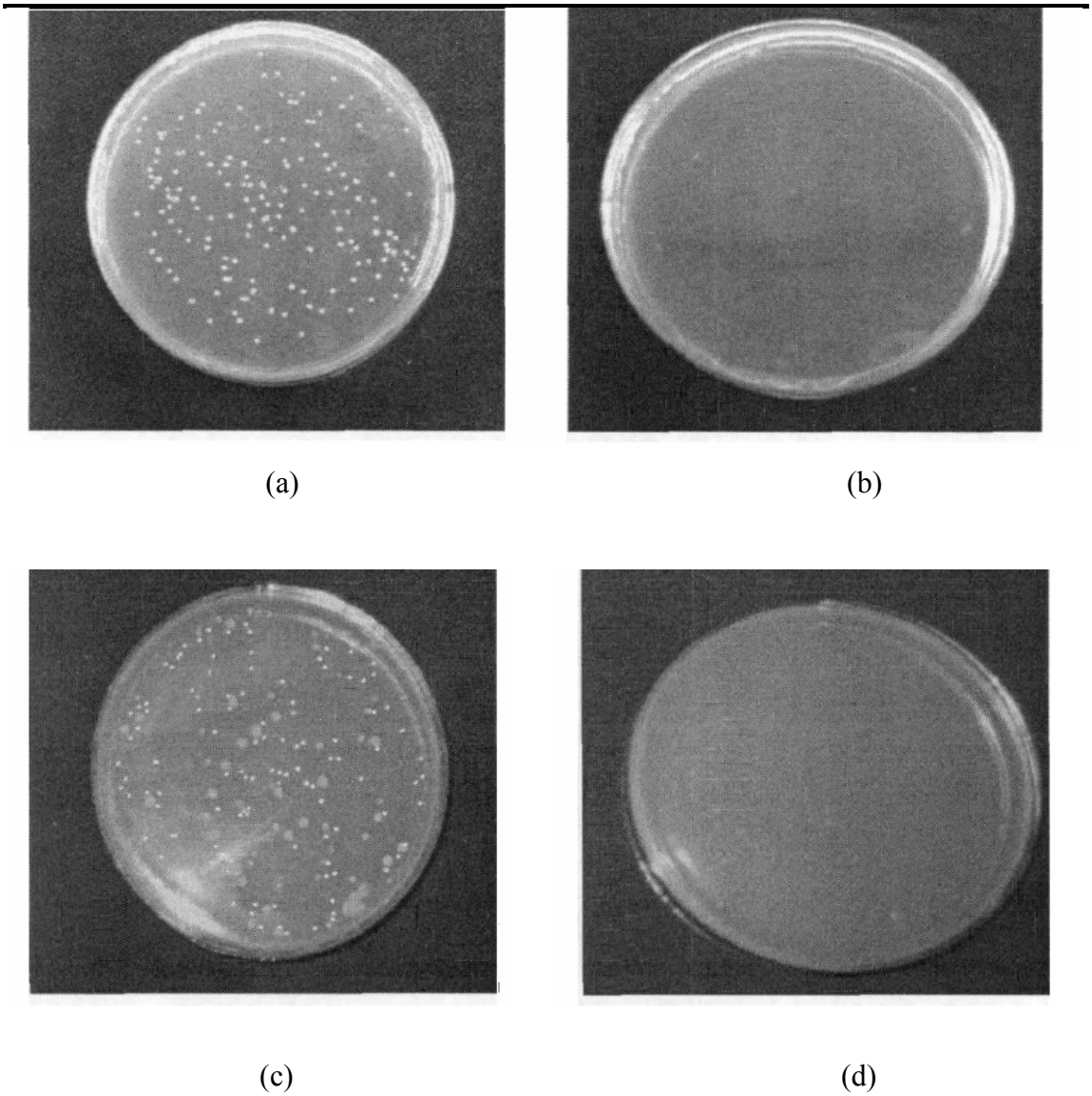

(a) (b)

(c) (d)

Figure 6.11 Images of antibacterial effect of ramie fabrics finished by TiO_2 working bath in which the 0.8g/L TiO_2 was involved. (a) control sample in Escherichia Coli suspension; (b) TiO_2 loaded fabric in Escherichia Coli suspension; (c) control sample in Staphylococcus Aureus suspension; (d) TiO_2 loaded fabric in Staphylococcus Aureus suspension.

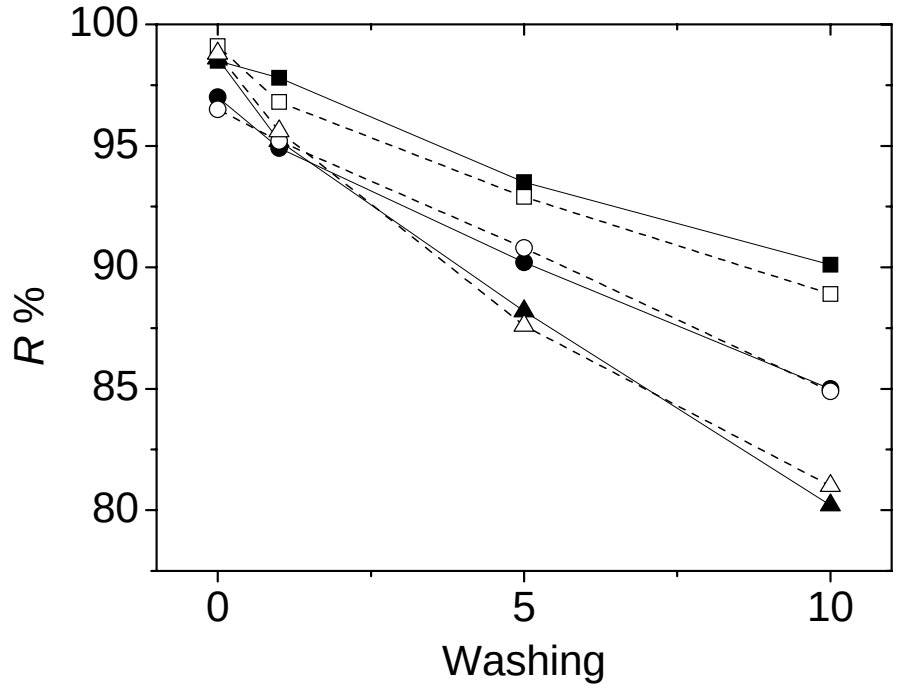

Figure 6.12 Antibacterial properties of ramie fabrics prepared differently before washing and after repeated washing cycles: (■) and (□) finished by only 0.8g/L TiO_2; (●) and (○) finished by 0.8g/L TiO_2 and 5g/L PU emulsion; (▲) and (Δ) pretreated by 7% owf citric acid and finished by 0.8g/L TiO_2. The solid symbols (■), (●) and (▲) refer to the antibacterial property against Escherichia Coli while the empty symbols (□), (○) and (Δ) represent the antibacterial property against Staphylococcus Aureus.

Figure 6.12 shows the antibacterial property of ramie fabrics prepared differently before washing and after repeated washing cycles. As would be expected, for all the ramie fabrics prepared differently the antibacterial property decreased with the increase of washing time, suggesting the loss of TiO_2 nanoparticles in repeated laundry cycles. For the untreated ramie fabric, the antibacterial property decreased rapidly with the increasing washing time because the TiO_2 nanoparticles were attached to ramie fibers only be physical interactions. The ramie fabric loaded with both TiO_2 and PU exhibited better washing durability because the polymer binder improved the attachment of TiO_2 to ramie fibers. The ramie fabric subjected to the pretreatment of citric acid presented the best washing durability because the some TiO_2 nanoparticles were anchored to

ramie fibers via covalent ester bonds and the strong electrostatic interaction between –COOH and TiO_2 as illustrated in Scheme 6.1. Hence chemical cross-linking agent is better than polymer adhesive for fixing TiO_2 nanoparticles on ramie fibers.

6.3.4 UV protective effect

Table 6.2 shows the UV absorbance of the untreated and the TiO_2 loaded ramie fabrics prepared differently. As can be seen, the UPF of untreated ramie fabric is only 5.85. In contrast, the UPF of the TiO_2 loaded ramie fabrics was above 30 at least. With the increase of content of TiO_2 in working bath, the UPF of the TiO_2 loaded ramie fabrics increased prominently. When the content of TiO_2 in working bath was above 0.6g/L, the UPF of the TiO_2 loaded ramie fabrics rose to above 60 which were rated as 50+, i.e, excellent UV protection. It is noteworthy that the UPF of the ramie fabric finished by TiO_2 and PU was slightly higher than the fabric coated only by TiO_2. This is likely because the PU film formed on ramie fibers blocked some UV light and gave rise to a small increase of UPF.

Table 6.2 UV protective property of the untreated and the TiO_2 loaded ramie fabrics.

Sample	UPF	UPF rating	UV protection category
Control (not coated with TiO_2)	5.86	5	-
0.2g/L TiO_2 in working bath	33.9	35	Very good
0.4g/L TiO_2 in working bath	45.3	45	Excellent
0.6g/L TiO_2 in working bath	60.5	50+	Excellent
0.8g/L TiO_2 in working bath	75.6	50+	Excellent
0.8g/L TiO_2 and 5g/L PU emulsion in working bath	78.9	50+	Excellent
7% owf citric acid pretreatment +0.8g/L TiO_2 working bath	76.3	50+	Excellent

Figure 6.13 presents the UPF change before and after washing of the ramie fabric differently prepared. Similar to the cases of photocatalytic degradation and antibacterial property, the UPF of the ramie fabrics also decreased gradually with the increase of washings. Moreover, the ramie fabrics subjected to pretreatment by citric acid exhibited the best washing durability due the same mechanism described above.

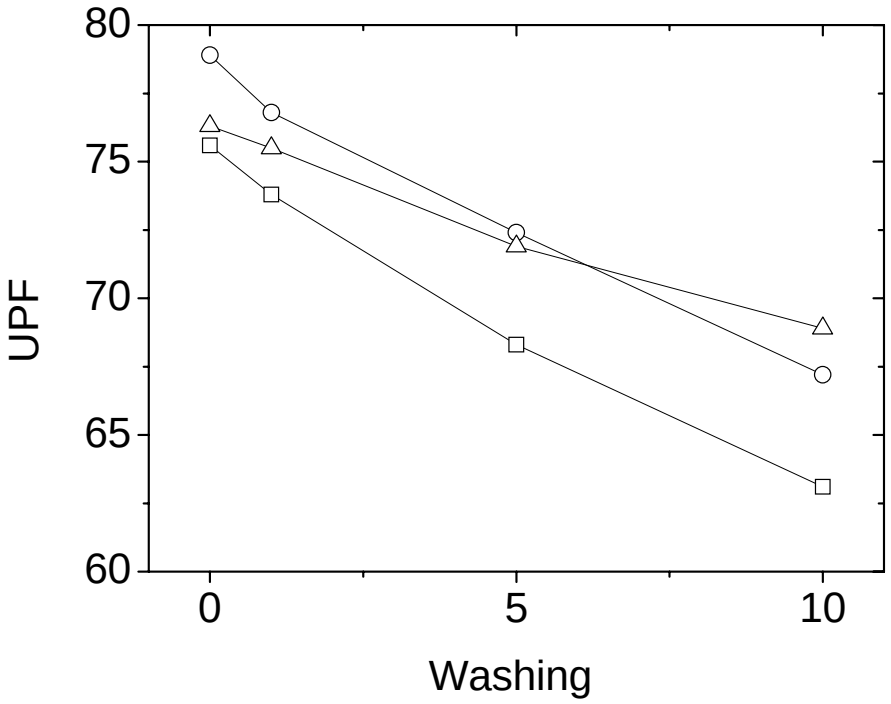

Figure 6.13 UPF change before and after washing of the ramie fabric differently prepared: (□) finished by only 0.8g/L TiO_2; (○) finished by 0.8g/L TiO_2 and 5g/L PU emulsion; (Δ) pretreated by 7% owf citric acid and finished by 0.8g/L TiO_2.

Conclusion

Although nanotechnology has been extensively used in the finishing of textile materials the application of nanoparticles for the modification of ramie fabrics has less been investigated. In this study, a kind of TiO_2 nanoparticle product was employed in the multi-functional finishing of ramie fabric. At first, for optimizing the dispersion conditions of TiO_2 nanoparticles in aqueous suspension, the influencing factors such dispersant type and content, pH, dispersion temperature and time were studied systematically. It was found that a kind of hydrophilic silica aerogel product was

suitable for serving as dispersant for producing TiO_2 aqueous suspension. In addition, the optimal pH, dispersion temperature and ultrasonic time were also experimentally determined. A series of working baths with varying content of TiO_2 were prepared and the ramie fabrics were coated with TiO_2 via a dip-pad-dry process. In order to enhance the washing durability of the TiO_2 modified fabric the ramie fabrics were pretreated by citric acid. It was proved that the efficiency of photocatalytic degradation of formaldehyde rose with the increase of content of TiO_2. The ramie fabrics coated with TiO_2 nanoparticles exhibited good antibacterial property. When the working bath contained 0.8 g/L TiO_2 the percentage of bacteria reduction approached to 100%. Using 5g/L PU emulsion as the binder of TiO_2 in working bath could enhance the washing resistant of the TiO_2 loaded ramie fabric. The ramie fabrics loaded with TiO_2 also exhibited excellent UV protective property when the content of TiO_2 increased to 0.8 g/L. Using PU emulsion as the binder of TiO_2 could raise the washing durability of the TiO_2 loaded ramie fabrics. In contrast, the pretreatment of fabric by citric acid before TiO_2 coating was more effective for improving the washing durability of TiO_2 loaded ramie fabrics.

CHAPTER 7
CONCLUSIONS

In this chapter, the experimental findings achieved from all the investigations in the PhD study were summarized as follows.

7.1 Natural dying of ramie fabrics with rare earth as mordant

At present, ramie fabrics are mostly dyed with synthetic colorants which can give rise to serious environmental pollution and potential harm to mankind health. Thus the natural and healthy features of ramie fabric are greatly weakened. In this study, ramie fabrics were dyed with the natural extracts of caesalpinia sappan, rhizoma coptidis, gardenia and areca catechu. The post-mordanting, dyeing temperature of 90^{o}C and dyeing time of 50-70 min and dyeing bath pH of 7-8 were determined as the optimal dyeing conditions. The fabrics dyed in presence of rare earth as mordant exhibited higher color shade stability against pH variation owing to the stable coordination bonds among the rare earth, natural dye and fiber. It was found that the color fastness to washing, rubbing and light of the ramie fabrics was raised significantly when rare earth was used as mordant in natural dyeing. As compared with Fe^{2+} and Cr^{6+}, rare earth could greatly reduce the ionic concentration employed in natural dyeing. This study proved that rare earth represented a kind of promising mordant in natural dyeing.

7.2 Wrinkle resistant treatment of ramie fabrics using liquid NH_3 technology

In order to raise the wrinkle resistant properties or ramie fabric, the combination of liquid NH_3 pretreatment and resin finishing was explored in this study. The liquid NH_3 treatment was proved to decrease the crystallinity of ramie fiber and bring about apparent swelling effect. As a result, the accessibility of the ramie fabrics treated by liquid NH_3 was elevated. The liquid NH_3 treatment gave rise to the decrease of dyeing

rate but resulted in the increase of equilibrium dye uptake. The liquid NH_3 pretreatment prior to resin finishing could reduce strength loss. Employing reactive PU emulsion in resin finishing could raise the strength retention of the ramie fabric without influencing wrinkle resistant effect since the reactive PU molecule could react with ramie fibers. The influences of wrinkle resistant treatment conditions were explored systematically. After 10 launderings, the flat appearance and crease retention of these ramie fabrics were all above grade 3.0 when they were produced from liquid NH_3 pretreatment followed by resin finishing. Therefore the liquid NH_3 pretreatment combined with thermally reactive PU as protector was favorable for the wrinkle resistant finishing of ramie fabric.

.

7.3 Electromagetic shielding finishing of ramie fabrics using scCO2 technology

The electromagnetic shielding ramie fabrics were developing from electroless Cu plating using $scCO_2$ fluid technology in this study. It was found that the $scCO_2$ fluid could greatly remove impurities of ramie fibers. In comparison with the conventionally method where a large amount of strong alkaline solutions is employed, the $scCO_2$ fluid is a better way to eliminate lignin from the ramie fibers. In particular, the removal of lignin in $scCO_2$ fluid could be raised to over 80% in presence of some swelling agent. The $scCO_2$ fluid could result in the swelling of ramie fiber, which would raise the accessibility of ramie fiber to additives. By using scCO2 fluid, the Pd(hfa)2 could be impregnated into the ramie fibers, especially when ethanol was used as co-solvent in the impregnation of Palladium complex. After the Cu plating, the ramie fabrics deposited with Palladium were plated by a Cu film of 18-20g/m^2. The Cu plated ramie fabrics exhibited good shielding effect. This study presented a new way for upgrading ramie fabric.

7.4 Multi-function finishing of ramie fabric using TiO_2 nanoparticles

Although nanotechnology has been extensively used in the finishing of textile materials the application of nanoparticles for the modification of ramie fabrics has less been investigated. In this study, the multifunctional ramie fabrics finished by TiO_2

nanoparticles were developed. It was found that a kind of hydrophilic silica aerogel was suitable for serving as dispersant in producing TiO_2 suspension. The ramie fabrics were coated with TiO_2 nanoparticles via a dip-pad-dry process. In order to enhance finishing durability in repeated launderings the ramie fabric samples were pretreated by citric acid. When the working bath contained 0.8 g/L TiO_2 the TiO_2 coated ramie fabrics exhibited excellent antibacterial property and UV protection. In addition, the TiO_2 coated ramie fabrics showed high capability of decomposing formaldehyde. Using PU emulsion as the binder could raise the washing durability of the TiO_2 loaded ramie fabrics. In contrast, the pretreatment of ramie fabric by citric acid before TiO_2 coating was more effective for improving washing durability.

7.5 Investigations by collaborating with other researchers

Apart from the studies mentioned above, the I also collaborated with other researchers investigations and published several refereed papers as co-author. I cooperated with Dr Shouxiang Jiang in the development of metal coated fabrics via either electroless plating or magnetron sputtering. The fabrics exhibited either good electromagnetic shielding effect or excellent antibacterial property. Through the collaboration with Prof Zheng Qingkang, I conducted the study of transfer printing with disperse dyes on cotton fabric modified with an aqueous tolylene diisocyanate derivative. It was found that the printing fastness was raised by the aqueous tolylene diisocyanate derivative.

REFERENCES

1. Pandey, S. N. Ramie fibre: part I. Chemical composition and chemical properties. A critical review of recent developments, Textile Progress 2007; 39: 1–66.

2. Bruhlmann, F., Leupin, M., Erismann, K. H., Fiechter, A. Enzymatic degumming of ramie bast fibers, J. Biotechnol. 2000; 76: 43–50.

3. Jin, C., Maekawa, M. Evaluating an enzyme treatment of ramie fabrics, Text. Res. J. 2001; 71 779-782.

4. Batra, S. K., Other long vegetable fibers In *Handbook of fiber science and technology*, 1985; Vol. 4, pp 727-807.

5. Kalia, S., Kaith, B. S., Kaur, I. Pretreatments of Natural Fibers and their Application as Reinforcing Material in Polymer Composites—A Review, Polym. Eng. Sci. 2009; 49: 1253-1279.

6. Basu, S., Saha, M. N., Chattopadhyay, D., Chakrabarti, K. Degumming and characterization of ramie fibre using pectate lyase from immobilized Bacillus pumilus DKS1, Letters in Applied Microbiology 2009; 48: 593-597.

7. Bhattacharya, S. D., Shah, S. R. Degumming of ramie: the role of the individual constituents of the gummy material, Color. Technol. 2002; 118: 295-299.

8. Basu, S., Saha, M. N., Chattopadhyay, D., Chakrabarti, K. Large-scale degumming of ramie Wbre using a newly isolated bacillus pumilus DKS1 with high pectate lyase activity, J. Ind. Microbiol. Biotechnol. 2009; 36: 239–245.

9. Saikia, R., Brouah, P., Samanta, R. Microbial degumming decoticated ramie and its fiber characteristics, Indian Journal of Fiber and Textile Research 2009; 34: 187-190.

10. Pandey, S. N. Ramie fibre: part II. Physical fibre properties. A critical appreciation of recent developments, Textile progress 2007; 39: 189–268.

11. Ishikawa, A., Okano, T., Sugiyama, J. Fine structure and tensile properties of ramie fibres in the crystalline form of cellulose I, II, Illl and IV, Polymer 1997; 38: 463-468

12. Marchessault, R. H., Howsmon, J. A. Experimental evaulation of the lateral-order in cellulose Text. Res. J. 1957; 27: 30-41.

13. Knight, J. A., Hicks, L. H., Stephen, K. W. Crystallinity study of cellulosic fibers

empolying deuteration and infrared spectroscopy, Text. Res. J. 1969; 39: 324-328.

14. Ray, P. K., Das, B. K. The effect of strong alkali treatment on the cell-wall structure of ramie fiber, Text. Res. J. 1977; 47: 437-440.

15. Nishimura, H., Sarko, A. Mercerization of cellulose, 3 changes in crystallite size, J. Appl. Polym. Sci. 1987; 33: 855-866.

16. Sao, K. P., Samantaray, B. K., Bhattacherjee, S. Radial distribution function analysis study on alkali and heat-treated ramie fiber, J. Appl. Polym. Sci. 1994; 52: 1917-1923.

17. Sao, K. P., Mathew, M. D., Ray, P. K. Infrared spetra of alkali treated degummed ramie Text. Res. J. 1987; 57: 407-414.

18. Liu , Q. H., Wang, H. J., S., W. J. The fine structure and physical properties of mercerised ramie, Journal of China textile university 1991; 17: 45-54.

19. Okano, T., Sarko, A. Mercerization of cellulose, I: X-ray diffration evidence for intermediate structures, J. Appl. Polym. Sci. 1984; 29: 4175-4182.

20. Cheek, L., Roussel, L. Mercerization of ramie: Comparison with flax and cotton part I: Effect on physical, mechanical and accessability characteristics Text. Res. J. 1989; 59: 478-483.

21. Cheek, L., Roussel, L. Mercerization of ramie: Comparison with flax and cotton part II: Effect on dyeing and behavior Text. Res. J. 1989; 59: 541-546.

22. Zhao, W. B. Cyanoethylation of ramie fiber, Journal of textile research (in Chinese) 1993; 14: 30-33.

23. Wakida, T., Kida, K., Lee, M., Bae, S., Yoshioka, H., Yanai, Y. Dyeing and mechanical properties of cotton fabrics treated with sodium hydroxide/liquid ammonia and liquid ammonia/sodium hydroxide, Text. Res. J. 2000; 70: 4, 328-332.

24. Wakida, T., Kitamura, Y., Lee, M., Bae, S., Chen, M., Yoshioka, H., Yanai, Y. Effect of hot water processing on dyeing and mechanical properties of cottons treated with liquid ammonia and sodium hydroxide, Text. Res. J. 2000; 70: 9, 769-774.

25. Wakida, T., Moriya, T., Lee, M., Yoshioka, H., Yanai, Y. Effect of liquid ammonia, sodium hydroxide/liquid ammonia, and subsequent cellulase treatments on mechanical properties of cotton fabric, Text. Res. J. 2000; 70: 2, 161-165.

26. Li, J., Feng, J., Zhang, H., Zhang, J. Wear properties of hemp, ramie and linen fabrics after liquid ammonia/crosslinking treatment, Fibers & Textiles in Eastern Europe

2001; 18: 5, 82-85.

27. Wakida, T., Hayashi, A., Lee, M. S., Lee, M., Doi, C., Okada, S., Yanai, Y. Dyeing and mechanical properties of ramie fabric treated with liquid ammonia, Sen'i Gakkashi 2001; 51: 5, 148-152.

28. Wakida, T., Hayashi, A., Lee, M. S., Lee, M., Okada, S., Yanai, Y. Liquid ammonia treatment of lyocell, Sen'i Gakkashi 2001; 57: 2, 355-358.

29. Wakida, T., Hayashi, A., Saito, M., Lee, M. S., Lee, M., Okada, S., Yanai, Y. Liquid ammonia treatment of polyester/cotton fabric, Sen'i Gakkashi 2001; 57: 2, 60-63.

30. Yanai, Y., Hamada, K., Shimizu, Y. The liquid ammonia treatment of cotton fibers-Structural change of cotton fibers under different method of liquid ammonia removal, Sen'i Gakkashi 2001; 61: 11, 204-302.

31. Park, S.-J., Lee, M., Wakida, T., Hayashi, A., Okada, S., Yanai, Y. Effect of dry heat and hot water processings on cellulose III crystallites of cotton and lyocell fibers treated with liquid ammonia, Sen'i Gakkashi 2002; 58: 8, 299-303.

32. Wakida, T., Lee, M., Park, S.-J., Saito, M. Effect of hot mercerization on liquid ammonia treated cottons, Sen'i Gakkashi 2002; 58: 5, 185-187.

33. Lee, M., Wakida, T., Tokuyama, T., Doi, C., Lim, Y. J., Jeon, S.-K. Liquid ammonia treatment of regenerated cellulosic fabrics, Textile Res. J. 2005; 75: 1 13–18

34. Yanai, Y., Hamada, K., Shimizu, Y. The liquid ammonia treatment of cotton fibers-Structural change of cotton fibers under various treatment conditions in practical units, Sen'i Gakkashi 2005; 61: 15, 287-293.

35. Dornyi, B., Csiszár, E., Somlai, C., Sajó, I. Effect of Liquid Ammonia on the Fine Structure of Linen Fabrics, Text. Res. J. 2006; 76: 8, 629–636.

36. Yanai, Y., Hamada, K., Shimizu, Y. The liquid ammonia treatment of cotton fibers-comparison and combination with mercerization using a practial unit, Sen'i Gakkashi 2006; 62: 4, 81-88.

37. Yanai, Y., Shimizu, Y. The liquid ammonia treatment of cotton fibers-Structural change of cotton fibers after liquid ammonia treatment and hot water treatment, Sen'i Gakkashi 2006; 62: 5, 100-105.

38. Dornyi, B., Csiszár, E., Somlai, P. Improving quality of linen-cotton fabrics with liquid ammonia treatment, Journal of Natural Fibers 2007; 4: 4, 41-57.

39. Buschle-Diller, G., Zeronian, S. H., Pan, N., Yoon, M. N. Enzymatic hydrolysis of

cotton, linen, ramie and visocous rayon fabrics, Text. Res. J. 1994; 64: 270-279.
40. Ishikawa, A. Effects of cellulose treatment on tensile properties of ramie fibers, Mokuzai Gakkaishi 1997; 43: 337-341.
41. Bechtold, T., Mahmud-Ali, A., Mussak, R. Natural dyes for textile dyeing: A comparison of methods to assess the quality of Canadian golden rod plant material, Dyes pigments 2007; 75: 287-293.
42. Lee, Y.-H., Kim, H.-D. Dyeing Properties and Colour Fastness of Cotton and Silk Fabrics Dyed with Cassia tora L. Extract, Fiber. Polym. 2004; 5: 303-308.
43. Bechtold, T., Turcanu, A., Ganglberger, E., Geissler, S. Natural dyes in modern textile dyehouses — how to combine experiences of two centuries to meet the demands of the future?, J. Clean. Prod. 2003; 11: 499–509.
44. Samanta, A. K., Agarwal, P., Singhee, D., Datta, S. Application of single and mixtures of red sandalwood and other natural dyes for dyeing of jute fabric: studies on colour parameters/colour fastness and compatibility, J. Text. Inst. 2009; 100: 565–587.
45. Santis, D. D., Moresi, M., Gallo, A. M., Petruccioli, M. Assessment of the dyeing properties of pigments from Monascus purpureus, J. Chem. Technol. Biotechnol. 2005; 80: 1072–1079.
46. Vankar, P. S., Shanker, R., Dixit, S. Chemical characterisation of extract derived from Daphne papyraceae and sonicator dyeing of cotton, silk and wool with the extract, Pigm. Resin Technol. 2009; 38 181–187.
47. Yi, E., Cho, J.-Y. Color Analysis of Natural Colorant-Dyed Fabrics, Color Res. Appl. 2008; 33: 148 – 157.
48. Ke, G., Yu, W., Xu, W. Color Evaluation of Wool Fabric Dyed With Rhizoma coptidis Extract J. Appl. Polym. Sci. 2006; 101: 3376–3380
49. Mongkholrattanasit, R., Krystufek, J., Wiener, J. Dyeing and fastness properties of natural dyes extracted from eucalyptus leaves using padding techniques, Fibers and Polymers 2010; 11: 346-350.
50. Chairat, M., Bremner, J. B., Chantrapromma, K. Dyeing of Cotton and Silk Yarn with the Extracted Dye from the Fruit Hulls of Mangosteen, Garcinia mangostana Linn, Fiber. Polym. 2007; 8: 613-619.
51. Vankar, P. S., Shanker, R. Dyeing of cotton, wool and silk with extract of Allium cepa, Pigm. Resin Technol. 2009; 38: 242–247.

52. Wang, L., Li, J., Feng, H. Dyeing of flax fabric with natural dye from chestnut shells, Pigm. Resin Technol. 2009; 38: 347–352.

53. Sumanta, A. K., Agarwal, P. Dyeing of jute and cotton fabrics using Jackfruit wood extract: Part I-effect of mordanting and dyeing process variables on color yield and color fastness properties Indian J. Fiber Text. Res. 2007; 32: 466-476.

54. El-Shishtawy, R. M., Shokry, G. M., Ahmed, N. S. E., Kamel, M. M. Dyeing of Modified Acrylic Fibers with Curcumin and Madder Natural Dyes, Fiber. Polym. 2009; 10: 617-624.

55. Shin, Y., Son, K., Yoo, D. I. Dyeing properties and color of silk fabrics dyed with safflower yellow dye, J. Korean Soc. Cloth. Text. 2008; 32: 928~934.

56. Lee, Y.-H. Dyeing, Fastness, and Deodorizing Properties of Cotton, Silk, and Wool Fabrics Dyed with Coffee Sludge (Coffea arabica L.) Extract, J. Appl. Polym. Sci. 2007; 103: 251–257.

57. Hwang, E.-K., Lee, Y.-H., Kim, H.-D. Dyeing, Fastness, and Deodorizing Properties of Cotton, Silk, and Wool Fabrics Dyed with Gardenia, Coffee Sludge, Cassia tora. L., and Pomegranate Extracts, Fiber. Polym. 2008; 9: 334-340.

58. Raisanen, R., Nousiainen, P., Hynninen, P. H. Emodin and dermocybin natural anthraquinones as mordant dyes for wool and polyamide, Text. Res. J. 2001; 71: 1016-1022

59. Perumal, K., Stalin, V., Chandrasekarenthiran, S., Sumathi, E., Saravanakumar, A. Extraction and characterization of pigment from Sclerotinia sp. and its use in dyeing cotton, Text. Res. J. 2009; 79: 1178–1187.

60. Lee, D.-K., Cho, D.-H., Lee, J.-H., Shin, H. Y. Fabrication of nontoxic natural dye from sappan wood, Korean J. Chem. Eng. 2008; 25: 354-358.

61. Park, Y., Koo, K., Kim, S., Choe, J. Improving the Colorfastness of Poly(ethylene terephthalate) Fabrics with the Natural Dye of Caesalpinia sappan L. Wood Extract and the Effect of Chitosan and Low-Temperature Plasma, J. Appl. Polym. Sci. 2008; 109: 160–166.

62. Lee, Y., Lee, J., Kim, Y., Choi, S., Hamc, S. W., Kim, K.-J. Investigation of natural dyes and ancient textiles from korea using TOF-SIMS, Appl. Surf. Sci. 2008; 255: 1033–1036.

63. Wang, J., Hu, P., Liu, B., Jin, X., Kong, Y., Gao, J., Wang, D., Wang, B., Xu, R.,

Zhang, X. Investigation on coordination number and geometrical conformation of rare earth complexes with catenulate aminopolycarboxylic acid ligands J Coord. Chem. 2010; 63: 2193 - 2222.

64. Komboonchoo, S., Bechtold, T. Natural dyeing of wool and hair with indigo carmine (C.I. Natural Blue 2), a renewable resource based blue dye, J. Clean. Prod. 2009; 17 1487–1493.

65. Vankar, P. S., Shanker, R., Dixit, S., Mahanta, D., Tiwari, S. C. Sonicator Dyeing of Natural Polymers with Symplocos spicata by Metal Chelation, Fiber. Polym. 2008; 9: 121-127.

66. Kongkachuichaya, P., Shitangkoonb, A., Chinwongamorna, N. Studies on dyeing of silk yarn with lac dye: effects of mordants and dyeing conditions, ScienceAsia 2002; 28: 161-166.

67. Andrew, B. A. K. Saft, comfortable, durable press cottons: A natural progress for a natural fiber, , Textile chemist and colorist 1992; 24.

68. Andrew, B. A. K. Wrinkle resistant cotton and formaldehyde release Colorage annual 1995; 41.

69. Can, Y., Akaydin, M., Turban, Y., Ay, E. Effect of wrinkle resistance on cotton fabric properties, Indian Journal of Fiber and Textile Research 2009; 34: 183-86.

70. Yuen, C. W. M., Ku, S. K. A., Li, Y., Cheng, Y. F., Kan, C. W., Choi, P. S. R. Improvement of wrinkle-resistant treatment by nanotechnology The Journal of The Textile Institute 2009; 100: 173–180.

71. Oh, K. H., Jung, E. J. Nonformaldehyde crease-resistant finishing of ramie with glyoxal in the presence of a swelling agent, Text. Res. J. 2001; 71: 225-230.

72. Zhou, L. M., W., Y. K., Yuen, C. W. M., Zhou, X. Effect of mercerization and crosslinking on the dyeing properties of ramie fabric, Color. Technol. 2003; 119: 170-176.

73. Zhou, L. M., Yeung, K. W., Yuen, C. W. M., Zhou, X. Effect of mercerization on the crosslinking of ramie fabric using 1,2,3,4- butanetetracarboxylic acid: physical properties and crosslink distribution, Text. Res. J. 2002; 72: 795-802.

74. Zhou, L. M., Yeung, K. W., Yuen, C. W. M., Zhou, X. Characterization of ramie yarn treated with sodium hydroxide and crosslinked by 1,2,3,4-butanetetracarboxylic acid, J. Appl. Polym. Sci. 2004; 91: 1857–1864.

75. Zhou, L. M., Yeung, K. W., Yuen, C. W. M., Zhou, X. Effect of NaOH mercerisation on the crosslinking of ramie fabric using 1, 2, 3, 4-butanetetracarboxylic acid-reaction kinetics, Journal of the textile institute 2005 96: 213–220.

76. Zhou, L. M., Yeung, K. W. P., Yuen, C. W. M. Effect of NaOH mercerization on the crosslinking of ramie yarn using 1,2,3,4-butanetetracarboxylic acid, Text. Res. J. 2002; 72: 531-538.

77. Beltrame, P., Castelli, A., Selli, E., Mossa, A., Testa, G., Bonfattic, A. M., Sevesc, A. Dyeing of Cotton in Supercritical Carbon Dioxide, Dyes Pigments 1998; 39: 335-340.

78. Liu, Z. T., Sun, Z., Liu, Z. W., Lu, J., Xiong, H. Benzylated Modification and Dyeing of Ramie Fiber in Supercritical Carbon Dioxide, J. Appl. Polym. Sci. 2008; 107: 1872–1878.

79. Montero, G. A., Smith, C. B., Hendrix, W. A., Butcher, D. L. Supercritical fluid technology in textile processing: an overview, Ind. Eng. Chem. Res. 2000; 39 4806-4812.

80. Park, M. W., Bae, H. K. Dye distribution in supercritical dyeing with carbon dioxide, J. Supercrit. Fluid. 2002 22 65–73.

81. Sawadaa, K., Uedab, M. Evaluation of the dyeing mechanism of an acid dye on protein fibers in supercritical CO2, Dyes Pigments 2004 63: 77-81.

82. Montero, G., D., H., Hooker, J. Reducing problems of cyclic trimer deposits in supercritical carbon dioxide polyester dyeing machinery, J. of Supercritical Fluids 2003; 26: 47-54.

83. Cid, M. V. F., Spronsen, J. V., Kraan, M. V. D., Veugelers, W. J. T., Woerleeb, G. F., Witkampa, G. J. Excellent dye fixation on cotton dyed in supercritical carbon dioxide using fluorotriazine reactive dyes, Green Chem. 2005; 7: 609–616.

84. Maeda, S., Kunitou, K., Hihara, T., Mishima, K. One-Bath Dyeing of Polyester/Cotton Blends with Reactive Disperse Dyes in Supercritical Carbon Dioxide, Textile Res. J. 2004; 77: 989-994.

85. Ozcan, A. S., Clifford, A. A., Bartle, K. D., Lewis, D. M. Dyeing of Cotton Fibres with Disperse Dyes in Supercritical Carbon Dioxide, Dyes Pigments 1998; 36 103-110.

86. Cid, M. V. F., Spronsen, J. V. , Kraan, M. V. D., Veugelers, W. J. T., Woerlee, G. F., Witkamp, G. J. Acid-catalysed methanolysis reaction of non-polar triazinyl reactive dyes in supercritical carbon dioxide, J. Supercrit. Fluid. 2007 39 389–398.

87. Cid, M. V. F., Spronsen, J. V., Kraan, M. V. D., Veugelers, W. J. T., Woerlee, G. F., Witkamp, G. J. A significant approach to dye cotton in supercritical carbon dioxide with fluorotriazine reactive dyes, J. Supercrit. Fluid. 2007 40 477–484.

88. Guzel, B., Akgerman, A. Mordant dyeing of wool by supercritical processing, J. Supercrit. Fluid. 2000; 18: 247–252.

89. Kraan, M. V. D., Cid, M. V. F., Woerlee, G. F., Veugelers, W. J. T., Peters, C. J., Witkamp, G. J. Equilibrium distribution of water in the two-phase system supercritical carbon dioxide–textile, J. Supercrit. Fluid. 2007 40 336–343.

90. Kraan, M. V. D., Cid , M. V. F., Woerlee, G. F., Veugelers, W. J. T., Witkamp, G. J. Dyeing of natural and synthetic textiles in supercritical carbon dioxide with disperse reactive dyes, J. Supercrit. Fluid. 2007 40: 470–476.

91. Liu, Z. T., Zhang, L., Liu, Z. W., Gao, Z., Dong, W., Xiong, H., Peng, Y., Tang, S. Supercritical CO2 Dyeing of Ramie Fiber with Disperse Dye, Ind. Eng. Chem. Res. 2006; 45: 8932-8938.

92. Bao, P., Dai, J. Relationships between the Solubility of C. I. Disperse Red 60 and Uptake on PET in Supercritical CO2, J. Chem. Eng. Data 2005; 50: 838-842.

93. Cid, M. V. F., Spronsen, J. V. , Kraan, M. V. D., Veugelers, W. J. T., Woerlee, G. F., Witkamp, G. J. Acid-catalysed methanolysis reaction of non-polar triazinyl reactive dyes in supercritical carbon dioxide, J. Supercrit. Fluid. 2007 39 389–398.

94. Hou, A., Xie, K., Dai, J. Effect of Supercritical Carbon Dioxide Dyeing Conditions on the Chemical and Morphological Changes of Poly(ethylene terephthalate) Fibers, J. Appl. Polym. Sci. 2004; 92 2008–2012

95. Kawahara, Y., Yoshioka, T., Sugiura, K., Ogawa, S., Kikutani, T. Dyeing behavior of high-speed spun poly(ethylene terephthalate) fibers in supercritical carbon dioxide, J. Macromol. Sci. Phys. 2001; B40 189–197

96. Liao, S. K. Dyeing Nylon-6,6 with some hydrophobic reactive dyes by supercritical processing, J. Polym. Res. 2004; 11 285–291.

97. Liao, S. K., Ho, Y. C., Chang, P. S. Dyeing of nylon 66 with a disperse–reactive dye using supercritical carbon dioxide as the transport medium, JSDC(Journal of the Society of Dyers and Colourists.) 2000 116 403-407.

98. Ozcan, A. S., Ozcan, A. Adsorption behavior of a disperse dye on polyester in supercritical carbon dioxide, J. of Supercritical Fluids 2005 35 133–139.

99. Park, M. W., Bae, H. K. Dye distribution in supercritical dyeing with carbon dioxide, Journal of Supercritical Fluids 2002 22 65–73.

100. Park, S. C., Tuma, D., Kim, S., Lee, Y., Shim, J. J. Sorption of C. I. Disperse Red 60 in polystyrene and PMMA films and polyester and Nylon 6 textiles in the presence of supercritical carbon dioxide, Korean J. Chem. Eng. 2010; 27 299-309

101. Santos, W. L. F., Porto, M. F., Muniz, E. C., Povh, N. P., Rubira, A. F. Incorporation of disperse dye in N,N-dimethylacrylamide modified poly(ethylene terephthalate) fibers with supercritical, J. Supercrit. Fluid. 2001; 19 177–185.

102. Wen, H., Dai, J. J. Dyeing of polylactide fibers in supercritical carbon dioxide, J. Appl. Polym. Sci. 2007; 105 1903-1907

103. Domínguez, C., Jover, E., Bayona, J. M., Erra, P. Effect of the Carbon Dioxide Modifier on the Lipid Composition of Wool Wax Extracted from Raw Wool, Anal. Chim. Acta 2003; 477: 233–242.

104. Alzaga, R., Pascual, E., Erra, P., and Bayona, J. M.,. Development of a Novel Supercritical Fluid Extraction Procedure for Lanolin Extraction from Raw Wool, Anal. Chim. Acta 1999; 381: 39–48.

105. Zhao, X., Hirogaki, K., Tabata, I., Okubayashi, S., Hori, T. A new method of producing conductive aramid fibers using supercritical carbon dioxide, Surf. Coat. Tech. 2006 201 628–636.

106. Gittard, S. D., Hojo, D., Hyde, G. K., Scarel, G., Narayan, R. J., Parsons, G. N. Antifungal Textiles Formed Using Silver Deposition in Supercritical Carbon Dioxide, J. Mater. Eng. Perform. 2010; 19: 368–373.

107. Ma, X., Tomasko, D. L. Coating and Impregnation of a Nonwoven Fibrous Polyethylene Material with a Nonionic Surfactant Using Supercritical Carbon Dioxide, Ind. Eng. Chem. Res. 1997; 36 1586-1597.

108. Wong, Y. W. H., Yuen, C. W. M., Leung, M. Y. S., Ku, S. K. A., Lam, H. L. I. Selected applications of nanotechnology in textiles, AUTEX Research Journal 2006; 6: 1-8.

109. Kathirvelu, S., Souza, L. D., Dhurai, B. Nanotechnology applications in textiles, Indian Journal of Science and Technology 2008; 1: 5, 1-10.

110.Abidi, N., Cabrales, L., Hequet, E. Functionalization of a cotton fabric surface with titania nanosols: applications for self-cleaning and UV-protection properties, ACS Appl.

Mater. Inter. 2009; 1 10, 2141–2146

111. Kathirvelua, S., Souza, L. D., Dhurai, B. UV protection finishing of textiles using ZnO nanoparticles, Indian Journal of Fibre & Textile Research 2009; 34: 267-273.

112. Yuranova, T., Mosteo, R., Bandara, J., Laub, D., Kiwi, J. Self-cleaning cotton textiles surfaces modified by photoactive SiO_2/TiO_2 coating, J. Mol. Catal. A: Chem. 2006; 244: 160–167.

113. Bozzi, A., Yuranova, T., Kiwi, J. Self-cleaning of wool-polyamide and polyester textiles by TiO_2-rutile modification under daylight irradiation at ambient temperature, J. Photoch. Photobio. A: Chem. 2005 172 27–34.

114. Surassmo, S., Lauruengtana, V., Kangwansupamongkol, W., Ruktanonchai, U. Antibacterial effect of apatite coated titanium dioxide for textiles and coating applications, Proceedings of the 2nd IEEE International, Conference on Nano/Micro Engineered and Molecular Systems, Bangkok, Thailand, 2007, Jan. 16-19.

115. Deng, H., Zheng, W., Wen, C., Xiao, C. Low temperature preparation of nano TiO2 and its application as antibacterial agents, Trans. Nonferrous Met. Soc. China 2007; 17: 700-703.

116. Gupta, K. K., Jassal, M., Agrawal, A. K. Sol-gel derived titanium dioxide finishing of cotton fabric for self cleaning, Ind. J. Fiber Text. Res. 2008; 33: 443-450.

117. Kathirvelu, S., Souza, L. D., Dhurai, B. UV protection finishing of textiles using ZnO nanoparticles, Ind. J. Fiber Text. Res. 2009; 34: 267-273.

118. Ugur, S. S., Sarıısık, M., Aktas, A. H. The fabrication of nanocomposite thin films with TiO2 nanoparticles by the layer-by-layer deposition method for multifunctional cotton fabrics, Nanotechnology 2010 21 doi:10.1088/0957-4484/21/32/325603.

119. Karimi, L., Mirjalili, M., Yazdanshenas, M. E., Nazari, A. Effect of nano TiO2 on self-cleaning property of cross-linking cotton fabric with succinic acid under UV irradiation, Photochem. Photobiol. 2010; 86: 1030–1037.

120. Xue, C.-H., Jia, S.-T., Chen, H.-Z., Wang, M. Superhydrophobic cotton fabrics prepared by sol–gel coating of TiO_2 and surface hydrophobization, Sci. Technol. Adv. Mater. 2008 9 doi:10.1088/1468-6996/9/3/035001.

121. Wu, D., Long , M., Zhou, J., Cai, W., Zhu, X., Chen, C., Wu, Y. Synthesis and characterization of self-cleaning cotton fabrics modified by TiO_2 through a facile approach, Surf. Coat. Tech. 2009; 203: 3728–3733.

122. Paul, R., Bautista, L., Varga, M. D., Botet, J. M., Casals, E., Puntes, V., Marsal, F. Nano-cotton fabrics with high utraviolet protection, Text. Res. J. 2009; doi:10.1177/0040517509342316.

123. Bizani, E., Fytianos, K., Poulios, I., Tsiridis, V. Photocatalytic decolorization and degradation of dye solutions and wastewaters in the presence of titanium dioxide, J. Hazard. Mater. 2006; 136: 85–94.

124. Khataeea, A. R., Ponsb, M. N., Zahraac, O. Photocatalytic degradation of three azo dyes using immobilized TiO_2 nanoparticles on glass plates activated by UV light irradiation: influence of dye molecular structure, J. Hazard. Mater. 2009 168 451–457.

125. Kangwansupamonkon, W., Jitbunpot, W., Kiatkamjornwong, S. Photocatalytic efficiency of TiO_2/poly[acrylamide-co-(acrylic acid)] composite for textile dye degradation, Polym. Degrad. Stabil. 2010 95: 1894-1902.

126. Peralta-Hernandez, J. M., Manrıquez, J., Meas-Vong, Y., Rodrıguez, F. J., Chapman, T. W., Maldonado, M. I., Godınez, L. A. Photocatalytic properties of nano-structured TiO_2-carbon films obtained by means of electrophoretic deposition, J. Hazard. Mater. 2007; 147 588–593.

127. Bedford, N. M., Steckl, A. J. Photocatalytic self cleaning textile fibers by coaxial electrospinning, ACS Appl. Mater. Inter. 2010; 2: 8, 2448–2455

128. Meilert, K. T., Laubb, D., Kiwi, J. Photocatalytic self-cleaning of modified cotton textiles by TiO_2 clusters attached by chemical spacers, J. Mol. Catal. A: Chem. 2005 237 101–108.

129. Shivaraju, H. P., Byrappa, K., Ananda, S. Photocatalytic treatment of paper and pulp industrial effluents using TiO_2 deposited calcium alumino-silicate beads, Int. J. Chem. Eng. Res. 2010; 2: 2, 219–230.

130. Konstantinou, I. K., Albanis, T. A. TiO2-assisted photocatalytic degradation of azo dyes in aqueous solution: kinetic and mechanistic investigations: A review, Appl. Catal. B: Environ. 2004 49 1–14.

131. Haque, M. M., Muneer, M. TiO_2-mediated photocatalytic degradation of a textile dye derivative, bromothymol blue, in aqueous suspensions, Dye. Pigment. 2007; 75: 443-448.

132. Mihailovic, D., Šaponjic, Z., Radoicic, M., Radetic, T., Jovancic, P., Nedeljkovic, J., Radetic, M. Functionalization of polyester fabrics with alginates and

TiO2 nanoparticles, Carbohyd. Polym. 2010 79 526–532.

133. Bozzi, A., Yuranova, T., Guasaquillo, I., Laub, D., Kiwi, J. Self-cleaning of modified cotton textiles by TiO_2 at low temperatures under daylight irradiation, Journal of Photochemistry and Photobiology A: Chemistry 2005 174 156–164.

134. Yang, H., Zhu, S., Pan, N. Studying the Mechanisms of Titanium Dioxide as Ultraviolet-Blocking Additive for Films and Fabrics by an Improved Scheme, J. Appl. Polym. Sci. 2004; 92: 3201–3210.

135. Han, F., Kambala, V. S. R., Srinivasan, M., Rajarathnam, D., Naidu, R. Tailored titanium dioxide photocatalysts for the degradation of organic dyes in wastewater treatment: A review, Appl. Catal. A: Gen. 2009; 359: 25–40.

136. Dong, Y., Bai, Z., Liu, R., Zhu, T. Preparation of fibrous TiO2 photocatalyst and its optimization towards the decomposition of indoor ammonia under illumination, Catal. Today 2007; 126: 320–327.

137. Ku, Y., Ma, C.-M., Shen, Y.-S. Decomposition of gaseous trichloroethylene in a photoreactor with TiO2-coated nonwoven fiber textile, Appl. Catal. B: Environ. 2001; 34: 181–190.

138. Chen, R. Q. Nanometer materials and health-care textiles, Dyestuff Industry 2002; 39: 24-28.

139. Xin, J. H., Daoud, W.A., and Kong, Y.Y.,. A New Approach to UV-Blocking Treatment for Cotton Fabrics, Text. Res. J. 2004; 74: 97-100.

140. Saito, M. Antibacterial, Deodorizing, and UV Absorbing Materials Obtained with Zinc Oxide (ZnO) Coated Fabrics, Journal of Coated Fabrics 1993; 23: 150-164.

141. Yu, Q.-Z., Shen, A.-A. Anti-ultraviolet Treatment for Cotton Fabrics by Dyeing and Finishing in one Bath and Two Steps, Journal of Fiber Bioengineering and Informatics 2008; 1: 65-72.

142. Ibrahim, N. A., El-Gamal, A.R. , Gouda, M., Mahrous, F. A new approach for natural dyeing and functional finishing of cotton cellulose, Carbohyd. Polym. 2010; 82: 1205–1211.

143. Ali, S., Hussain, T., Nawaz, R. Optimization of alkaline extraction of natural dye from Henna leaves and its dyeing on cotton by exhaust method, J. Clean. Prod. 2009; 19: 61–66.

144. Vankar, P. S., Shanker, R., Dixit, S., Mahanta, D., Tiwari, S. C. Sonicator

dyeing of cotton with the leaves extract Acer pectinatum Wallich, Pigm. Resin Technol. 2008; 37: 308–313.

145. Huang, C.-H., *Rare Earth Coordination Chemistry: Fundamentals and Applications*. Wiley: 2010.

146. Gao, M., Chen, S., Han, J., Luo, D., Zhao, L., Zheng, Q. Effects of a pretreatment with N-methylmorpholine-N-oxide on the structures and properties of ramie, J. Appl. Polym. Sci. 2010; 117: 2241–2250.

147. Zhou, L. M., Yeung, K. W., Yuen, C. W. M., Zhou, X. Tensile strength loss of mercerized and crosslinked ramie fabric, Text. Res. J. 2003; 73: 367-372.

148. Kim, E., Csiszáár, E. Chemical finishing of linen and ramie fabrics, Journal of natural fibers 2005; 2: 39-52.

149. Liu, Z.-T., Yang, Y., Zhang, L., Sun, P., Liu, Z.-W., Lu, J., Xiong, H., Peng, Y., Tang, S. Study on the performance of ramie fiber modified with ethylenediamine, Carbohyd. Polym. 2008; 71 18–25.

150. Lee, M., Lee, M. S., Wakida, T., Hayashi, A., Okada, S., Yanai, Y. Liquid Ammonia Treatment of Nylon 6 Fabric, Text. Res. J. 2002; 72: 6, 539-544.

151. Mormman, W., Michel, U. Hydrocellulose with low degree of polymerisation from liquid ammonia treated cellulose, Carbonhyd. Polym. 2002; 50: 349-353.

152. Lu, Y. Electroless copper plating on 3-mercaptopropyltriethoxysilane modified PET fabric challenged by ultrasonic washing, Appl. Surf. Sci. 2009; 255: 8430–8434.

153. Perumlraj, R., Nalankilli, G., Dasaradan, B. S. Textile Composite Materials for EMC, J. Reinf. Plast. Comp. 2010; 29: 2992-3005.

154. Han, E. G., Kim, E. A., Oh, K. W. Electromagnetic interference shielding effectiveness of electroless Cu-plated PET fabrics., Synthetic Met. 2001; 123: 469~476.

155. Onar, N., Aksit, A. C., Ebeoglugil, M. F., Birlik, I., Celik, E., Ozdemir, I. Structural, electrical, and electromagnetic properties of cotton fabrics coated with polyaniline and polypyrrole, J. Appl. Polym. Sci., 2009; 114: 2003–2010.

156. Montero, G. A., Smith, C. B., Hendrix, W. A., Butcher, D. L. Supercritical Fluid Technology in Textile Processing: An Overview, Ind. Eng. Chem. Res. 2000; 39: 4806-4812.

157. Kongdee, A., Okubayashi, S., Tabata, I., Hori, T. Impregnation of Silk Sericin

into Polyester Fibers Using Supercritical Carbon Dioxide, J. Appl. Polym. Sci. 2007; 105: 2091–2097

158. Ahmed, N. S. E., El-Shishtawy, R. M. The use of new technologies in coloration of textile fibers, J. Mater. Sci. 2010; 45: 1143–1153.

159. Hendrix, W. A. Progress in Supercritical CO2 Dyeing, J. Ind. Text. 2001; 31: 43-56.

160. Ramsey, E., Sun, Q., Zhang, Z., Zhang, C., Gou, W. Mini-Review: Green sustainable processes using supercritical fluid carbon dioxide, J. Environmental Sciences 2009 21: 720–726.

161. Muthukumaran, P., Gupta, R. B., Sung, H. D., Shim t, J. J., Bae, H. K. Dye solubility in supercritical carbon dioxide. Effect of hydrogen bonding with cosolvents, Korean J. Chem. Eng. 1999; 16: 111-117

162. Sawadaa, K., Takagia, T., Uedab, M. Solubilization of ionic dyes in supercritical carbon dioxide: a basic study for dyeing fiber in non-aqueous media, Dyes Pigments 2004 60 129–135.

163. Xu, Y., Wu, N., Wei, Q., Pi, X. Preparation and the light transmittance of TiO2 deposited fabrics, J. Coat. Technol. Res. 2009; 6: 4, 549–555.

164. Lam, Y. L., Kan, C. W., Yuen, C. W. M. Effect of concentration of titanium dioxide acting as catalyst or co-catalyst on the wrinkle-resistant fnishing of cotton fabric, Fiber. Polym. 2010; 11: 4, 551-558.

PUBLICATIONS IN PHD STUDY

1. Guang Hong Zheng, Xi Zhao and Teuro Hori The application of supercritical CO_2 fluid technology for the electroless copper plating on ramie fabrics. *Textile Asia*, 2011, May, 17-22.

2. Guang Hong Zheng, Hong Bin Fu, and Guang Ping Liu Application of rare earth as mordant for the dyeing of ramie fabrics with natural dyes. Korean J. Chem. Eng. 28(11), 2148-2155 (2011),DOI: 10.1007/s11814-011-0090-9

3. Guang Hong Zheng, Yu Zhou, Dong Jie Yang. The application of liquid ammonia technique for the wrinkle resistant treatment of ramie fabric. *Textile Asia*, 2012, Jan-Feb, 31-33.

4. Shou Xiang Jiang, Rong Hui Guo, Guang Hong Zheng. Characterization of Ag-plated silk fabric by electroless plating. *Advanced Materials Research*, 2011, vol. 175-176, 509-513.

5. Yu Guan, Ya-Hong Mao, Qing-Kang Zheng, Guang Hong Zheng and Tian Tian, Transfer Printing with Disperse Dyes on Cotton Fabric Modified with an Aqueous Tolylene Diisocyanate Derivative, *Fibers and Polymers*, 2009, vol.10, No.4, 488-495.

6. Qiang Lin Li, Xiu Li Wang, De Yi Wang, Yu Zhong Wang, Xi Ning Feng and Guang Hong Zheng, Durable Flame Retardant Finishing of PET/Cotton Blends Using a Novel PVA-Based Phosphorus-Nitrogen, *Journal of Applied Polymer Science*, 2011, vol. 122, 342-353.

7. R. H. Guo, S. Q. Jiang, C. W. M. Yuen, M. C. F. Ng, Guang Hong Zheng, Influence of nickel ions for electroless Ni–P plating on polyester fabric, *Journal of Coating Technology Research*, DOI 10.1007/s11998-009-9227-8.

8. Shou Qiang Jiang, Rong Hui Guo, Guang Hong Zheng, Characterization of

silver-coated polyester fabric between magnetron sputting and electroless plating, *The Tenth International Symposium on Sputtering and Plasma Processes*, July 8-10, 2009, Kanazawa, Japan.

9. Zheng. G. H, Zhao. X, Tabata. I, Hori.T. Modification of the inner structure of ramie fabric using supercritical carbon dioxide fluid. *Proceedings of The Textile 83rd World Conference(83 rd TIWC),* Volume 2. P829-831 (2004)*,* Edited by College of Textil, Donghua University, May 23-27 Shanghai China.（2004）

10. Zhuo Yu, Zheng Guang Hong, Feng Chao Yang, A study on application of new type crosslinking additive for sil fabrics. *The Collections of The Theses For The 2002 Sino-Japanese Fiber Symposium* P254-260，Organizing Committee Of SJFS（2002）

ACKNOWLEDGMENT

At first, I would like express my sincerest gratitude to my supervisor Professor Teuro Hori for his consistent guidance and encouragement. Without his genuine help and constant support, it would be impossible for me to accomplish my PhD study. I indeed learned much from him. I was greatly influenced by his professional academic knowledge as well as his great passion for work and smart working style. The experience of working with him shall be a valuable treasure for my whole life.

I am sincerely grateful to my friend Dr Xi Zhao who has ever gave me a lot of warm hearted helps when we worked together in University of Fukui. In the past several years, his unselfish practical helps, invaluable discussions and endless encouragements have greatly improved my PhD study.

My acknowledgement also goes to Miss Rong Hui Guo, Mr Hong Bin Fu and Mr Yu Zhou, my colleagues in Chengdu Textile College for their helps in sample preparation and data collection during my PhD study. I also express my acknowledgements to all my colleagues who have ever helped me in different ways. Their unselfish helps are greatly appreciated.

I also give my acknowledgement to the Dr Shouxiang Jiang from Hong Kong Polytechnic University for his cooperation in the study of electroless plating of fabrics and Prof Zheng Qingkang from Sichuan University for his collaboration in the study of transfer printing of cotton fabric.